AD_________________

AWARD NUMBER: W81XWH-05-1-0627

TITLE: Systems Biology and Bioinformatics in Medical Applications

PRINCIPAL INVESTIGATOR: Bruce A. Holm, Ph.D.

CONTRACTING ORGANIZATION: New York State University Research Foundation, Buffalo
Amherst, NY 14260

REPORT DATE: October 2009

TYPE OF REPORT: Final Addendum

PREPARED FOR: U.S. Army Medical Research and Materiel Command
Fort Detrick, Maryland 21702-5012

DISTRIBUTION STATEMENT: Approved for Public Release;
Distribution Unlimited

REPORT DOCUMENTATION PAGE

Form Approved
OMB No. 0704-0188

1. REPORT DATE	**2. REPORT TYPE**	**3. DATES COVERED**
1 October 2009	Final Addendum	30 Sep 2007 – 29 Sep 2009

4. TITLE AND SUBTITLE

Systems Biology and Bioinformatics in Medical Applications

5a. CONTRACT NUMBER

5b. GRANT NUMBER
W81XWH-05-1-0627

5c. PROGRAM ELEMENT NUMBER

6. AUTHOR(S)

Bruce A. Holm, Ph.D.

E-Mail: baholm@buffalo.edu

5d. PROJECT NUMBER

5e. TASK NUMBER

5f. WORK UNIT NUMBER

7. PERFORMING ORGANIZATION NAME(S) AND ADDRESS(ES)

New York State University Research Foundation, Buffalo
Amherst, NY 14260

8. PERFORMING ORGANIZATION REPORT NUMBER

9. SPONSORING / MONITORING AGENCY NAME(S) AND ADDRESS(ES)
U.S. Army Medical Research and Materiel Command
Fort Detrick, Maryland 21702-5012

10. SPONSOR/MONITOR'S ACRONYM(S)

11. SPONSOR/MONITOR'S REPORT NUMBER(S)

12. DISTRIBUTION / AVAILABILITY STATEMENT
Approved for Public Release; Distribution Unlimited

13. SUPPLEMENTARY NOTES

14. ABSTRACT
Acinetobacter baumannii is a bacterial pathogen of increasing medical significance in military and civilian healthcare fa cilities. The importance of A. baumannii infections in war-related injuries is well established. A. baumannii was the mo st common gram-negative bacillus recovered from traumatic injuries to the lower extremities during the Vietnam War. More recently a new series of infections was reported in U.S. service personnel injured in the Iraq/Kuwait/Afghanistan regions during Operation Iraqi Freedom and in Afghanistan during Operation Enduring Freedom and many of these iso lates expressed a high degree of antimicrobial resistance. In addition, the incidence of multidrug-resistant (MDR) A. ba umannii infections, associated with significant morbidity and mortality, are increasing worldwide. Thus there is a critical need to identify potential vaccine antigens and new drug targets expressed by A. baumannii. In the past year we h ave made significant progress in our research. We identified three surface polysaccharides and three proteins that ma y serve as vaccine candidates and/or drug targets. We have developed an animal model that will allow us to test the se bacterial components in vivo. Finally, we completely sequenced and annotated the genome of A. baumannii 307, which allows us to search for novel targets in silico.

15. SUBJECT TERMS
Acinetobacter baumannii, respiratory pathogen, vaccine antigens, drug targets, biofilm

16. SECURITY CLASSIFICATION OF:			**17. LIMITATION OF ABSTRACT**	**18. NUMBER OF PAGES**	**19a. NAME OF RESPONSIBLE PERSON**
					USAMRMC
a. REPORT	**b. ABSTRACT**	**c. THIS PAGE**			**19b. TELEPHONE NUMBER** *(include area code)*
U	U	U	UU	49	

Standard Form 298 (Rev. 8-98)
Prescribed by ANSI Std. Z39.18

Table of Contents

INTRODUCTION:

The opportunistic human pathogen *Acinetobacter baumannii* is a gram-negative, nonmotile, nonfastidious member of the family *Moraxellaceae* within the order *Pseudomonadales*. *A. baumannii* is best known for causing health-care associated infections, however it is now emerging as a community-acquired pathogen as well. This bacterium accounts for 1-3% of hospital acquired infections primarily in immunocompromised hosts or those in Intensive Care Units (ICU). In some centers, the incidence of infections, particularly due to antibiotic resistant strains, is increasing making treatment challenging. The respiratory tract, particularly in ventilated patients, and IV devices (particularly for non-*A. baumannii* species) are the primary sites of infection [36]. Interestingly, *A. baumannii* has been described to uncommonly cause severe community-acquired pneumonia, usually in abnormal hosts (e.g. alcoholics), with the preponderance of cases reported from warm and humid geographic locales [5, 6, 15]. Further, a recent report from Kenya, described *A. baumannii* as the sixth most common pathogen responsible for bacteremia and sepsis in children [10]. The importance of *A. baumannii* infections in war-related injuries is now well established. *A. baumannii* was the most common gram-negative bacillus recovered from traumatic injuries to the lower extremities during the Vietnam War [51]. A new series of infections due has been reported in U.S. service members injured in the Iraq/Kuwait region during Operation Iraqi Freedom and in Afghanistan during Operation Enduring Freedom [2, 34]. The majority of patients had sustained traumatic injuries and *A. baumannii* was associated with soft-tissue infection, osteomyelitis, pneumonia, and bacteremia. In 67% of these cases *A. baumannii* was detected in blood cultures 48 hours after arrival to Landstulhl Regional Medical Center in Germany (LRMC) and 62% (18/29) had *A. baumannii* detected in blood cultures obtained within 48 hours of arrival at Walter Reed Army Medical Center (WRAMC). LRMC. These data are consistent with the concept that the majority of these *A. baumannii* infections were acquired from the combat field although subsequent acquisition in field hospitals or referral centers remains a possibility. Particularly disconcerting was the degree of antimicrobial resistance detected in the clinical isolates. Historically, imipenem has been the most active antimicrobial (>95% sensitivity) and β-lactam-β-lactamase combinations, cefepime, and amikacin have been often active [26, 50, 52]. However, only 87% and 82% of isolates from LRMC and WRAMC were sensitive to imipenem and from WRAMC 35% were sensitive only to impenem and 4% were resistant to all antimicrobials tested.

BODY/RESEARCH ACCOMPLISHMENTS:

Milestones/Task 1: Computer analysis of open reading frames.

We identified 1,862 putative open reading frames and annotated the complete genome of *A. baumannii* 307. **Completed 06/01/06.**

Milestones/Task 2: Lipoprotein determinations.

We have identified all the putative lipoprotein proteins and determined their characteristics. **Completed 07/01/06.**

Milestones/Task 3: Outer membrane transport analysis.

We identified 35 proteins that were apparently transported to the outer membrane. These were characterized by mass spectroscopy and database searches. Given the complexity in the characterization of optimal targets, we elected to pursue a more effective method to identify proteins of interest. **Completed 08/31/06.**

Milestones/Task 4: Homology searches.

We analyzed 102 different spots that represented outer membrane proteins expressed under different conditions. Using our selection process 71 of these proteins were analyzed to find putative vaccine antigens, iron regulated proteins, novel drug targets and/or virulence factors. **Completed 12/22/06.**

Milestones/Task 5: Identification of iron-regulated outer membrane proteins.

IROMPS were identified and characterized. From this group we identified an FHA homologue to the Bordetella FHA. This component is in the currently licensed DPT vaccine and thus we began to focus or efforts on determining the vaccine potential of this *A. baumannii* protein. We have also developed a series of monoclonal antibodies to *A. baumannii* and have characterized the epitopes recognized by three of these antibodies. Mab 6E3 reacts to an epitope expressed on the FHA homologue of Acinetobacter described above in task 1 and this epitope is present on the surface of 41% of the clinical isolates tested to date. Mab 13C11 reacts to a surface exposed carbohydrate epitope present on 33% of our strains and Mab 4E5 reacts with an epitope expressed on the surface of 38% of all isolates tested. **Completed 05/09/07.**

Milestones/Task 6: Isolation and Characterization of IROMPs.

We initially focused these studies on the Ton B dependent putative receptor proteins as are important for other human pathogens. In the pathogenic Neisseria and also in *Haemophilus influenzae*, iron-regulated Ton B dependent bacterial proteins have been expressed on the surface, conserved among strains, expressed in vivo and immunogenic in humans. These are all characteristics that constitute an ideal vaccine candidate thus we identified these homologues in *A. baumannii* isolates 307 and 855. To our surprise the biofilm-associated protein (BAP) was identified in this analysis and decided to pursue this protein further. Some of this data is presented in publication 1 in the appendix. **Completed 09/24/07.**

Milestone/Task 7: Molecular Epidemiologic Assessment of Military and Civilian Healthcare Associated *Acinetobacter* Strain Collections.

We performed a comprehensive antibody analysis combining our monoclonal and polyclonal antibodies to screen all our isolates for BAP reactivity. These data are shown in publication 1 in the appendix. It is important to note that a significant number of *A. baumannii* express the Bap epitope recognized by our Mab 6E3.

We have also performed static biofilm assays on our entire *A. baumannii* collection in order to define any obvious phenotypic differences among the strains. The plate on the right shows that some strains form very strong biofilms (well H/6); some strain form intermediate biofilms (well G/1); some strains form weak biofilms (well B/3); while other strains form no detectable biofilm using this method (well H/12). We have begun to explore these differences by comparative genomics among the different phenotypes.

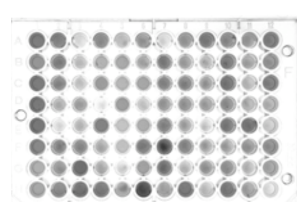

We also focused our efforts on identifying conserved genes in following three categories:
1) Adherence/colonization factors
2) Biofilm associated proteins and polysaccharides
3) Siderophores and siderophore receptors
Completed 09/29/08.

Milestone/Task 8: Genome Sequencing of Representative Military Associated and Civilian Healthcare Associated *A. baumannii* Strains.
We completed the complete genome sequence of Ab 307 reported this data publication 2 of the appendix. As we had a no cost extension we continued to sequence other relevant *A. baumannii* isolates as the additional milestones added (and approved) to the original proposal. **Completed 09/18/08.**

Milestone/Task 9: Comparative prevalence of virulence factors, antibiotic resistance genes, and genes that encode surface-exposed epitopes between military and civilian healthcare associated *A. baumannii* isolates by microarray analysis.
We have identified numerous *A. baumannii* components that represent novel drug targets, virulence factors and potential vaccine antigens. Most of the data derived from this proposal is presented the publications in the appendix. However, we did not have enough time or funding design a logical microarray chip. In addition it appears that with the changing technology there is no longer a need to perform microarray studies as we have already identified viable targets with defined phenotypes. Thus we have completed all of the proposed studies in each milestone with the exception of the remaining 20% of milestone 9.

KEY RESEARCH ACCOMPLISHMENTS:
1) We have developed an animal model to study infections associated with *A. baumannii.* Including in vivo biofilm formation on medically relevant material.
2) We have sequenced and annotated complete *A. baumannii* genomes.
3) We have identified 18-25 novel targets for novel therapeutic development.
4) We have identified and characterized single gene targets that disrupt biofilm formation.
5) We have identified a Bap, which may be a potential vaccine antigen.
6) We have performed extensive comparative genomic studies on multiple isolates of A. baumannii.
7) We have present some of our data at the First Wound Conference at the WRAMRC; at two meetings of the American Society for Microbiology; at the the recent TATRC meeting in Frederick, MD.
Appendix is attached.

REPORTABLE OUTCOMES: None

CONCLUSIONS:
We have identified targets that warrant further analysis as putative vaccine antigens, therapeutic targets and virulence factors. The next steps would be to continue these studies towards the development of deliverables that can be used to prevent and eradicate *A. baumannii* infections.

References:

1. Tong, M. J. (1972). Septic complications of war wounds. *JAMA* **219**(8): 1044-7.
2. Center for Disease Control and Prevention (2004). *Acinetobacter baumannii* infections among patients at military medical facilities treating injuried U.S. service members, 2002-2004. *MMWR* **53**: 1063-1066.
3. Department of Veterans Affairs. (2004). Update of the Colleagues' Letter sent April 23, 2004 concerning *Acinetobacter baumanii.* In, p. 539/111. Department of Veterans Affairs, Veterans Health Administration, Washington, D.C.
4. Davis, K. A., et al. (2005). Multidrug-resistant Acinetobacter extremity infections in soldiers. *Emerg Infect Dis* **11**(8): 1218-24.
5. Russo, T. A. (2005). Diseases caused by Gram-negative enteric bacilli. In *Harrison's Principles of Internal Medicine* (Kasper, D. L., et al. eds.), pp. 878-885. McGraw-Hill.
6. Chen, M. Z., et al. (2001). Severe community-acquired pneumonia due to *Acinetobacter baumannii*. *Chest* **120**(4): 1072-7.
7. Anstey, N. M., et al. (2002). Community-acquired bacteremic Acinetobacter pneumonia in tropical Australia is caused by diverse strains of Acinetobacter baumannii, with carriage in the throat in at-risk groups. *J Clin Microbiol* **40**(2): 685-6.
8. Anstey, N. M., Currie, B. J. and Withnall, K. M. (1992). Community-acquired Acinetobacter pneumonia in the Northern Territory of Australia. *Clin Infect Dis* **14**(1): 83-91.
9. Jain, R. and Danziger, L. H. (2004). Multidrug-resistant Acinetobacter infections: an emerging challenge to clinicians. *Ann Pharmacother* **38**(9): 1449-59. Epub 2004 Jul 27.
10. Tognim, M. C., et al. (2004). Resistance trends of Acinetobacter spp. in Latin America and characterization of international dissemination of multi-drug resistant strains: five-year report of the SENTRY Antimicrobial Surveillance Program. *Int J Infect Dis* **8**(5): 284-91.
11. Van Looveren, M. and Goossens, H. (2004). Antimicrobial resistance of Acinetobacter spp. in Europe. *Clin Microbiol Infect* **10**(8): 684-704.
12. Data from the Department of Defense. Military Casualty Information. www.dior.whs.mil/mmid/casualty/castop.htm Accessed April 21st, 2006.
13. Johnson, J. R. and Russo, T. A. (2005). Molecular epidemiology of extraintestinal pathogenic (uropathogenic) *Escherichia coli*. *Int J Med Microbiol* **295**(6-7): 383-404.
14. Johnson, J. R., et al. (1997). Characteristics and prevalence within serogroup O4 of a J96-like clonal group of uropathogenic *Escherichia coli* O4:H5 containing the class I and class III alleles of papG. *Infect Immun* **65**(6): 2153-9.
15. Johnson, J. R., et al. (2001). Molecular comparison of extraintestinal *Escherichia coli* isolates of the same electrophoretic lineages from humans and domestic animals. *J Infect Dis* **183**(1): 154-9. Epub 2000 Nov 28.
16. Grundmann, H. J., et al. (1997). Multicenter study using standardized protocols and reagents for evaluation of reproducibility of PCR-based fingerprinting of Acinetobacter spp. *J Clin Microbiol* **35**(12): 3071-7.
17. Bartual, S. G., et al. (2005). Development of a multilocus sequence typing scheme for characterization of clinical isolates of *Acinetobacter baumannii*. *J Clin Microbiol* **43**(9): 4382-90.
18. Fournier, P. E., et al. (2006). Comparative Genomics of Multidrug Resistance in *Acinetobacter baumannii*. *PLoS Genet* **2**(1): e7.
19. Luke, N. R. and Campagnari, A. A. (1999). Construction and characterization of *Moraxella catarrhalis* mutants defective in expression of transferrin receptors. *Infect Immun* **67**(11): 5815-9.
20. Luke, N. R., et al. (1999). Use of an isogenic mutant constructed in *Moraxella catarrhalis* To identify a protective epitope of outer membrane protein B1 defined by monoclonal antibody 11C6. *Infect Immun* **67**(2): 681-7.

21. Russo, T. A., et al. (1995). Loss of the O4 antigen moiety from the lipopolysaccharide of an extraintestinal isolate of *Escherichia coli* has only minor effects on serum sensitivity and virulence in vivo. *Infect Immun* **63**(4): 1263-9.
22. Margulies, M., et al. (2005). Genome sequencing in microfabricated high-density picolitre reactors. *Nature* **437**(7057): 376-80.
23. Berkley, J. A., et al. (2005). Bacteremia among children admitted to a rural hospital in Kenya. *N Engl J Med* **352**(1): 39-47.
24. Actis, L. A., et al. (1993). Effect of iron-limiting conditions on growth of clinical isolates of *Acinetobacter baumannii*. *J Clin Microbiol* **31**(10): 2812-5.
25. Ducey, T. F., et al. (2005). Identification of the iron-responsive genes of *Neisseria gonorrhoeae* by microarray analysis in defined medium. *J Bacteriol* **187**(14): 4865-74.
26. Hughes, T. R., et al. (2000). Functional discovery via a compendium of expression profiles. *Cell* **102**(1): 109-26.
27. Smoot, L. M., et al. (2001). Global differential gene expression in response to growth temperature alteration in group A Streptococcus. *Proc Natl Acad Sci U S A* **98**(18): 10416-21.
28. Stintzi, A. (2003). Gene expression profile of *Campylobacter jejuni* in response to growth temperature variation. *J Bacteriol* **185**(6): 2009-16.
29. Campagnari, A. A., Ducey, T. F. and Rebmann, C. A. (1996). Outer membrane protein B1, an iron-repressible protein conserved in the outer membrane of *Moraxella* (*Branhamella*) *catarrhalis*, binds human transferrin. *Infect Immun* **64**(9): 3920-4.
30. Campagnari, A. A., Shanks, K. L. and Dyer, D. W. (1994). Growth of *Moraxella catarrhalis* with human transferrin and lactoferrin: expression of iron-repressible proteins without siderophore production. *Infect Immun* **62**(11): 4909-14.
31. Luke, N. R., et al. (2004). Expression of type IV pili by *Moraxella catarrhalis* is essential for natural competence and is affected by iron limitation. *Infect Immun* **72**(11): 6262-70.
32. Russo, T. A., Carlino, U. B. and Johnson, J. R. (2001). Identification of a new iron-regulated virulence gene, *ireA*, in an extraintestinal pathogenic isolate of *Escherichia coli*. *Infect Immun* **69**(10): 6209-16.
33. Russo, T. A., et al. (1999). Identification of genes in an extraintestinal isolate of *Escherichia coli* with increased expression after exposure to human urine. *Infect Immun* **67**(10): 5306-14.
34. Russo, T. A., et al. (2002). IroN functions as a siderophore receptor and is a urovirulence factor in an extraintestinal pathogenic isolate of *Escherichia coli*. *Infect Immun* **70**(12): 7156-60.
35. Russo, T. A., et al. (1998). Identification, genomic organization, and analysis of the group III capsular polysaccharide genes kpsD, kpsM, kpsT, and kpsE from an extraintestinal isolate of *Escherichia coli* (CP9, O4/K54/H5). *J Bacteriol* **180**(2): 338-49.
36. Russo, T. A., Liang, Y. and Cross, A. S. (1994). The presence of K54 capsular polysaccharide increases the pathogenicity of *Escherichia coli* in vivo. *J Infect Dis* **169**(1): 112-8.

JOURNAL OF BACTERIOLOGY, Feb. 2008, p. 1036–1044 Vol. 190, No. 3
0021-9193/08/$08.00+0 doi:10.1128/JB.01416-07

Identification and Characterization of an *Acinetobacter baumannii* Biofilm-Associated Protein▽

Thomas W. Loehfelm,[1,3] Nicole R. Luke,[1,4] and Anthony A. Campagnari[1,2,3,4]*

Department of Microbiology and Immunology[1] and Department of Medicine, Division of Infectious Diseases,[2] and Witebsky Center for Microbial Pathogenesis and Immunology,[3] University at Buffalo, The State University of New York, and NYS Center of Excellence in Bioinformatics and Life Sciences,[4] Buffalo, New York

Received 31 August 2007/Accepted 7 November 2007

We have identified a homologue to the staphylococcal biofilm-associated protein (Bap) in a bloodstream isolate of *Acinetobacter baumannii*. The fully sequenced open reading frame is 25,863 bp and encodes a protein with a predicted molecular mass of 854 kDa. Analysis of the nucleotide sequence reveals a repetitive structure consistent with bacterial cell surface adhesins. Bap-specific monoclonal antibody (MAb) 6E3 was generated to an epitope conserved among 41% of *A. baumannii* strains isolated during a recent outbreak in the U.S. military health care system. Flow cytometry confirms that the MAb 6E3 epitope is surface exposed. Random transposon mutagenesis was used to generate *A. baumannii bap1302*::EZ-Tn*5*, a mutant negative for surface reactivity to MAb 6E3 in which the transposon disrupts the coding sequence of *bap*. Time course confocal laser scanning microscopy and three-dimensional image analysis of actively growing biofilms demonstrates that this mutant is unable to sustain biofilm thickness and volume, suggesting a role for Bap in supporting the development of the mature biofilm structure. This is the first identification of a specific cell surface protein directly involved in biofilm formation by *A. baumannii* and suggests that Bap is involved in intercellular adhesion within the mature biofilm.

Acinetobacter spp. are gram-negative aerobic coccobacilli that are ubiquitous in nature, persistent in the hospital environment, and cause a variety of opportunistic nosocomial infections (1). A number of species of *Acinetobacter* are associated with human infection, including genomic species 3 and 13TU (8, 46), although *A. baumannii* is generally regarded as the major pathogen. *A. baumannii* is a causative agent of nosocomial pneumonia, bacteremia, meningitis, and urinary tract infection (1) and more recently has caused serious infections among American military personnel serving in Iraq and Afghanistan (12, 38). Because it is often multi- or pan-drug resistant, infections are difficult to treat (17), resulting in attributable mortalities of up to 23% for hospitalized patients and 43% for patients under intensive care (16). Indeed, the Antimicrobial Availability Task Force of the Infectious Diseases Society of America recently identified *A. baumannii*, along with *Aspergillus* spp., extended-spectrum β-lactamase-producing *Enterobacteriaceae*, vancomycin-resistant *Enterococcus faecium*, *Pseudomonas aeruginosa*, and methicillin-resistant *Staphylococcus aureus*, as "particularly problematic pathogens" for which there is a desperate need for new drug development (42). In the case of *A. baumannii*, there is an additional unmet need for an understanding of its basic pathogenesis.

Most *A. baumannii* research to date has focused on cataloging and understanding the variety of antimicrobial resistance genes and mechanisms found within the species (3, 30, 45, 50). An intriguing observation that ethanol stimulates the virulence of *A. baumannii* (39) led to the identification of a number of genes affecting virulence toward *Caenorhabditis elegans* and *Dictyostelium discoideum* (40) that await further characterization. A well-characterized porin of *A. baumannii*, the 38-kDa outer membrane protein A, has been shown to induce apoptosis of eukaryotic cells (9) and to activate dendritic cells, leading to the differentiation of $CD4^+$ T cells toward a Th1 phenotype (26). Finally, it was noted that *A. baumannii* forms biofilms with enhanced antibiotic resistance (48, 49) and, more recently, that a chaperone-usher secretion system involved in pilus assembly affects biofilm formation (44).

Biofilms are highly structured communities of bacteria attached to a surface (41) and are recognized as a common cause of human infection (10). It has been proposed that all bacterial biofilms have a number of functionally conserved components in common, including the production of an extracellular polysaccharide matrix, GGDEF/EAL-domain-mediated intracellular signaling, and large surface adhesins homologous to the biofilm-associated protein (Bap) first identified in *S. aureus* (23). Bap family members are defined as high-molecular-weight proteins that are present on the bacterial surface, contain a core domain of tandem repeats, and confer on bacteria the ability to form a biofilm (24). Since the initial identification of Bap, homologues have been identified in at least 13 pathogenic species (24, 25), and the proteins generally share structural and functional similarities, although not necessarily primary sequence similarity.

In the present study, we have identified and fully sequenced a gene encoding a Bap homologue in *A. baumannii* 307-0294. We have generated a transposon-insertion mutant deficient in Bap surface expression and a specific monoclonal antibody (MAb), 6E3, recognizing Bap. The epitope recognized by MAb 6E3 is surface accessible and conserved among 41% of *A.*

* Corresponding author. Mailing address: Department of Microbiology and Immunology, University at Buffalo, Rm. 140, Biomedical Research Building, 3435 Main St., Buffalo, NY 14214. Phone: (716) 829-2673. Fax: (716) 829-3889. E-mail: aac@buffalo.edu.

▽ Published ahead of print on 16 November 2007.

TABLE 1. Sequences of oligonucleotide primers used for RT-PCR

Primer	Sequence (5′–3′)	Position[a]	Target
1124	TCATACGTCTGAAA AATGGCGAG	152–174	5′ region of *bap*
1125	CATCAAGTGCTACT GTCGGCG	1151–1171(c)	5′ region of *bap*
1461	CAGATGTGCCTCAT TTGTCGG	25025–25045	3′ region of *bap*
1462	CCTGTATTCACTCC TTGACCAGCAG	25259–25283(c)	3′ region of *bap*
1160	AAGGAGTGAATAC AGGCGAAG	25268–25288	3′ *bap* to A1S_2695
1330	CATTTGCATCGTAG CGACTCG	26572–26592(c)	3′ *bap* to A1S_2695
1437	ACCAAATAGAGCA GCAGGTTC	26278–26298	A1S_2695
1438	CTCCCCTTCTTTACC ATCAATC	26888–26909(c)	A1S_2695

[a] That is, relative to the predicted *bap* start codon. The predicted *bap* coding sequence is from positions 1 to 25863, and that of A1S_2695 is from positions 26160 to 27665. The "(c)" indicates that the primer anneals to the cDNA strand.

baumannii isolates recovered during the U.S. military health care system outbreak. Quantitative comparison of biofilms formed by a Bap-deficient mutant and wild-type bacteria demonstrates that the mutant is unable to sustain biovolume and biofilm thickness development.

MATERIALS AND METHODS

Bacterial strains and culture conditions. Wild-type *A. baumannii* strain 307-0294 was isolated from the bloodstream of a patient in 1994. A library of 98 *Acinetobacter* strains was obtained from the Walter Reed Army Medical Center, including 76 isolates of *A. baumannii*, 13 isolates of genome species 3, 5 isolates of species 13TU, 1 isolate of genome species 10, and 3 isolates of otherwise-uncharacterized *Acinetobacter* sp. *Escherichia coli* XL1-Blue (Stratagene, La Jolla, CA) was used as the host strain for all plasmid manipulations.

All *Acinetobacter* strains were cultured in Mueller-Hinton (MH) medium (broth or agar), supplemented with kanamycin (50 μg/ml) and carbenicillin (200 μg/ml) when appropriate. For biofilm studies, FAB medium [0.1 mM $CaCl_2$, 0.15 mM $(NH_4)_2SO_4$, 0.33 mM Na_2HPO_4, 0.5 mM NaCl, and 0.2 mM KH_2PO_4] supplemented with 10 mM sodium citrate and, unless otherwise indicated, 0.5% (wt/vol) Casamino Acids (FAB-citrate) was used. Static culture biofilm experiments for time course confocal microscopy were incubated at 37°C in room air on a heated microscope stage; in all other cases, bacteria were grown at 35.5°C in 5% CO_2.

Plasmid pMU125, an *E. coli-Acinetobacter* shuttle vector conferring green fluorescent protein (GFP) expression (14), was generously provided by Luis Actis.

DNA and RNA manipulations. Routine DNA manipulations were performed using standard procedures (37). Chromosomal DNA was purified as previously described (36). Restriction endonucleases were supplied by New England Biolabs, Inc. (Ipswich, MA), and Promega Corp. (Madison, WI); assays were performed as recommended by the manufacturer. Oligonucleotide primers were purchased from Integrated DNA Technologies (Coralville, IA).

Total RNA was isolated by using an RNeasy minikit (Qiagen, Santa Clara, CA), and transcriptional analysis was performed by using a OneStep reverse transcriptase-PCR (RT-PCR) kit (Qiagen) and the primers listed in Table 1.

MAb development. MAb 6E3, an immunoglobulin G1 isotype that reacts to an epitope on Bap, was developed by injecting BALB/c mice intraperitoneally with live *A. baumannii* 307-0294 suspended in phosphate-buffered saline according to a previously described protocol (5). Hybridoma supernatants were screened by immunodot and Western blot assays for the presence of antibody reactive to whole bacteria, whole-cell lysate, and proteinase K-digested whole-cell lysate of *A. baumannii* 307-0294.

Hybridoma cell line 6E3 produced antibody reactive to a proteinase K-sensitive epitope on a high-molecular-weight antigen. This cell line was used to generate high-titer mouse ascites fluid and protein A affinity-purified antibody at a stock concentration of 2.2 mg/ml (Rockland Immunochemicals, Gilbertsville, PA).

Transposon mutagenesis. EZ-Tn*5* Kan-2 Transposomes (Epicenter, Madison, WI) were electroporated into electrocompetent *A. baumannii* 307-0294, prepared by washing log-phase bacteria (optical density at 600 nm [OD_{600}] ≈ 1) three times with ice-cold sterile ultrapure water and resuspending them in ice-cold sterile 10% glycerol. Electrocompetent cells were stored in 50-μl single-use aliquots at −80°C. Transformants were selected with kanamycin and screened for surface reactivity to MAb 6E3 by colony lift assay.

Flow cytometry. Wild-type *A. baumannii* 307-0294 and *bap1302*::EZ-Tn*5* from late-log-phase growth (OD_{600} ≈ 1.8) in MH broth cultures were diluted in sterile saline to an OD_{600} of 0.03. MAb 6E3 was labeled with the Zenon Alexa Fluor 488 Mouse IgG1 kit (Invitrogen Corp., Carlsbad, CA) according to the manufacturer's protocol. Blocking antibody, supplied with the kit, was labeled separately as a control for nonspecific binding. A total of 1 μg of labeled antibody was added to 100 μl of diluted bacteria, followed by incubation at room temperature for 20 min. Then, 900 μl of sterile saline was added to the samples, and the cells were analyzed in a FACSCalibur flow cytometer (BD, Franklin Lakes, NJ) with the following settings: forward scatter voltage, E02 (log); side scatter voltage, 582 (log); FL1 voltage, 665 (log); event threshold, forward scatter = 434 and side scatter = 380.

DNA sequencing and computer analysis. The DNA sequence was determined by the dideoxy chain termination method using an ABI Prism 3130XL genetic analyzer (Applied Biosystems, Foster City, CA) at the Biopolymer Resource facility at Roswell Park Cancer Institute (Buffalo, NY). PCR products were cloned into the pGEM-T Easy vector (Promega), and genomic DNA was cloned into pUC18 after appropriate restriction endonuclease digestion. For sequencing the internal, highly repetitive region of *bap*, chromosomal DNA from nine transposon-insertion mutants, each with insertions in *bap*, was partially digested with Sau3AI, separated by 1.5% agarose gel electrophoresis to allow the selection of specific fragment sizes, and ligated into BamHI-digested pUC18. In some cases, nested deletions of the resultant plasmids were generated by using the Erase-a-Base system (Promega). The sequence of the genomic regions neighboring *bap* was determined by pyrophosphate-based sequencing by synthesis on a 454 Genome Sequencer 20 DNA sequencing system (Roche Applied Science, Indianapolis, IN) at the New York State Center of Excellence in Bioinformatics and Life Sciences (Buffalo, NY). Sequence similarity searches were performed by using the BLAST and BLASTP programs at the National Center for Biotechnology Information (NCBI). All other sequence assembly and analysis was performed by using the MacVector software package (v7.2.3; MacVector, Inc., Cary, NC).

SDS-PAGE, Western blotting, and colony lift immunoassay. Sodium dodecyl sulfate-polyacrylamide gel electrophoresis (SDS-PAGE), Western blotting, and colony lift analyses were performed according to standard procedures (37), with the exception that protein samples were not boiled prior to gel electrophoresis. Equal amounts of protein were loaded in each lane, and gels were stained with a Colloidal Blue staining kit (Invitrogen). Western blots and colony lift immunoassays were probed with MAb 6E3 and detected colorimetrically with horseradish peroxidase-conjugated secondary antibody (KPL, Inc., Gaithersburg, MD). Whole-cell protein extracts were prepared with a BugBuster protein extraction reagent (Novagen) according to the manufacturer's protocol. Zwittergent-extracted outer membrane proteins were prepared as described previously (6).

NanoLC-MS/MS. The protein identification work was performed by ProtTech, Inc. (Norristown, PA) using nanoscale liquid chromatography with tandem mass spectrometry (NanoLC-MS/MS) peptide sequencing technology. In brief, each protein gel band was destained, cleaned, and digested in-gel with sequencing-grade modified trypsin. The resultant peptide mixture was analyzed by an LC-MS/MS system, and the mass spectrometric data acquired were used to search the most recent nonredundant and patent protein databases with ProtTech's proprietary software suite.

Static culture biofilm growth for confocal microscopy. For single-time-point biofilm imaging, *A. baumannii* 307-0294 and *bap1302*::EZ-Tn*5* were resuspended from an overnight MH plate and inoculated into 35-mm glass-bottom petri dishes (MatTek, Corp., Ashland, MA). The plates were incubated at 35.5°C for 48 h and then stained with a LIVE/DEAD *Bac*Light bacterial viability kit (Invitrogen) according to the manufacturer's instructions. Image stacks were acquired by confocal laser scanning microscopy (CLSM) at ×630 magnification on a Zeiss Axiovert 200M inverted microscope with an attached Zeiss LSM 510 Meta NLO imaging system. Images were produced from the raw LSM files by using ImageJ (freely available from the National Institutes of Health).

For time course biofilm imaging, *A. baumannii* 307-0294 and *bap1302*::EZ-Tn*5* were transformed by electroporation with pMU125. The resultant GFP-express-

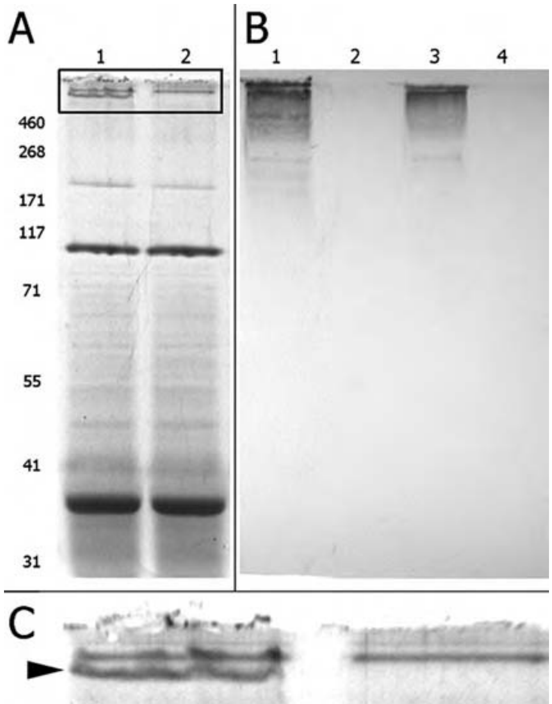

FIG. 1. Coomassie blue-stained SDS–7% polyacrylamide gel (A and C) and immunoblot (B) demonstrating reactivity of MAb 6E3 to a high-molecular-weight antigen in *A. baumannii* 307-0294 whole-cell lysate (lane 1) and outer membrane proteins (lane 3) but not the corresponding samples from *A. baumannii bap1302*::EZ-Tn*5* (lanes 2 and 4, respectively). (C) Enlargement of the region outlined in panel A to clearly show the high-molecular-weight antigen present in wild type and absent in *A. baumannii bap1302*::EZ-Tn*5* whole-cell lysate. This band was excised from a similar gel and identified by NanoLC-MS/MS. Molecular mass standards are indicated in kilodaltons.

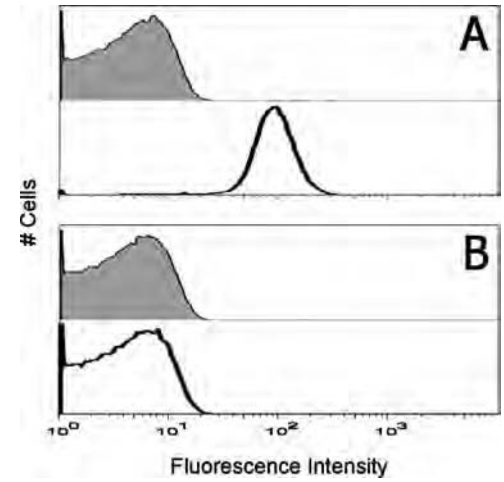

FIG. 2. Flow cytometric analysis of *A. baumannii* 307-0294 (A) and *bap1302*::EZ-Tn*5* (B) demonstrates the surface accessibility of the MAb 6E3 epitope. Cells from late-log-phase cultures were probed with Alexa Fluor 488-conjugated control nonspecific antibody (shaded histograms) or MAb 6E3 (unshaded histograms). Each histogram shows the fluorescence intensity distribution of >50,000 flow cytometer events.

ing strains were incubated overnight at 35.5°C on MH agar with appropriate antibiotics. Cells were resuspended in FAB-citrate to an OD_{600} of 0.4, and 10 μl was inoculated into four-well chambered coverglass slides (Nunc; Lab-Tek catalog no. 136420) containing 1 ml of FAB-citrate. The slides were loaded onto the motorized preheated stage of the CLSM system, and image stacks were acquired every 60 min for 14 h from two nonoverlapping fields of view at ×400 magnification, covering a total slide surface area of 10^5 μm^2, in order to obtain a representative sample of the biofilm (21). The CLSM image stacks were manually edited to remove extraneous images (defined as any image including and below those containing reflections of the glass coverslip and any images including and above the first image to contain no bright pixels representing bacterial cells) to minimize bias during quantitative image analysis (29). The manually edited image stacks were analyzed by using the Image Structure Analyzer-3D program to calculate 20 parameters describing the three-dimensional biofilm structure (2), including biovolume and average thickness at each time point for each field of view. Statistical analyses were performed with Prism (version 4.0c; GraphPad Software, Inc.) by fitting the data with the best-fit fourth-order polynomial equation and performing an F test of the null hypothesis that the curves describing biofilm development by wild-type and mutant bacteria were best described by the same equation. Inverse biofilm experiments using 96-well polystyrene plates were performed as described previously (28).

Nucleotide sequence accession number. The *A. baumannii* 307-0294 *bap* locus, with each repeat unit annotated, has been deposited in GenBank under accession number EU117203.

RESULTS

Characterization of MAb 6E3. Immunodot assay was initially used to identify MAb 6E3, which reacted to whole-cell lysates of *A. baumannii* 307-0294 (data not shown). Western blot analysis demonstrated that the MAb 6E3 epitope is detected on a high-molecular-weight antigen present in whole-cell lysate and outer membrane proteins of *A. baumannii* 307-0294 (Fig. 1B). The epitope is sensitive to proteinase K digestion, and the electrophoretic mobility of the antigen is modified by heat but not by SDS or β-mercaptoethanol (data not shown).

The MAb 6E3 antigen contains surface-exposed epitopes. Flow cytometry was used to determine whether the antigen recognized by MAb 6E3 was surface accessible. Figure 2 shows that MAb 6E3 binds to an epitope expressed on the surface of wild-type *A. baumannii* 307-0294 (Fig. 2A), whereas the Bap-deficient mutant *bap1302*::EZ-Tn*5* (described below) has lost

TABLE 2. Survey of MAb 6E3 reactivity among a representative library of *Acinetobacter* strains isolated during an outbreak in the U.S. military health care system

Acinetobacter species	Sequence type[a]	No. of strains: Isolated	No. of strains: Screened	No. of strains reactive to MAb 6E3 (%)
A. baumannii		189	76	31 (41)
	ST11	51	5	4 (80)
	ST14	22	6	6 (100)
	ST16	13	2	2 (100)
	ST10	12	2	2 (100)
	Other[b]	91	61	17 (28)
13TU		8	5	0 (0)
Genome sp. 3		13	13	11 (85)
Other[c]		6	4	0 (0)
Total		216	98	42 (43)

[a] Sequence type assignments were extracted from Fig. 2 in reference 15.
[b] Includes strains representing 35 other sequence types and two isolates of unknown sequence type.
[c] Includes one isolate of genome species 10 and three otherwise undescribed genomic species; additional single isolates of *A. ursingii* and *A. haemolyticus* were recovered during the outbreak, but these were not included in our screened library.

TABLE 3. Internal peptide fragments of Bap identified by NanoLC-MS/MS from a single band on a protein gel

Peptide mass (Da)	Peptide sequence	Position (start-end)
1,141.64	VAASDVLVVNR	35–45
2,630.35	NIPADAANTAVTVVINGVTYNATVDK	228–253
1,900.95	AAGTWTVSVPGSGLVADADK	254–273
2,596.33	TVVADSSDTGVIDLLGIFGSEVQFK	8032–8056
1,642.78	VDSFTYTVSDPVTGR	8181–8195
1,690.84	PLDSAANATVDVIDYK	8444–8459

reactivity to this antibody (Fig. 2B). These data confirm that the epitope on the high-molecular-weight antigen recognized by MAb 6E3 is surface exposed.

The MAb 6E3 epitope is conserved among recent clinical isolates. A panel of 98 *Acinetobacter* strains, representing the 216 isolates recovered during an outbreak in the U.S. military health care system (15), was screened by colony lift assay to determine the level of conservation of the MAb 6E3 epitope. The results of these studies demonstrate that 43% of *Acinetobacter* isolates are reactive to MAb 6E3 (Table 2).

Peptide sequence from the MAb 6E3 antigen. The high-molecular-weight protein band reactive to MAb 6E3 was excised from a Coomassie blue-stained SDS-polyacrylamide gel and identified by LC-MS/MS peptide sequencing. Six peptides were sequenced (Table 3), and the sequences were concatenated and subjected to BLASTP analysis against the patented protein sequence database at the NCBI, which identified sequence 5503 from U.S. patent 6562958 (entitled "Nucleic acid and amino acid sequences relating to *Acinetobacter baumannii* for diagnostics and therapeutics"). A similar search performed against the nonredundant protein sequence database identified a small number of repetitive surface proteins, as well as two predicted proteins from *A. baumannii* ATCC 17978: A1S_2724, a putative hemagglutinin/hemolysin-related protein, and A1S_2696, a hypothetical protein.

Random transposon mutagenesis. In order to identify the gene encoding the high-molecular-weight proteinaceous antigen described above, we screened 550 kanamycin-resistant EZ-Tn*5* insertional mutants and identified nine that lost surface reactivity to MAb 6E3. We obtained DNA sequence flanking the transposon insertion site for each of the nine mutants that suggested a common gene was disrupted.

The full-length coding sequence of the disrupted gene was assembled from sequence data obtained as described in Materials and Methods. BLASTP analysis against the nonredundant protein sequences database at the NCBI showed that this coding sequence was similar to Baps from various bacterial species. The predicted full-length *A. baumannii* 307-0294 *bap* open reading frame is 25,863 bp and composed primarily of four similar, tandem repeated modules (designated modules A to D), ranging in size from 237 to 315 bp (Fig. 3A). The 3′ end of the coding sequence contains additional repeat modules (designated modules E to G) that are not similar to modules A to D.

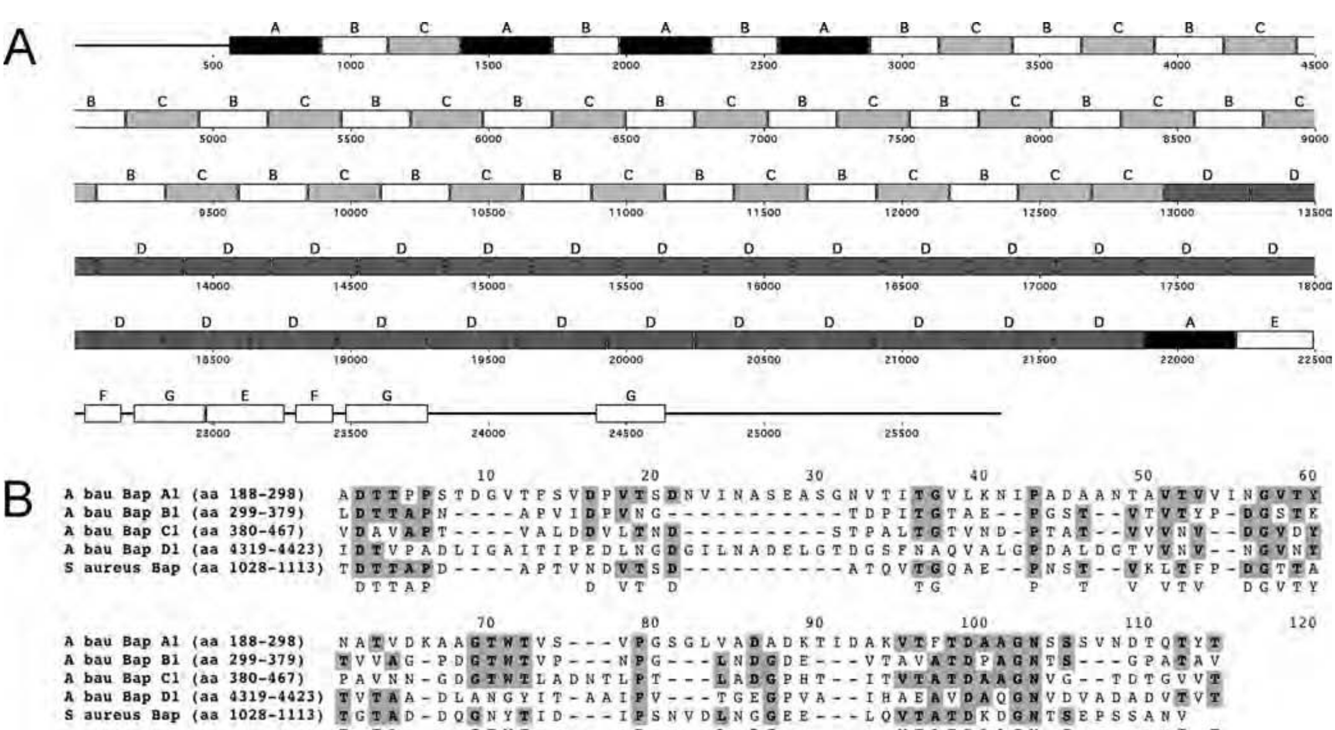

FIG. 3. Graphical representation of *bap* demonstrating the repetitive structure (A) and a CLUSTAL alignment (B) showing sequence similarity between the $Bap_{A.\ baumannii}$ and $Bap_{S.\ aureus}$ repeat units. (A) The 25,863-bp *A. baumannii bap* open reading frame is composed almost entirely of tandemly arranged repeats, labeled A to D. The 3′ end of the coding sequence contains additional repetitive units E to G that are not similar to A to D. (B) CLUSTAL alignment of an example of each of the major repeat types found in $Bap_{A.\ baumannii}$ and of the "C" repeat unit from $Bap_{S.\ aureus}$. For both proteins, the start and end of each repeat, indicated in parentheses, was defined by comparison to the seed alignment of the HYR domain (PFAM accession no. PF02494).

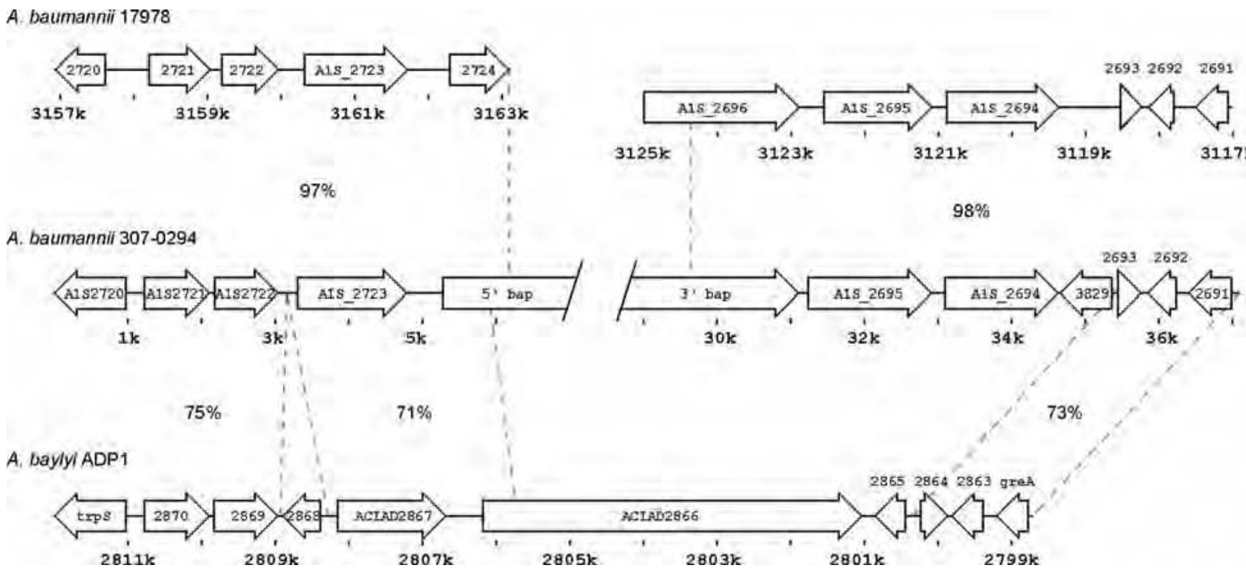

FIG. 4. The publicly available *Acinetobacter* genomes *A. baumannii* 17978 (NCBI accession no. NC_009085.1) and *A. baylyi ADP1* (NCBI accession no. NC_005966.1) contain regions homologous to the *bap* locus in *A. baumannii* 307-0294. The rulers indicate the size (*A. baumannii* 307-0294) and genomic coordinates (*A. baumannii* 17978 and *A. baylyi* ADP1) of the fragments. The percent nucleotide identity is shown for the regions delimited by dashed lines. Predicted open reading frames in *A. baumannii* 307-0294 are annotated with the identifier of the homologous open reading frame in *A. baumannii* 17978 (prefix A1S_, except for AS1_3829), and those in *A. baylyi* ADP1 are annotated with the gene symbol when available and the serially numbered identifiers (prefix ACIAD) otherwise. Note that the rulers for the two *A. baumannii* 17978 fragments are not continuous and not even in the same direction: the fragments in the assembled genome are in opposition relative to the arrangement in *A. baumannii* 307-0294 and *A. baylyi* ADP1 and are separated by over 30 kb of intervening genomic DNA that is not similar to *bap*.

Each of the peptides identified by nanoLC-MS/MS (Table 3) is found within the translated predicted *bap* open reading frame. As mentioned above, BLASTP analysis of the predicted amino acid sequence against the nonredundant protein database at the NCBI demonstrates regions of sequence similarity to the Baps from several staphylococcal species, including *S. hyicus* Bap (accession no. AAY28520.1), *S. aureus* Bap (accession no. AAK38834.2), and *S. epidermidis* Bap (accession no. AAY28519.1).

A. baumannii bap1302::EZ-Tn*5* was selected from the nine available *bap*-insertional mutants because it contains a transposon insertion closest to the predicted *bap* start codon, preventing translation of the 95% of the gene that is 3′ to the insertion site. Whole-cell lysates of wild-type *A. baumannii* 307-0294 and *bap1302*::EZ-Tn*5* were analyzed by SDS-PAGE (Fig. 1A), demonstrating that the wild type contained a high-molecular-weight band (Fig. 1C, lane 1) that was missing in the mutant (lane 2). In addition, Western blot analysis confirmed that whole-cell lysate and outer membrane proteins of *A. baumannii bap1302*::EZ-Tn*5* lost reactivity to MAb 6E3 (Fig. 1B, lanes 2 and 4).

Characterization of *bap* transcription by RT-PCR. *A. baumannii bap1302*::EZ-Tn*5* was further analyzed to determine whether the transposon insertion resulted in downstream polar effects. We performed RT-PCR to determine whether *bap* and A1S_2695 were cotranscribed (see Fig. 4 for the genetic arrangement of the *bap* locus in *A. baumannii* 307-0294). Oligonucleotide primers (Table 1) were designed to amplify regions of *bap* up- and downstream of the transposon insertion site; primers were also designed for an internal region of A1S_2695 and for a region spanning the intergenic region linking *bap* to A1S_2695. The results in Fig. 5 demonstrate that *bap* and A1S_2695 are not cotranscribed: therefore, disruption of *bap* does not appear to exert polar effects on neighboring genes.

Structural features of Bap. Bap is composed primarily of multiple copies of seven repeat units (designated A to G; see

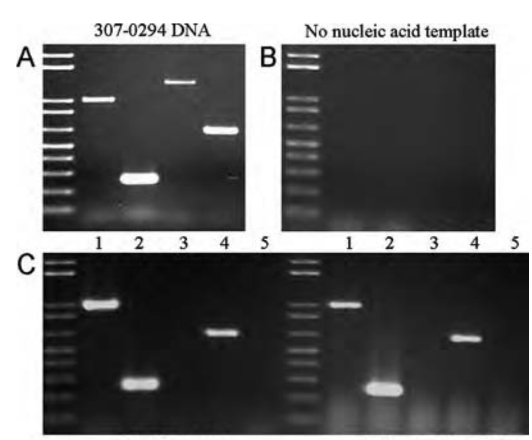

FIG. 5. RT-PCR and agarose gel electrophoresis demonstrates that *bap* and A1S_2695 are not cotranscribed and that transcription of A1S_2695 is not disrupted in *A. baumannii bap1302*::EZ-Tn*5*. (A) Each primer set amplifies a product from chromosomal DNA template. Pr1160-1330 (lane 3), however, fails to amplify a product from RNA template (C), indicating that *bap* and A1S_2695 are not present on the same fragment of RNA. The samples in lane 5 included RNA template but were not subject to the RT step, as a control for DNA contamination, and hence were not applicable to the reaction sets containing either chromosomal DNA (A) or no nucleic acid template (B). Primers (Table 1) were designed to target the indicated regions: lane 1, 5′ *bap*; lane 2, 3′ *bap*; lane 3, 3′ *bap*-A1S_2695; lane 4, A1S_2695; and lane 5, 3′ *bap* (no template control).

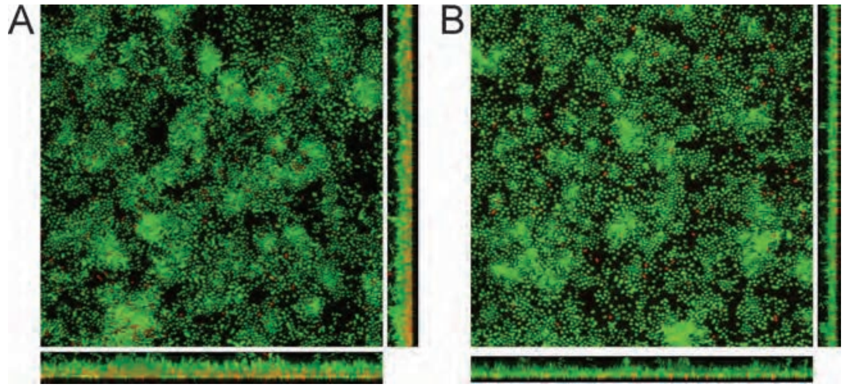

FIG. 6. CLSM images of biofilms formed by *A. baumannii* 307-0294 (A) and *bap1302*::EZ-Tn*5* (B) clearly demonstrate the decreased thickness achieved by the mutant after 48 h in static culture. Biofilms were grown in 35 mm glass-bottom petri dishes for 48 h and stained with the LIVE/DEAD *Bac*Light bacterial viability kit, which stains live cells green with SYTO-9 and dead cells red with propidium iodide. The images show the average intensity projections through the confocal image stack, with the maximum intensity *x-z* and *y-z* projections shown along the bottom and side of each image. Images were produced in ImageJ.

Fig. 3A); there are 5 copies of repeat module A (54 to 99% amino acid sequence identity between copies), 22 copies of module B (72 to 100%), 21 copies of module C (73 to 100%), 28 copies of module D (78 to 100%), 2 copies of module E (62%), 2 copies of module F (67%), and 3 copies of module G (36 to 51%). For the majority of the sequence (amino acids 188 to 7499, out of 8,621), the repeat modules are directly in tandem, with no additional amino acids between consecutive repeats.

Analysis of the primary structure reveals the absence of Cys and an abundance of Thr (1,389 residues; 16% of the total), Ala (1,176 residues; 14% of the total), and Val (1,109 residues; 13% of the total). In addition, Bap has a remarkably low isoelectric point (pI), estimated to be 2.9, placing it among the most acidic bacterial proteins thus far described. The low pI may explain why the presence of SDS during electrophoresis has no apparent effect (data not shown), since very acidic proteins do not bind SDS under standard SDS-PAGE conditions (18), and is a reflection of an 11:1 imbalance in the number of acidic and basic amino acids: there are 1,168 acidic (984 Asp + 184 Glu) and 105 basic residues (60 His + 34 Lys + 11 Arg). Since trypsin cleaves exclusively after Lys and Arg (33), the paucity of these amino acids explains why only a few peptides were sequenced after tryptic digestion of Bap (Table 3).

BLASTP analysis of the "D" repeat region, which in aggregate contains 35% of the total amino acids, identifies similarities to a putative outer membrane adhesin from *Shewanella* sp. strain ANA-3 (accession number YP_868031), whereas the similarity to the staphylococcal Baps is limited to the "A-C" repeats, which contain 48% of the total amino acids. CLUSTAL alignment of repeat units A to D from $\mathrm{Bap}_{A.\ baumannii}$ and C from $\mathrm{Bap}_{S.\ aureus}$ (Fig. 3B) indicated that sequence similarities are limited to small stretches of amino acids (particularly in positions 2 to 6 [consensus DTTAP] and 95 to 103 [consensus VTATDAAGN]), which are separated from each other by longer stretches with more divergent sequence.

Comparison of the *bap* locus in *A. baumannii* 307-0294 with homologous loci in other *Acinetobacter* species. There are two publicly available *Acinetobacter* genomes: *A. baylyi* ADP1 and *A. baumannii* 17978, and we have identified regions homologous to the *A. baumannii* 307-0294 *bap* locus in each (Fig. 4). *A. baumannii* 307-0294 *bap* is flanked by *nhaP* (A1S_2723) upstream, and a putative glucosyltransferase (A1S_2695) downstream, with all three genes in the same orientation. *A. baylyi* ADP1 contains a single contiguous genomic region with a 5-kb putative hemagglutinin in place of the 26-kb *bap* open reading frame. The published genome for *A. baumannii* 17978 (40), surprisingly, does not contain a single homologous locus but rather two loci separated by 30 kb of unrelated sequence and oriented in opposition relative to the organization in *A. baylyi* ADP1 and *A. baumannii* 307-0294. The nonrepetitive 5′ and 3′ ends of *bap* are annotated as two distinct putative open reading frames in *A. baumannii* 17978, and the internal repeats are not found in the assembled genome. *A. baumannii* 17978 and *A. baylyi* ADP1 are not reactive to MAb 6E3 (data not shown).

Disruption of *bap* diminishes biovolume and biofilm thickness. Biofilms formed by *A. baumannii* 307-0294 and *bap1302*::EZ-Tn*5* after 48 h of static culture in FAB-citrate supplemented with 0.05% (wt/vol) Casamino Acids were stained with a LIVE/DEAD stain and imaged by CLSM (Fig. 6). Upon examination of these confocal micrographs, the biofilm formed by wild-type bacteria was noticeably thicker than that formed by mutant bacteria. In order to more carefully analyze this difference, we designed an experiment that allowed us to quantify the dynamics of biofilm development over time.

Static cultures of GFP-expressing *A. baumannii* 307-0294 and *bap1302*::EZ-Tn*5* were imaged every hour for 14 h to visualize and quantify biofilm development on glass coverslips. The resultant image stacks were analyzed by using the ISA-3D software program (2) and, of the 20 calculated parameters, 2 followed significantly different trends over time for the mutant compared to wild-type biofilms: mean biofilm thickness and total biovolume (Fig. 7). Specifically, biofilms formed by wild-type and mutant bacteria are distinguishable after 6 h, when the mutant reaches a biofilm thickness plateau that is less than half that ultimately achieved by wild-type bacteria. The mutant also steadily loses biovolume for the remainder of the experiment, in contrast to the stable biovolume maintained by wild-

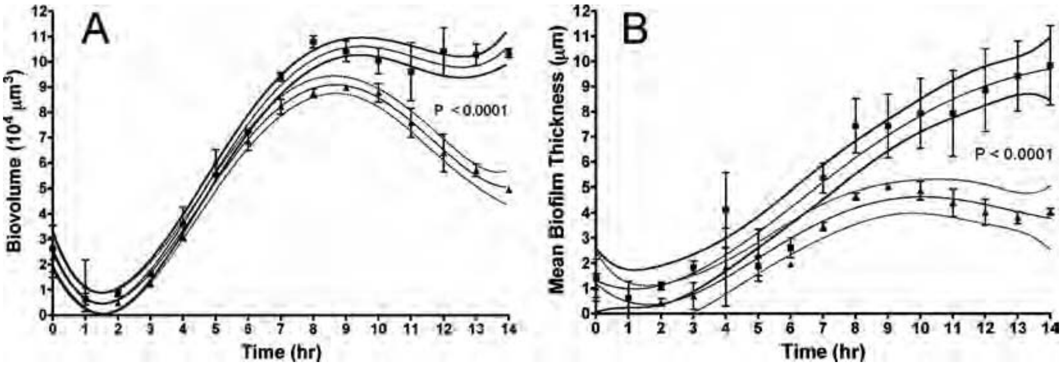

FIG. 7. Comparison of biovolume (A) and mean biofilm thickness (B) achieved by *A. baumannii* 307-0294 (■) and *A. baumannii bap1302*::EZ-Tn*5* (▲) during static culture. The data points are the means ± the standard deviations for two separate high-power fields of view, representing a total slide surface area of 10^5 μm^2 per sample. The best-fit nonlinear regression curve is shown as a thin trend line with 95% confidence bands. Because the biofilms formed by wild-type and mutant bacteria cannot be described with the same curve ($P < 0.0001$), we conclude that the biofilms differ significantly with respect to biovolume and mean biofilm thickness development over time.

type bacteria. It is important to note that these differences are specific to biofilm formation, since these strains are indistinguishable by growth curve analysis in shaking broth cultures in the same FAB-citrate media used in the static culture biofilm experiments (data not shown).

Semiquantitative analysis of biofilms grown on polystyrene pins in 96-well plates is consistent with the results obtained from the confocal experiments: the biofilm formed by the *bap1302*::EZ-Tn*5* retains less crystal violet stain, indicative of less accumulated biovolume, compared to the wild type (data not shown).

DISCUSSION

A. baumannii is an opportunistic pathogen that is particularly successful at colonizing and persisting in the hospital environment, able to resist desiccation (19, 20, 53) and survive on inanimate surfaces for months (22). It is among the most common causes of device-related nosocomial infection (13, 43, 52), which result when the organism is able to resist physical and chemical disinfection, often by forming a biofilm (7, 27, 34). We chose to study biofilm formation by *A. baumannii* in order to understand how this pathogen persists in the hospital environment to cause outbreaks worldwide (51).

Baps were first characterized in *S. aureus* (11) and have since been identified in a number of other gram-positive and gram–negative pathogenic bacteria (reviewed in references 24 and 25). They are defined by shared structural and functional characteristics and are essentially high-molecular-weight, repetitive surface proteins involved in biofilm formation (24). The prototypical Bap from *S. aureus* is involved in the primary attachment step of biofilm formation, as well as in promoting intercellular adhesion and biofilm maturation (11); other Baps are involved in the various stages of biofilm formation and in adhesion to eukaryotic host cells (25).

We have identified a protein produced by *A. baumannii* 307-0294 that satisfies all of the criteria to be included in the Bap family: it is high molecular weight, with a predicted molecular mass of 854 kDa; it is repetitive, composed of multiple copies of seven repeat modules (A to G); it is exposed on the surface; and it is involved in biofilm formation and development.

There are several conceptual, sequential stages in bacterial biofilm formation (reviewed in reference 41): (i) reversible primary attachment of individual cells to a surface, (ii) progression to irreversible attachment mediated by extracellular polysaccharide, (iii) early development of biofilm architecture, (iv) maturation of biofilm architecture, and (v) dispersal of single cells from the biofilm. $\text{Bap}_{A.\ baumannii}$ does not appear to be involved in the primary attachment of cells to glass or polystyrene, in contrast to $\text{Bap}_{S.\ aureus}$ (11). Our data suggest that $\text{Bap}_{A.\ baumannii}$ appears to be involved in maintaining the mature biofilm architecture (steps 3 and 4), since biofilms formed by the mutant are neither as thick nor as voluminous as those formed by the wild type. There are at least three potential Bap-mediated interactions to explore in future studies: (i) $\text{Bap}_{A.\ baumannii}$ may mediate direct intercellular adhesion from one bacterium to a surface receptor on a neighboring bacterium, (ii) this may be an example of autoadhesion between Bap molecules on adjacent bacteria, or (iii) cells may be linked indirectly via shared interactions with some extracellular biofilm matrix component. While these are all logical hypotheses, further studies are needed in order to carefully determine the actual function of $\text{Bap}_{A.\ baumannii}$.

Bap is a remarkable protein: it contains 8,621 amino acids, making it one of the largest bacterial proteins yet described; it has a predicted pI of 2.9, making it one of the most acidic bacterial proteins; and it is composed of tandemly arranged repeat modules. The protein is divided almost equally in two parts: the first contains modules A to C, alternating one after the other; the second contains 28 direct tandem repeats of module D. Each repeat unit A-D appears to be related to the HYR domain (4) (PFAM accession no. PF02494) based on the conserved amino acids DTTAP and VTATDAAGN (Fig. 3), although the HYR seed alignment contains two conserved cysteines that are conspicuously absent from Bap. HYR was first identified in eukaryotic proteins involved in cellular adhesion and is found in a number of large repetitive prokaryotic proteins as well, including several adhesins (4). Three-dimensional structure prediction using the PHYRE server (http:

//www.sbg.bio.ic.ac.uk/phyre/) suggests that each module A-D folds into a seven-stranded β-sandwich similar to proteins within the immunoglobulin-like fold superfamily (PFAM accession no. CL0159, which includes the HYR domain as a family member). This suggests Bap adopts a "beaded-filament" tertiary structure and that each module might redundantly contribute to the overall function. Other bacterial proteins that adopt a tertiary structure similar to that predicted for Bap include invasin from *Yersinia pseudotuberculosis* and intimin, FimH, and PapG from enteropathogenic *E. coli* (32). The latter two proteins are actually individual subunits that resemble an isolated repeat unit of Bap and are assembled into filamentous pili that recapitulate in quaternary structure what Bap is predicted to accomplish in tertiary structure. The pattern of sequence similarity to $\text{Bap}_{S.\ aureus}$ (Fig. 3B), with short stretches of highly conserved residues separated by longer regions of divergence, suggests that the conserved regions might function to maintain a common structural motif, while the divergent regions might confer unique functionality to the respective proteins. In this light, it is interesting that $\text{Bap}_{A.\ baumannii}$ contains four distinct modules (A to D), each based on the same HYR motif, whereas $\text{Bap}_{S.\ aureus}$ seems to contain multiple copies of only a single repeat type.

Using a previously reported typing scheme (15), *A. baumannii* 307-0294 is a sequence type ST15 (data not shown). ST15 is phylogenetically linked with European hospital clone I (15, 35), which is associated with epidemic behavior and multidrug resistance (31, 35, 47). Although at least 39 sequence types of *A. baumannii* were distinguished among the military outbreak strains (15), four of them (ST11, ST14, ST16, and ST10) accounted for over half of the isolates, suggesting either that the outbreak was clonal in nature or that particular sequence types of *A. baumannii* are more likely to cause human infection. It is intriguing that MAb 6E3 recognizes 14 of 15 (93%) of the representatives from these four sequence types compared to 17 of 61 (28%) of the representatives from the other 35 sequence types (Table 2), although the significance of this observation is not clear. For example, we do not know whether the strains that failed to react to MAb 6E3 did not express a Bap homologue, or whether they expressed a variant that simply lacked the recognized epitope. For these reasons, and because we do not have access to disease severity information for the patients involved in the military outbreak, we are unfortunately unable to comment on the contribution of Bap to disease severity. Nevertheless, MAb 6E3 will be a useful tool for future studies designed to answer such questions.

In conclusion, we have identified a novel *A. baumannii* protein, Bap, expressed on the surface of these bacteria that is involved in biofilm formation in static culture. Bap has a predicted structure similar to bacterial adhesins within the immunoglobulin-like fold superfamily and may function as an intercellular adhesin in such a way that supports the mature biofilm structure. Although more studies are needed to test this hypothesis, a better understanding of the contribution of this Bap to *A. baumannii* biofilm formation and maturation may help to explain why *Acinetobacter* remains a common cause of nosocomially acquired device-related infection.

ACKNOWLEDGMENTS

David Craft and Paul Scott and the Walter Reed Army Medical Center generously provided a panel of 98 *Acinetobacter* strains recently isolated from infected military personnel serving in Iraq and Afghanistan (15). Thomas Russo provided *A. baumannii* 307-0294, originally isolated from the bloodstream of a patient in 1994. Luis Actis provided plasmid pMU125, an *E. coli-Acinetobacter* shuttle plasmid able to confer GFP expression in *Acinetobacter*. Haluk Beyenal generously provided the Image Structure Analyzer-3D software program, and Wade Sigurdson acquired the confocal microscopy images. Steven Gill provided a helpful critique of the manuscript.

Funding for this study was provided by U.S. Army Medical Research Acquisition Activity under contract W81XWH-05-1-0627.

REFERENCES

1. **Bergogne-Berezin, E., and K. J. Towner.** 1996. *Acinetobacter* spp. as nosocomial pathogens: microbiological, clinical, and epidemiological features. Clin. Microbiol. Rev. **9:**148–165.
2. **Beyenal, H., C. Donovan, Z. Lewandowski, and G. Harkin.** 2004. Three-dimensional biofilm structure quantification. J. Microbiol. Methods **59:**395–413.
3. **Bonomo, R. A., and D. Szabo.** 2006. Mechanisms of multidrug resistance in *Acinetobacter* species and *Pseudomonas aeruginosa*. Clin. Infect. Dis. **43**(Suppl. 2)**:**S49–S56.
4. **Callebaut, I., D. Gilges, I. Vigon, and J. P. Mornon.** 2000. HYR, an extracellular module involved in cellular adhesion and related to the immunoglobulin-like fold. Protein Sci. **9:**1382–1390.
5. **Campagnari, A. A., T. F. Ducey, and C. A. Rebmann.** 1996. Outer membrane protein B1, an iron-repressible protein conserved in the outer membrane of *Moraxella* (*Branhamella*) *catarrhalis*, binds human transferrin. Infect. Immun. **64:**3920–3924.
6. **Campagnari, A. A., K. L. Shanks, and D. W. Dyer.** 1994. Growth of *Moraxella catarrhalis* with human transferrin and lactoferrin: expression of iron-repressible proteins without siderophore production. Infect. Immun. **62:**4909–4914.
7. **Cappelli, G., L. Sereni, M. G. Scialoja, M. Morselli, S. Perrone, A. Ciuffreda, M. Bellesia, P. Inguaggiato, A. Albertazzi, and C. Tetta.** 2003. Effects of biofilm formation on haemodialysis monitor disinfection. Nephrol. Dial. Transplant. **18:**2105–2111.
8. **Chang, H. C., Y. F. Wei, L. Dijkshoorn, M. Vaneechoutte, C. T. Tang, and T. C. Chang.** 2005. Species-level identification of isolates of the *Acinetobacter calcoaceticus-Acinetobacter baumannii* complex by sequence analysis of the 16S-23S rRNA gene spacer region. J. Clin. Microbiol. **43:**1632–1639.
9. **Choi, C. H., E. Y. Lee, Y. C. Lee, T. I. Park, H. J. Kim, S. H. Hyun, S. A. Kim, S. K. Lee, and J. C. Lee.** 2005. Outer membrane protein 38 of *Acinetobacter baumannii* localizes to the mitochondria and induces apoptosis of epithelial cells. Cell Microbiol. **7:**1127–1138.
10. **Costerton, J. W., P. S. Stewart, and E. P. Greenberg.** 1999. Bacterial biofilms: a common cause of persistent infections. Science **284:**1318–1322.
11. **Cucarella, C., C. Solano, J. Valle, B. Amorena, I. Lasa, and J. R. Penades.** 2001. Bap, a *Staphylococcus aureus* surface protein involved in biofilm formation. J. Bacteriol. **183:**2888–2896.
12. **Davis, K. A., K. A. Moran, C. K. McAllister, and P. J. Gray.** 2005. Multidrug-resistant *Acinetobacter* extremity infections in soldiers. Emerg. Infect. Dis. **11:**1218–1224.
13. **Dima, S., E. I. Kritsotakis, M. Roumbelaki, S. Metalidis, A. Karabinis, N. Maguina, F. Klouva, S. Levidiotou, E. Zakynthinos, J. Kioumis, and A. Gikas.** 2007. Device-associated nosocomial infection rates in intensive care units in Greece. Infect. Control Hosp. Epidemiol. **28:**602–605.
14. **Dorsey, C. W., A. P. Tomaras, and L. A. Actis.** 2002. Genetic and phenotypic analysis of *Acinetobacter baumannii* insertion derivatives generated with a transposome system. Appl. Environ. Microbiol. **68:**6353–6360.
15. **Ecker, J. A., C. Massire, T. A. Hall, R. Ranken, T. T. Pennella, C. Agasino Ivy, L. B. Blyn, S. A. Hofstadler, T. P. Endy, P. T. Scott, L. Lindler, T. Hamilton, C. Gaddy, K. Snow, M. Pe, J. Fishbain, D. Craft, G. Deye, S. Riddell, E. Milstrey, B. Petruccelli, S. Brisse, V. Harpin, A. Schink, D. J. Ecker, R. Sampath, and M. W. Eshoo.** 2006. Identification of *Acinetobacter* species and genotyping of *Acinetobacter baumannii* by multilocus PCR and mass spectrometry. J. Clin. Microbiol. **44:**2921–2932.
16. **Falagas, M. E., I. A. Bliziotis, and I. I. Siempos.** 2006. Attributable mortality of *Acinetobacter baumannii* infections in critically ill patients: a systematic review of matched cohort and case-control studies. Crit. Care **10:**R48.
17. **Falagas, M. E., and E. A. Karveli.** 2007. The changing global epidemiology of *Acinetobacter baumannii* infections: a development with major public health implications. Clin. Microbiol. Infect. **13:**117–119.
18. **Garcia-Ortega, L., V. De los Rios, A. Martinez-Ruiz, M. Onaderra, J. Lacadena, A. Martinez del Pozo, and J. G. Gavilanes.** 2005. Anomalous electrophoretic behavior of a very acidic protein: ribonuclease U2. Electrophoresis **26:**3407–3413.
19. **Jawad, A., J. Heritage, A. M. Snelling, D. M. Gascoyne-Binzi, and P. M.**

Hawkey. 1996. Influence of relative humidity and suspending menstrua on survival of *Acinetobacter* spp. on dry surfaces. J. Clin. Microbiol. **34:**2881–2887.
20. **Jawad, A., H. Seifert, A. M. Snelling, J. Heritage, and P. M. Hawkey.** 1998. Survival of *Acinetobacter baumannii* on dry surfaces: comparison of outbreak and sporadic isolates. J. Clin. Microbiol. **36:**1938–1941.
21. **Korber, D. R., J. R. Lawrence, M. J. Hendry, and D. E. Caldwell.** 1993. Analysis of spatial variability within Mot^+ and Mot^- *Pseudomonas fluorescens* biofilms using representative elements. Biofouling **20:**334–358.
22. **Kramer, A., I. Schwebke, and G. Kampf.** 2006. How long do nosocomial pathogens persist on inanimate surfaces? A systematic review. BMC Infect. Dis. **6:**130.
23. **Lasa, I.** 2006. Towards the identification of the common features of bacterial biofilm development. Int. Microbiol. **9:**21–28.
24. **Lasa, I., and J. R. Penades.** 2006. Bap: a family of surface proteins involved in biofilm formation. Res. Microbiol. **157:**99–107.
25. **Latasa, C., C. Solano, J. R. Penades, and I. Lasa.** 2006. Biofilm-associated proteins. C. R. Biol. **329:**849–857.
26. **Lee, J. S., J. C. Lee, C. M. Lee, I. D. Jung, Y. I. Jeong, E. Y. Seong, H. Y. Chung, and Y. M. Park.** 2007. Outer membrane protein A of *Acinetobacter baumannii* induces differentiation of $CD4^+$ T cells toward a Th1 polarizing phenotype through the activation of dendritic cells. Biochem. Pharmacol. **74:**86–97.
27. **Loukili, N. H., B. Granbastien, K. Faure, B. Guery, and G. Beaucaire.** 2006. Effect of different stabilized preparations of peracetic acid on biofilm. J. Hosp. Infect. **63:**70–72.
28. **Mampel, J., T. Spirig, S. S. Weber, J. A. Haagensen, S. Molin, and H. Hilbi.** 2006. Planktonic replication is essential for biofilm formation by Legionella pneumophila in a complex medium under static and dynamic flow conditions. Appl. Environ. Microbiol. **72:**2885–2895.
29. **Merod, R. T., J. E. Warren, H. McCaslin, and S. Wuertz.** 2007. Toward automated analysis of biofilm architecture: bias caused by extraneous confocal laser scanning microscopy images. Appl. Environ. Microbiol. **73:**4922–4930.
30. **Navon-Venezia, S., A. Leavitt, and Y. Carmeli.** 2007. High tigecycline resistance in multidrug-resistant *Acinetobacter baumannii*. J. Antimicrob. Chemother. **59:**772–774.
31. **Nemec, A., L. Dijkshoorn, and T. J. van der Reijden.** 2004. Long-term predominance of two pan-European clones among multi-resistant *Acinetobacter baumannii* strains in the Czech Republic. J. Med. Microbiol. **53:**147–153.
32. **Niemann, H. H., W. D. Schubert, and D. W. Heinz.** 2004. Adhesins and invasins of pathogenic bacteria: a structural view. Microbes Infect. **6:**101–112.
33. **Olsen, J. V., S. E. Ong, and M. Mann.** 2004. Trypsin cleaves exclusively C-terminal to arginine and lysine residues. Mol. Cell Proteomics **3:**608–614.
34. **Pajkos, A., K. Vickery, and Y. Cossart.** 2004. Is biofilm accumulation on endoscope tubing a contributor to the failure of cleaning and decontamination? J. Hosp. Infect. **58:**224–229.
35. **Pantophlet, R., A. Nemec, L. Brade, H. Brade, and L. Dijkshoorn.** 2001. O-antigen diversity among *Acinetobacter baumannii* strains from the Czech Republic and Northwestern Europe, as determined by lipopolysaccharide-specific monoclonal antibodies. J. Clin. Microbiol. **39:**2576–2580.
36. **Russo, T. A., J. E. Guenther, S. Wenderoth, and M. M. Frank.** 1993. Generation of isogenic K54 capsule-deficient *Escherichia coli* strains through TnphoA-mediated gene disruption. Mol. Microbiol. **9:**357–364.
37. **Sambrook, J., and D. W. Russell.** 2001. Molecular cloning: a laboratory manual, 3rd ed. Cold Spring Harbor Laboratory Press, Cold Spring Harbor, NY.
38. **Scott, P. T., K. Petersen, J. Fishbain, D. W. Craft, A. J. Ewell, K. Moran, D. C. Hack, G. A. Deye, S. Riddell, G. Christopher, J. D. Mancuso, B. P. Petrucelli, T. Endy, L. Lindler, K. Davis, E. G. Milstrey, L. Brosch, J. Pool, C. L. Blankenship, C. J. Witt, J. L. Malone, D. N. Tornberg, A. Srinivasan, et al.** 2004. *Acinetobacter baumannii* infections among patients at military medical facilities treating injured U.S. service members, 2002–2004. Morb. Mortal. Wkly. Rep. **53:**1063–1066.
39. **Smith, M. G., S. G. Des Etages, and M. Snyder.** 2004. Microbial synergy via an ethanol-triggered pathway. Mol. Cell. Biol. **24:**3874–3884.
40. **Smith, M. G., T. A. Gianoulis, S. Pukatzki, J. J. Mekalanos, L. N. Ornston, M. Gerstein, and M. Snyder.** 2007. New insights into *Acinetobacter baumannii* pathogenesis revealed by high-density pyrosequencing and transposon mutagenesis. Genes Dev. **21:**601–614.
41. **Stoodley, P., K. Sauer, D. G. Davies, and J. W. Costerton.** 2002. Biofilms as complex differentiated communities. Annu. Rev. Microbiol. **56:**187–209.
42. **Talbot, G. H., J. Bradley, J. E. Edwards, Jr., D. Gilbert, M. Scheld, and J. G. Bartlett.** 2006. Bad bugs need drugs: an update on the development pipeline from the Antimicrobial Availability Task Force of the Infectious Diseases Society of America. Clin. Infect. Dis. **42:**657–668.
43. **Thongpiyapoom, S., M. N. Narong, N. Suwalak, S. Jamulitrat, P. Intaraksa, J. Boonrat, N. Kasatpibal, and A. Unahalekhaka.** 2004. Device-associated infections and patterns of antimicrobial resistance in a medical-surgical intensive care unit in a university hospital in Thailand. J. Med. Assoc. Thai. **87:**819–824.
44. **Tomaras, A. P., C. W. Dorsey, R. E. Edelmann, and L. A. Actis.** 2003. Attachment to and biofilm formation on abiotic surfaces by *Acinetobacter baumannii*: involvement of a novel chaperone-usher pili assembly system. Microbiology **149:**3473–3484.
45. **Tsakris, A., A. Ikonomidis, S. Pournaras, N. Spanakis, and A. Markogiannakis.** 2006. Carriage of OXA-58 but not of OXA-51 beta-lactamase gene correlates with carbapenem resistance in *Acinetobacter baumannii*. J. Antimicrob. Chemother. **58:**1097–1099.
46. **van den Broek, P. J., J. Arends, A. T. Bernards, E. De Brauwer, E. M. Mascini, T. J. van der Reijden, L. Spanjaard, E. A. Thewessen, A. van der Zee, J. H. van Zeijl, and L. Dijkshoorn.** 2006. Epidemiology of multiple *Acinetobacter* outbreaks in The Netherlands during the period 1999–2001. Clin. Microbiol. Infect. **12:**837–843.
47. **van Dessel, H., L. Dijkshoorn, T. van der Reijden, N. Bakker, A. Paauw, P. van den Broek, J. Verhoef, and S. Brisse.** 2004. Identification of a new geographically widespread multiresistant *Acinetobacter baumannii* clone from European hospitals. Res. Microbiol. **155:**105–112.
48. **Vidal, R., M. Dominguez, H. Urrutia, H. Bello, A. Garcia, G. Gonzalez, and R. Zemelman.** 1997. Effect of imipenem and sulbactam on sessile cells of *Acinetobacter baumannii* growing in biofilm. Microbios **91:**79–87.
49. **Vidal, R., M. Dominguez, H. Urrutia, H. Bello, G. Gonzalez, A. Garcia, and R. Zemelman.** 1996. Biofilm formation by *Acinetobacter baumannii*. Microbios **86:**49–58.
50. **Vila, J., S. Marti, and J. Sanchez-Cespedes.** 2007. Porins, efflux pumps, and multidrug resistance in *Acinetobacter baumannii*. J. Antimicrob. Chemother. **59:**1210–1215.
51. **Villegas, M. V., and A. I. Hartstein.** 2003. *Acinetobacter* outbreaks, 1977–2000. Infect. Control Hosp. Epidemiol. **24:**284–295.
52. **Wang, S. S., N. K. Chou, R. B. Hsu, W. J. Ko, H. Y. Yu, Y. S. Chen, S. C. Huang, N. H. Chi, C. S. Liau, and Y. T. Lee.** 2004. Heart transplantation in the patient under ventricular assist complicated with device-related infection. Transplant Proc. **36:**2377–2379.
53. **Wendt, C., B. Dietze, E. Dietz, and H. Ruden.** 1997. Survival of *Acinetobacter baumannii* on dry surfaces. J. Clin. Microbiol. **35:**1394–1397.

JOURNAL OF BACTERIOLOGY, Dec. 2008, p. 8053–8064 Vol. 190, No. 24
0021-9193/08/$08.00+0 doi:10.1128/JB.00834-08

Comparative Genome Sequence Analysis of Multidrug-Resistant *Acinetobacter baumannii*▽†

Mark D. Adams,[1]* Karrie Goglin,[1]‡ Neil Molyneaux,[1] Kristine M. Hujer,[2] Heather Lavender,[1] Jennifer J. Jamison,[3] Ian J. MacDonald,[3] Kristienna M. Martin,[3] Thomas Russo,[3,4,5,7] Anthony A. Campagnari,[3,7] Andrea M. Hujer,[2] Robert A. Bonomo,[2,6] and Steven R. Gill[3,8]

Department of Genetics[1] and Departments of Pharmacology and Molecular Biology and Microbiology,[6] Case Western Reserve University School of Medicine, Cleveland, Ohio; Louis Stokes Cleveland Department of Veterans Affairs Medical Center, Cleveland, Ohio[2]; and New York State Center of Excellence in Bioinformatics and Life Sciences,[3] Veterans Administration Western New York Healthcare System,[4] and Department of Medicine,[5] Department of Microbiology & Immunology,[7] and Department of Oral Biology,[8] The State University of New York at Buffalo, Buffalo, New York

Received 16 June 2008/Accepted 6 October 2008

The recent emergence of multidrug resistance (MDR) in *Acinetobacter baumannii* has raised concern in health care settings worldwide. In order to understand the repertoire of resistance determinants and their organization and origins, we compared the genome sequences of three MDR and three drug-susceptible *A. baumannii* isolates. The entire MDR phenotype can be explained by the acquisition of discrete resistance determinants distributed throughout the genome. A comparison of closely related MDR and drug-susceptible isolates suggests that drug efflux may be a less significant contributor to resistance to certain classes of antibiotics than inactivation enzymes are. A resistance island with a variable composition of resistance determinants interspersed with transposons, integrons, and other mobile genetic elements is a significant but not universal contributor to the MDR phenotype. Four hundred seventy-five genes are shared among all six clinical isolates but absent from the related environmental species *Acinetobacter baylyi* ADP1. These genes are enriched for transcription factors and transporters and suggest physiological features of *A. baumannii* that are related to adaptation for growth in association with humans.

Among gram-negative pathogens that are reported as "multidrug resistant" (MDR), *Acinetobacter baumannii* is rapidly becoming a focus of significant attention (1, 10, 35, 56). *A. baumannii*, a pleomorphic, gram-negative coccobacillus, is currently recognized by the Infectious Diseases Society of America as one of the most important pathogens threatening our health care delivery system (48). Global surveillance programs conducted over the last decade show an unparalleled increase in resistance rates among clinical *Acinetobacter* isolates (26). *Acinetobacter* spp. are now the third leading cause of respiratory tract infections among patients in intensive care units, and *A. baumannii* is responsible for up to 10% of hospital-acquired infections (26). These nosocomial infections are typically found in immunocompromised patients and are associated with an increased length of stay and excess morbidity (13, 25, 38, 47). In intensive care units, up to 30% of *A. baumannii* clinical isolates are resistant to at least three classes of antibiotics (26).

A significant nosocomial outbreak of MDR *A. baumannii* in the United States occurred in the period 2003–2005 in a military treatment facility caring for injured service personnel and civilians (Walter Reed Army Medical Center [WRAMC]) (19, 40). Molecular typing of isolates from this outbreak revealed eight major clone types, and about 60% of the isolates were related to three pan-European types (5, 52), suggesting multiple independent origins (40). Examination of specific resistance determinants in the WRAMC isolates demonstrated considerable variability in the composition of resistance genes within each clone type and similar patterns across certain divergent clone types. Thus, genetic relatedness was a poor predictor of the MDR phenotype. This led to the hypothesis that there exist multiple independent genetic mechanisms leading to MDR in *A. baumannii*. A large cluster of antibiotic resistance genes and mobile genetic elements is present as an 86-kb "resistance island" (RI) in the *A. baumannii* AYE genome (15). The RI is not present in the genomes of the drug-susceptible *A. baumannii* isolates ATCC 17978 (43) and SDF (51), suggesting that it is an important contributor to the MDR phenotype.

In an effort to understand the significance of the RI and the integration of genetic factors that permit *A. baumannii* to successfully infect patients in multiple clinical settings, we undertook a whole-genome sequence analysis of six clinical isolates in comparison to a nonhuman *A. baumannii* isolate (SDF) and an environmental *Acinetobacter* strain, *Acinetobacter baylyi* ADP1. We compared three MDR isolates to three drug-susceptible isolates in order to explore common features of their evolution and the diversity of mechanisms by which resistance is demonstrated. Our goals were (i) to determine the repertoire and phylogeny of resistance determinants among recent clinical isolates, (ii) to see how these "successful" clinical iso-

* Corresponding author. Mailing address: Department of Genetics, Case Western Reserve University School of Medicine, 10900 Euclid Ave., Cleveland, OH 44106-4955. Phone: (216) 368-2791. Fax: (216) 368-3432. E-mail: mda13@case.edu.

† Supplemental material for this article may be found at http://jb.asm.org/.

‡ Present address: Scripps Healthcare, San Diego, CA.

▽ Published ahead of print on 17 October 2008.

TABLE 1. Selected genetic and phenotypic properties of *A. baumannii* genomes

Genome	Accession no.	Genome size (bp)	No. of genes	Source (reference)	Size of RI (kb)	Beta-lactamase gene(s)			Plasmid-carried beta-lactamase gene	Resistance gene(s)			*gyrA*/*parC* QRDR[a]
						Class A	Class C	Class D		Tetra-cycline	Chloram-phenicol	Trimetho-prim-sulfa	
AB0057	ABJM01000001	4,050,513	3,853	WRAMC	42 + 18	$bla_{\text{TEM-1}}$	Two copies of *ampC*	$bla_{\text{OXA-69}}$, $bla_{\text{OXA-23}}$		*tetA*	*cat*	Two copies of *sulI*, *dhfrX*	RR
AB307-0294	CP001172	3,760,981	3,458	Buffalo, NY			*ampC*	$bla_{\text{OXA-69}}$				*dhfrX*	RS
AYE	CU459141	3,936,291	3,607	France (51)	86	$bla_{\text{VEB-1}}$	*ampC*	$bla_{\text{OXA-69}}$, $bla_{\text{OXA-10}}$		*tetA*	*cat*, *cmlA*	Four copies of *sulI*, *dhfrX*, *dhfrI*	RR
AB900	ABXK00000000	3,913,289		WRAMC			*ampC*	$bla_{\text{OXA-51-like}}$				*dhfrX*	SS
ATCC 17978	CP000521	3,976,747	3,791	ATCC (43)			*ampC*	$bla_{\text{OXA-51}}$				*sulI*, *dhfrX*	SS
ACICU	CP000863	3,904,116	3,667	Rome, Italy (20)	17		*ampC*	$bla_{\text{OXA-66}}$, $bla_{\text{OXA-20}}$	Two copies of $bla_{\text{OXA-58}}$			*sulI*, *dhfrX*	RS
SDF	CU468230	3,421,954	2,913	Louse in France (51)				$bla_{\text{OXA-75}}$				*dhfrX*	SS
ADP1	CR543861	3,598,621	3,325	Soil (3)			*ampC*					*dhfrX*	

[a] RR, resistance-associated Ser83Leu mutation found in *gyrA* and Ser80Ile mutation found in *parC*; SS, susceptibility-associated alleles in both *gyrA* and *parC*; RS, resistance-associated mutation found only in *gyrA*.
[b] R, resistant. Numbers in bold indicate resistance, and numbers in italics indicate intermediate susceptibility. Resistance data were published previously for AYE (15, 36), SDF (14, 24), and ACICU (20).

lates differ from pathogenic and nonpathogenic strains/species already examined, (iii) to assess the function and purpose of the RI, and (iv) to evaluate the importance and impact of insertion sequences (IS) in the evolution of the resistance phenotype. Our results show that the RI is variable in composition and is only one contributor to the MDR phenotype. Based on closely matched MDR and drug-susceptible isolates, it appears that the MDR phenotype is largely due to the acquisition of a series of genes encoding drug-inactivating enzymes that are located on mobile genetic elements. Moreover, we identified a series of genes that may define the ability of *A. baumannii* to live in association with the human host and describe extensive diversity in genes that contribute to the lipopolysaccharide barrier.

MATERIALS AND METHODS

***A. baumannii* isolates.** The origins and certain genetic and phenotypic properties of the *A. baumannii* isolates studied here are presented in Table 1. *A. baumannii* ATCC 17978 was obtained from a case of fatal meningitis in 1951. Its antibiotic susceptibility profile has not previously been reported. *A. baumannii* ACICU was isolated from the cerebrospinal fluid of a patient in an intensive care unit in Rome, Italy, in 2005 (20). *A. baumannii* AYE was cultured from a patient with pneumonia and a urinary tract infection in France in 2001 (36). *A. baumannii* SDF was recovered from a human body louse (24). *A. baumannii* isolate AB307-0294 was obtained from the blood of a patient hospitalized in Buffalo, NY, in 1994. *A. baumannii* strain AB900 is a perineal isolate obtained in 2003 from an active duty military patient at WRAMC. *A. baumannii* AB0057 is an MDR bloodstream isolate collected in 2004 from a patient at WRAMC (19).

Resistance profiles. Resistance profiles reported for AYE, SDF, and ACICU are given in Table 1. Profiles for AB0057, AB307-0294, AB900, and ATCC 17978 were determined using Vitek2 and interpreted by Clinical Laboratory Standards Institute standards (7); these are also given in Table 1. Results for AB0057 are consistent with those reported previously (19).

Genome sequencing and annotation. AB307-0294 and AB900 were sequenced by pyrosequencing, and AB0057 was sequenced by a combination of pyrosequencing and traditional Sanger shotgun sequencing. Finished genome sequences with no gaps were completed for AB307-0294 and AB0057. Genome annotation was performed at The Institute for Genomic Research (TIGR) and later at the J. C. Venter Institute, Rockville, MD, and the Institute for Genome Sciences, Baltimore, MD, using the TIGR Annotation Engine (www.jcvi.org/ems/research/projects/annotation_service/overview/) followed by manual curation. Details of the sequencing, assembly, gap filling, and annotation methods are given in the supplemental material.

PCR. PCR was performed using the primers listed in Table S1 in the supplemental material and as described by Hujer et al. (19).

Nucleotide sequence accession numbers. The genome sequences of AB0057, AB307-0294, and AB900 have been deposited in the DDBJ/EMBL/GenBank databases under the accession numbers CP001182-3, CP001172, and ABXK00000000, respectively.

RESULTS

Genomes. We have completed the genome sequences of three recent clinical isolates, the MDR isolate AB0057 and two drug-susceptible isolates, AB307-0294 and AB900 (Table 1). Within the past year, genome sequences of four *A. baumannii* isolates have been published (20, 43, 51). Two of these, AYE and ACICU, are MDR, while ATCC 17978 is susceptible to many standard antibiotics. SDF was isolated from a human body louse, and its status as a human pathogen has not been determined.

Despite acquisition from geographically diverse regions, AYE, AB0057, and AB307-0294 are remarkably similar at the DNA level, averaging over 99.9% nucleotide sequence identity in orthologous regions (Fig. 1). The other isolates are each ~98% identical to one another. Interestingly, the >50-year-old isolate (ATCC 17978) and the louse isolate (SDF) are not more divergent than any of the other isolates at the sequence identity level (Fig. 1A). The relationship of isolates to one another based on shared gene content differs from the relationships inferred based on analysis of conserved genes, reflecting a considerable contribution of lateral gene transfer in the evolution of *A. baumannii* (Fig. 1B). SDF has a much smaller genome than the other *A. baumannii* isolates, presumably as a result of extensive IS-mediated deletion events (51). The extent of divergence in gene content in SDF and its questionable role as a human pathogen have prompted us to focus most of our analysis on comparisons among the six human clinical isolates.

Comparison between ADP1 and *A. baumannii* isolates. Based on reciprocal best BLAST matches, there are 2,688 genes shared among the six clinical isolates; these define the core

TABLE 1—*Continued*

Resistance gene(s)			MIC[b]												
AME gene	Ampicillin	Ampicillin-sulbactam	Piperacillin-tazobactam	Cefazolin	Ceftriaxone	Cefepime	Meropenem	Imipenem	Tigecycline	Aztreonam	Gentamicin	Amikacin	Tobramycin	Trimethoprim-sulfamethoxazole	Ciprofloxacin
aphA1, *aacC1*, *aadA1*	**≥32**	**≥32**	**≥128**	**≥64**	**≥64**	**≥64**	**≥16**	**≥16**	*4*	**≥64**	**≥16**	≤2	≤1	**160**	**≥4**
	≥32	≤2	≤4	**≥64**	*16*	8	≤0.25	≤1	≤0.5	**≥32**	*2*	≤2	≤1	≤20	*2*
aphA1, *aadB*, two copies of *aadA1*, *aacC1*	**R**		*8*			**512**	1	1		**≥512**	**R**	**R**	**R**	**R**	**R**
	16	≤2	≤4	**≥64**	*16*	2	≤0.25	≤1	≤0.5	**≥32**	≤1	≤2	≤1	≤20	≤0.25
	16	≤2	≤4	**≥64**	*16*	2	≤0.25	≤1	≤0.5	**≥64**	≤1	≤2	≤1	**160**	≤0.25
aac3	**R**		**R**			**R**	**R**	**R**		**R**		**R**	**R**	**R**	**R**
	ND														ND

genome of *A. baumannii*. These core genes encode basic functions involved in DNA replication, transcription, and translation, as well as many metabolic pathways (Fig. 2). Eighty-two percent of the core genes have orthologs in the environmental organism *A. baylyi* ADP1 (3, 53). For comparison, only 75% of the core genes are present in the louse isolate *A. baumannii* SDF.

The average percent identity between presumed orthologs in the *A. baumannii* isolates and ADP1 is 71%, but the range of identities among reciprocal best BLAST matches is 21% to 100%. This variation indicates a wide range of selective pressures acting on different genes since the split of these two

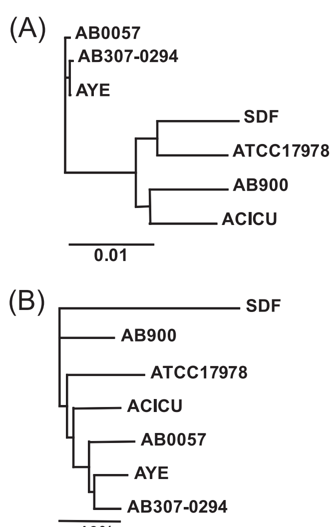

FIG. 1. Phylograms of *A. baumannii* isolates. The relationships of *A. baumannii* isolates were inferred based on the similarity of shared sequences that have most likely been retained in each genome from a common ancestor (A) and based on the extent of unique gene content in each isolate (B). (A) A maximum likelihood tree was constructed using *dnaml* from the PHYLIP package, based on the concatenated DNA sequences of 1,942 ORFs that were reciprocal best matches in each genome. Bar, 0.01 substitution per nucleotide. (B) A tree based on the shared content of accessory genes was constructed as described previously (44). Bar, 10% difference in gene content.

Acinetobacter lineages. An important feature of the ADP1 genome is a series of islands carrying genes related to the catabolism of a diverse array of complex organic compounds. Interestingly, three of the four catabolic islands are largely intact in the *A. baumannii* isolates, although they are rearranged so they are distributed over a larger genomic region rather than grouped into an archipelago as in ADP1 (3). The cluster that is missing carries the *ssu*, *sox*, *ats*, and *nth* genes, encoding products that metabolize alkanesulfonates, dibenzothiophene, sulfuric esters, and nitriles. Genes that encode proteins involved in catabolism of betaine, vanillate, urea, benzoate, catechol, protocatechuate, quinate, and several other complex organic compounds are retained in the *A. baumannii* isolates.

Adaptation to the human host. *A. baylyi* ADP1 is a naturally transformable soil isolate. We hypothesize that genes found in the *A. baumannii* isolates but not in ADP1 may contribute to features of growth in association with a human host. We found 475 genes that are shared by all six *A. baumannii* clinical isolates and that are missing from the ADP1 genome (pan-*A. baumannii* accessory genes [see Table S2 in the supplemental material]). Hence, we propose that these genes may play an important role in human adaptation. Reinforcing the significance of these genes for growth in association with humans, 279 (59%) have been lost in the SDF strain, which was isolated from a human body louse.

Gene annotations for each genome were classified using gene ontology (GO) terms to group related genes by molecular function, biological role, and cellular compartment (2). The pan-*A. baumannii* accessory genes are enriched in the categories of transport activity and transcription factor activity compared with core genes shared with ADP1 (Fig. 2). In contrast, GO categories for metabolism and cellular processes were overrepresented among core genes compared with pan-*A. baumannii* accessory genes. Remarkably, 59 of the pan-*A. baumannii* accessory genes are predicted to be transcription factors based on sequence similarity. This suggests a more extensive regulatory program in *A. baumannii* than in ADP1. Transporter genes comprise 22% of the pan-*A. baumannii* accessory genes, compared to 10% of all genes. Transport systems are identifiable for urea, taurine, oligopeptides, and

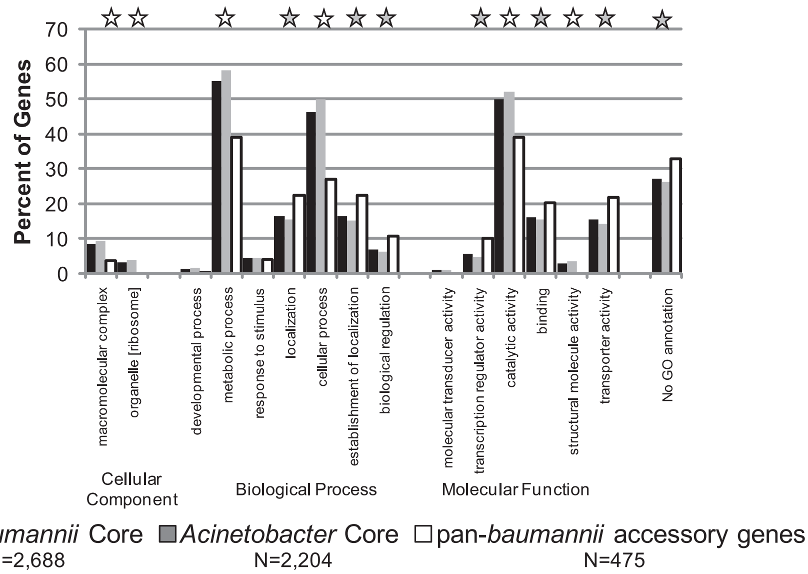

FIG. 2. GO categories of core and *A. baumannii*-specific genes. GO categories were inferred for AB0057 genes by using the JCVI Annotation Engine. The percentage of genes in each GO category was determined for core *A. baumannii* genes (those present in all six clinical isolates), *Acinetobacter* core genes (*A. baumannii* core genes that are also present in ADP1), and pan-*A. baumannii* accessory genes (core genes absent from ADP1), using WEGO (58). Percentages indicate the fractions of gene groups annotated with each GO category. Stars indicate GO categories that are significantly underrepresented (open) or overrepresented (filled) among pan-*A. baumannii* accessory genes compared to core genes ($P < 0.05$).

histidine. The presence of additional transport systems for amino acids and other nitrogen-containing compounds presumably reflects their greater availability in humans than in soil. Several amino acid utilization enzymes were also found, including arginine *N*-succinyltransferase and histidine decarboxylase.

Two hundred sixty-one of the 475 pan-*A. baumannii* accessory genes (55%) are present in clusters of at least four adjacent genes. As noted above, not all clusters should be presumed to be present due to lateral transfer into the *A. baumannii* ancestor. Although by definition none have orthologs in ADP1, 40% have orthologs in *Pseudomonas aeruginosa* PAO1 and may have been lost in the ADP1 lineage.

Two clusters are worthy of further note. One is a cluster of genes responsible for the biosynthesis of a homoserine lactone that is involved in quorum sensing (AB57_0151 to AB57_0161). The AbaI protein (AB57_0151) has been shown to be a homoserine lactone synthase which is involved in quorum sensing and is required for biofilm formation (33). The second cluster (AB57_2565 to AB57_2574) is a chaperone/usher pilus assembly gene cluster that has also been shown to be involved in adherence to mammalian cells and in biofilm formation (50).

Variation among *A. baumannii* isolates. As shown for *Haemophilus influenzae*, *P. aeruginosa*, *Streptococcus pneumoniae*, and other bacterial pathogens, there is considerable variation in the DNA content of each isolate (18, 29, 41, 42). The accessory genome of *A. baumannii* comprises 2,649 annotated genes that are present in one to five of the six isolates. This number will surely grow as additional isolates are characterized. The number of unique genes ranges from 80 (AB307-0294) to 528 (ATCC 17978).

Genomic regions of unique content (islands) have been noted in each of the reported *A. baumannii* genomes, but the availability of seven complete genomes enables a much more rigorous evaluation of the contents and distribution of these islands. A variety of terms have been applied to clustered groups of genes in *A. baumannii*, including (putative) alien islands, pathogenicity islands (PAIs), and RIs (11, 15, 23, 39, 43). Based on the gene content, the latter term seems appropriate for a subset of islands with a clear concentration of genes associated with resistance to several classes of antibiotics. However, the function of most islands is not proven, so we prefer the simple term genomic islands.

In AB0057, 60% of lineage-specific genes are within clusters of at least 10 genes located adjacent to one another. Some genomic islands are likely the result of lateral gene transfer, such as prophage insertions, which in general are the largest genomic islands in each isolate. The RI described below is comprised largely of genes that were likely acquired by lateral transfer. It is also clear that not all genomic islands were derived by lateral gene transfer, however. Some likely represent regions of an ancestral *Pseudomonadales* genome that have been lost in ADP1, for example, a leucine metabolism cluster at AB57_1597 to AB57_1604 that has orthologs in both *P. aeruginosa* and another closely related organism, *Psychrobacter cryohalolentis* (AB0057 numbers are given, but this cluster is shared by all of the *A. baumannii* isolates except for SDF).

Each genome contains a considerable number of unique genes, as 46% of accessory genes are isolate specific. A disproportionate number of these are hypothetical and are likely cryptic prophage regions. Of the 1,228 total genes that are annotated for only one of the six clinical isolates, 412 fall within prophage regions and 487 others are annotated as encoding hypothetical proteins (73% in the two categories combined). The phage regions are not orthologous, suggesting recent insertion and/or rapid loss and a large pool of potential bacteriophage genomes. One prophage was found in both AB0057

and ACICU, albeit at different chromosome locations in the two genomes (AB57_1230 to AB57_1300 and ACICU_02150 to ACICU_02228). The significance of these two independent insertion events in the context of the natural history of these isolates is unclear.

The excess of hypothetical proteins in the accessory genome could be due to several causes. First, incorrectly annotated (wrong frame, strand, or region) open reading frames (ORFs) that do not code for bona fide proteins will not match ORFs from the other isolates. Second, incomplete or inaccurate annotation can result in the unintended omission of identification of a set of orthologous proteins. Finally, frameshift errors in the DNA sequence can result in unpaired orthologs. The first two groups of hypothetical proteins are difficult to quantify. The number of frameshifted annotations was examined by comparison of the predicted protein set from each isolate to the genomes of the other isolates, using TBLASTN. Instances where the alignment was apportioned across two different frames were counted. The number of potentially frameshifted annotations varied from 21 in AYE to 162 in ATCC 17978 (see Table S3 in the supplemental material).

A. baumannii is thought of as a cousin of another human pathogen, *P. aeruginosa*, and 65% of the core genes have orthologs in *P. aeruginosa* PAO1. The accessory genome of *P. aeruginosa* has been shown to be inserted into limited locations around the genome, defined as regions of genome plasticity (29). In contrast, there does not seem to be a similar preference for strain-specific insertion locations in *A. baumannii*, with the exception of the location of the RI.

RIs of variable composition. An interesting feature of many drug-resistant genomes is the presence of a genomic island or RI containing a collection of genes encoding proteins related to antibiotic inactivation and efflux. RIs can be plasmid carried (20, 22) or located on the bacterial chromosome (15), and antibiotic resistance genes are usually interspersed with mobile genetic elements (11).

Comparison of the sequence and structure of the genomic island in each *A. baumannii* isolate revealed a series of insertion/deletion events at this locus (Fig. 3A). The 86-kb island in AYE (AbaR1) is the largest, with 90 annotated genes, including genes related to the inactivation of β-lactams, aminoglycosides, chloramphenicol, rifampin, and tetracycline. These resistance determinants are intermixed with a complex set of partial and complete integrons and transposons (15). The 49-kb AB0057 RI (AbaR3) is largely a subset of AbaR1. It contains eight genes associated with antibiotic resistance. Unique sequences in AbaR3 include a bla_{TEM} gene that is associated with a Tn*3* transposon and a small cluster of genes, including two that encode a DNA topoisomerase and a single-strand binding protein that are most similar to proteins from a broad-host-range plasmid (49). The ACICU RI contains the distal portion of the AYE/AB0057 RI, into which an ISAba1-flanked $bla_{\mathrm{OXA\text{-}20}}$ gene has been inserted (AbaR2). In ATCC 17978, only the initial and terminal segments are present, and these do not contain resistance determinants. An unrelated 37.7-kb insertion is present at the location of the RI in AB900. The AB900 island appears to have been transferred laterally based on the source of the best protein database matches. It contains a copper resistance operon and a high concentration of hypothetical proteins. ADP1 and AB307-0294 preserve the ancestral gene order across the location of the RI insertion. Given the close relationship between AYE and AB307-0294, it is likely that the larger AYE RI is more like an original insertion, with AB0057 and ACICU derived by series of subsequent deletion, insertion, and rearrangement events. Another interpretation, however, is that the RI represents a series of independent insertion events; this view is supported by the fact that ACICU and AYE/AB0057 are representatives of divergent European clone types II and I, respectively.

Supporting the notion that the RI may be mobile, a second copy of the resistance island is present in the AB0057 genome (AbaR4). AbaR4 is the location of a 4.9-kb ISAba1-flanked gene cassette including $bla_{\mathrm{OXA\text{-}23}}$, reinforcing the idea that the environment is permissive for resistance gene accumulation. The other five clinical isolates do not have a second copy of sequences related to the RI, and only two other closely related isolates amplified sequences related to AbaR4 by PCR (Fig. 3B).

A distinguishing feature of AbaR1 and AbaR3 in the MDR isolates AYE and AB0057 is the presence of a pair of ISPpu12 IS elements that flank the resistance gene portion of the island (Fig. 3A, fragments D to J). In the second AB0057 island (AbaR4), the *uspA* gene, encoding a universal stress protein, is present intact, while this gene is interrupted at the corresponding position in the main RI (AbaR3) by the ISPpu12-flanked insertion. The average G+C content of ORFs between the ISPpu12 elements is 57%, compared to 39% for segments A to C and K of the RI and the rest of the genome, suggesting a recent acquisition of the ISPpu12-flanked cassette by lateral transfer. Many of the predicted proteins in segments E to I are nearly identical to segments of a broadly distributed integron (45). In addition, as noted above, AbaR3 in AB0057 contains genes for a plasmid-derived DNA topoisomerase that may contribute to RI mobility. Only one ISPpu12 element is present in ACICU, perhaps reflecting deletion of one element along with a significant fraction of the 5′ end of the island, including the 5′-flanking sequence.

How much of the MDR phenotype can be explained by the RI? The RI is a dramatic feature of the MDR isolates AB0057 and AYE. A significant concentration of genes involved in antibiotic resistance is also present in an orthologous location in ACICU. It is tempting to speculate that the MDR phenotype is correlated with the presence of some variant of the RI. To test this hypothesis, we attempted to amplify segments of the RI from several drug-susceptible and MDR isolates (Fig. 3B). The basic structure of the RI, as found in AB0057 and AYE, appears to be restricted to closely related clones, as defined by PCR-electrospray ionization mass spectrometry (PCR/ESI-MS) typing (12). In other PCR/ESI-MS types, however, MDR isolates typically exhibit the presence of some of the resistance genes but not other markers of the RI per se, such as the ISPpu12 elements that flank the resistance gene region. It is possible that these genes either are not associated with an RI or are associated with islands with an alternate structure and/or location. One example is the presence of *aadB* in several isolates despite the absence of $bla_{\mathrm{VEB\text{-}1}}$, which is adjacent to *aadB* in the AYE RI, indicating that this segment of the RI is not widespread (Fig. 3C, RIN primers). The RI is completely missing in AB307-0294 and a subset of other isolates that are largely susceptible (Fig. 3C, RIH primers). An

(A)

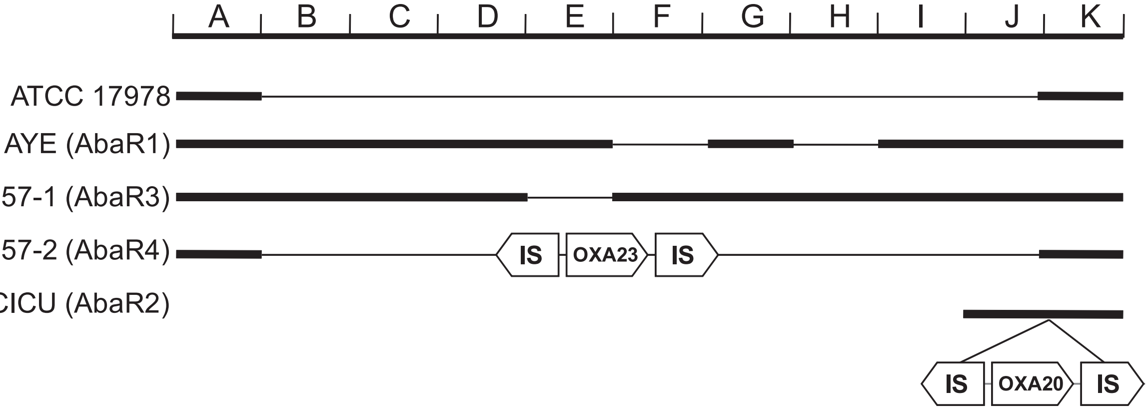

(B)

A	transposon
B	*trkA, trxB*
C	arsenate resistance operon
D	ISPpu12
E	AYE-specific sequence including *strA, strB, dfrI, cmlA, arr-2, tetR, tetA, aadA1, aadB, aac6,* bla_{VEB-1}, bla_{OXA-10}
F	AB0057-specific sequence including *topA, ssb*
G	including mercury resistance operon, *tetR, tetA, cat*
H	Tn3 including bla_{TEM}
I	including *aphA1, aac3, aadDA1*
J	ISPpu12
K	sulfate permease

(C)

	Fig Label	A	C	D/J	E	F	G	H	I	I	I											
	Primers	RIC	RIA	RIG	RIN	RID	RIE	Hujer	Hujer	Hujer	Hujer	RIH	RIK									
Isolate	PCR/ ESI-MS type	Trans-posase	Ars	ISPpu12	*aadB*	*topA*	*tetA*	*bla*-TEM	Int1	*aadA1*	*aacC1*	Island Presence[a]	2nd Island Presence[a]	AMP	CIP	CAZ	FEP	AMK	TOB	SAM	MEM	IPM
AB056	15	+	+	+	-	+	-	-	+	+	+	-	-	+	+	+	+			+	+	+
AB0057	15	+	+	+	-	+	+	+	+	+	+	-	-	+	+	+	+			+	+	+
AB058	15	+	+	+	+	+	-	-	-	-	-	-	+	+	+	+	+	+	+			
AB059	15	+	+	+	+	+	+	+	+	+	+	-	-	+	+	+	+	+		+	+	+
AB060	3	-	+	-	+	-	-	-	+	-	-	-	+	+	+	+	+		+	+	+	+
AB061	3	-	+	-	+	-	-	-	+	-	+	-	+	+	+	+	+		+	+	+	+
AB062	3	-	+	-	+	-	-	-	+	-	+	-	+	+	+	+	+		+	+	+	+
AB063	3	-	+	-	+	-	-	-	+	-	-	-	+	+	+	+	+	+		+		
AB064	3	-	+	-	+	-	-	-	-	-	+	-	+	+								
AB065	3	-	+	-	+	-	-	-	-	-	+	-	+	+	+		+		+	+	+	+
AB070	16	-	-	-	+	-	-	-	+	+	+	-	+	+	+	+	+		+			
AB074	39							-	-	-	-	+		+								
AB069	1							-	+	+	+	+		+	+	+	+		+			
AB072	48							-	-	-	-	+		+								
AB068	9							-	-	-	-	+		+		+		+	+			
ATCC17978*	ND	-	-	-	-	-	-	-	-	-	-	-	+	+								
AYE*	15	+	+	+	+	-	+	-	+	+	+	-	+	+	+		+	+	+			
AB307-0294*	46	-	-	-	-	-	-	-	-	-	-	+	+	+								
AB900*	19	-	-	-	-	-	-	-	-	-	-	-	+	+								
SDF*	ND	-	-	-	-	-	-	-	-	-	-	-	+									
ACICU*	ND	-	-	+	-	-	-	-	+	-	+	-	+	+	+		+	+	+		+	+

FIG. 3. RI composition. (A) Modules that comprise components of the RI in sequenced *A. baumannii* genomes are designated by the letters A to J. A bold bar indicates that the region is present in an isolate. (B) Representative genes present in each module are listed. (C) The presence of various RI components in additional *A. baumannii* isolates was tested by PCR. *, PCR results were inferred based on a BLAST search of each genome with primer sequences; [a], these primer pairs flank the island location, so successful PCR amplification (+) indicates that the island, an insertion that is too long for PCR amplification, is absent. AB0057 was reported previously as AB057 (19). Abbreviations: AMP, ampicillin; CIP, ciprofloxacin; CAZ, ceftazidime; FEP, cefepime; AMK, amikacin; TOB, tobramycin; SAM, ampicillin-sulbactam; MEM, meropenem; IPM, imipenem. Hujer, data obtained from reference 19.

insertion is present at this genomic location in a large majority of isolates. The genes present may be quite different, though, since completely unrelated sequences are present at this genome location in AB900 and SDF.

In the three MDR isolates, AB0057, AYE, and ACICU, a significant fraction of genes responsible for antibiotic resistance are located in mobile genetic elements, including the RIs in each isolate and a plasmid in ACICU. In AB0057, a second gene encoding ADC ($bla_{\mathrm{ADC-40}}$) is present, flanked by ISAba1 elements. The $bla_{\mathrm{ADC-40}}$ gene was likely obtained by lateral transfer because it contains a 15-bp insertion relative to most other bla_{ADC} genes as well as four amino acid substitutions and several silent changes compared with the chromosomal copy.

The corollary issue, i.e., how many resistance genes are not associated with mobile genetic elements, is equally compelling because it may provide a sense of the innate resources in the genome that are available to counter the antibiotic threat. Resistance to fluoroquinolones is mediated by mutations in *gyrA* and *parC*, which are not present on mobile elements. Resistance to aminoglycosides and β-lactams may be mediated by a combination of drug-inactivating enzymes, efflux pumps, and changes in the bacterial outer membrane that reduce drug uptake. Three multidrug efflux pumps, encoded by *adeABC*, *adeIJK*, and *abeM*, have been shown to contribute to drug resistance in *A. baumannii* (9, 27, 32, 46).

The very close relationship of the drug-susceptible isolate AB307-0294 with the MDR isolates AB0057 and AYE enables another perspective on the acquisition of resistance determinants. Virtually all of the AB307-0294 genome aligns with the AB0057 and AYE genomes, and the average percent identity between orthologs is >99.7%. The genes that are present in AYE and AB0057 but not in AB307-0294 are almost exclusively related to the RIs or to prophage or IS element insertions (see Table S4 in the supplemental material). Only ~3% of the AB307-0294 genome is not represented in AB0057 or AYE; this is virtually all in two prophage clusters. The significance of the genetic similarity among these three isolates rests with the observation that AB307-0294 retains all of the transport, metabolism, and regulatory capacities of the MDR isolates and yet is drug susceptible.

The *adeABC* and *adeIJK* genes encoding drug efflux pumps are present and the encoded proteins are 100% identical in sequence in all three isolates. The two-component regulatory proteins AdeR and AdeS are also present in AB307-0294, with only a single conservative amino acid substitution in each protein differing from the AB0057 sequence. In fact, the entire *adeRSABC* and *adeIJK* gene regions together have only three nucleotide differences in 12,436 bp between AB307-0294 and AB0057 or AYE, suggesting that both their regulation and function are similar among the three isolates. It has been suggested that the AdeIJK proteins contribute to intrinsic but not acquired antibiotic resistance in *A. baumannii* (9), and these proteins are also identical in AB307-0294, AB0057, and AYE. Regulators of AdeIJK expression have not been described, and it is likely that additional proteins that control the *adeABC* and *adeIJK* operons remain to be found.

There are 15 genomic islands in ACICU annotated as being involved in drug resistance (20). For most of these islands, the designation is based on the presence of one or more genes annotated as transporters of the DMT superfamily (21), and their substrates have not been verified experimentally. Most of these genes are also present in the drug-susceptible isolates AB307-0294, AB900, and ATCC 17978 and thus do not seem to be indicative of antibiotic susceptibility status.

In addition to the RIs and prophage regions, there are two additional clusters of genes in the MDR isolates AB0057 and AYE that are absent from AB307-0294: these are a copper resistance cluster and a cluster that includes a glycine/betaine transport operon. Betaines serve as organic osmolytes for protection against osmotic stress, drought, high salinity, or high temperature (57). At least some portion of the copper resistance cluster is present in ATCC 17978 and AB900, and the cluster is absent from ACICU, so these genes are unlikely to contribute directly to antibiotic resistance. The role, if any, of the cluster including the glycine/betaine transport genes in resistance and/or pathogenicity remains to be determined.

IS elements represent another potential source of variability between AB307-0294 and the MDR isolates. AB307-0294 does not contain ISAba1 elements, while AB0057 carries 9 copies and AYE carries 21 copies. Four of the nine ISAba1 elements in AB0057 flank β-lactamase genes that appear to have been transferred laterally into this isolate ($bla_{\mathrm{ADC-40}}$ and $bla_{\mathrm{OXA-23}}$). These ISAba1 elements are presumably involved in overexpression of the *bla* genes from outward-facing promoters in the IS element (17). Two AB0057 ISAba1 insertions are polymorphic and are thus unlikely to be related to drug resistance. One ISAba1 element appears to inactivate the *uup* gene, in which mutations have been reported to increase the precise excision of transposons (31). The final two insertions are in or adjacent to hypothetical protein genes. None of the ISAba1 insertion locations are shared between AB0057 and AYE, suggesting that any impact on expression of adjacent genes at the insertion sites is not a primary feature of drug resistance.

Other features of antibiotic resistance. The RI carries genes that encode resistance to chloramphenicol, an antibiotic that is not commonly used in contemporary acute care settings in developed countries. This suggests that the RI is not a recent acquisition. Further work will be required to assess the genetic stability of the RI.

All tested isolates of *A. baumannii* are resistant to aztreonam, which specifically targets penicillin-binding protein 3 (PBP-3) (8). The basis for this resistance has yet to be determined but could be related to the considerable divergence of PBP-3 in *Acinetobacter*. The AB0057 PBP-3 protein is only 40% identical to the orthologous proteins from the closest non-*Acinetobacter* relative, *Psychrobacter cryohalolentis* K5, and to *P. aeruginosa* PAO1.

All isolates of *A. baumannii* displayed high-level resistance to nitrofurantoin. Nitrofurantoin is a prodrug that is reduced by the bacterial enzyme nitrofuran reductase to form highly reactive intermediates that in turn produce DNA damage. Although present in the close *Acinetobacter* relative *Psychrobacter* sp. strain PRwf-1 and many other gammaproteobacteria, this enzyme is absent from ADP1 and all *A. baumannii* isolates examined to date.

Plasmids were identified during genome sequencing of AB0057 (1), ATCC17978 (2), AYE (4), SDF (3), and ACICU (2), but only in ACICU is there a direct contribution to antibiotic resistance. Two copies of $bla_{\mathrm{OXA-58}}$ are present on a plasmid in ACICU and are flanked by insertion sequences. No

TABLE 2. Distribution of O-antigen genes with first primer set

Isolate[a]	PCR/ESI-MS type[a]	PCR result with primer									
		AB57_0094	AB57_0095	AB57_0096	AB57_0097	AB57_0099	AB57_0100	AB57_0102	AB57_0103	AB57_0104	AB57_0105
ATCC 17978	ND	−	−	−	−	−	−	−	−	−	−
AB0076	15	+	+	+	+	+	+	+	+	+	+
AB0077	15	+	+	+	+	+	+	+	+	+	+
AB0078	15	+	+	+	+	+	+	+	+	+	+
AB0079	15	+	+	+	+	+	+	+	+	+	+
AB0080	15	+	+	+	+	+	+	+	+	+	+
AB0057	15	+	+	+	+	+	+	+	+	+	+
AB056	15	+	+	+	+	+	+	+	+	+	+
AB058	15	−	−	−	−	−	−	−	−	−	−
AB059	15	+	+	+	+	+	+	+	+	+	+
AB070	16	−	−	−	−	−	−	−	−	−	−
AB900	19	−	−	−	−	−	−	−	−	−	−
AB307-0294	46	−	−	−	−	−	−	−	−	−	−
AB066	46	−	−	−	−	−	−	−	−	−	−
AB067	46	−	−	−	−	−	−	−	−	−	−

[a] Isolate and PCR/ESI-MS type information is from reference 19.

plasmids were found after accounting for all genome sequence reads from AB900 and AB307-0294.

Evaluation of *esv* genes. Smith et al. identified 16 genes that, when mutated, resulted in attenuation of the virulence of *A. baumannii* ATCC 17978 in two invertebrate models of infection (43). They also identified 28 potential PAIs based on analysis of base composition and gene content. Surprisingly, only three of the attenuated virulence mutations mapped to PAIs, and the two PAIs containing mutations are prophage regions. Eleven of the 16 so-called *esv* genes (for *e*thanol-*s*timulated *v*irulence) have orthologs in the nonpathogenic organism *Acinetobacter baylyi* ADP1, and 4 of the remaining 5 are absent from all five recent clinical isolates of *A. baumannii* discussed here and from six additional tested isolates (data not shown). This suggests that they are not ubiquitous contributors to clinical infections. The one remaining *esv* gene (*esvB*; A1S_1232) encodes an HxlR family helix-turn-helix transcription factor of unknown specificity. *esvB* is also absent from the SDF strain. Further work to determine the role of this gene in pathogenicity of *A. baumannii* will be required, preferably with a mammalian model system.

Diversity at the O-antigen biosynthetic cluster. The outer surfaces of gram-negative bacteria are comprised of a lipopolysaccharide layer that serves as a barrier between the outer membrane and the environment. Considerable intraspecies variability has been observed in the composition of the O-antigen side chains of the lipopolysaccharide, and this contributes to antigenic variability among isolates. For *P. aeruginosa*, at least 11 highly divergent gene clusters encoding proteins involved in O-antigen biosynthesis at a conserved genome location have been reported (37). A similar arrangement is found in *A. baumannii.* Among the seven isolates analyzed here, there are six highly divergent sets of genes located at the O-antigen cluster. In each genome, the cluster is located at an orthologous position (between ACIAD0069 and ACIAD1016 in ADP1) and contains 17 to 30 genes. The sequences of AB307-0294 and AYE are identical across this region. Testing of the O-antigen gene content of other isolates by PCR showed that a subset of PCR/ESI-MS type 15 isolates share the AB0057 gene set, while other isolates match the AB307-0294/AYE gene set (Table 2). Among the closely related isolates defined by PCR/ESI-MS type 15, the amplification pattern is quite consistent across the gene cluster, and all type 15 isolates match either the AB0057 or AYE/AB307-0294 pattern (Table 2). With more diverse isolates, it is less common to see amplification with both of the tested primer pairs for each O-antigen cluster type, implying that the entire cluster is not always present intact (Table 3). Nonetheless, 18 of 20 isolates in the diverse set of isolates tested by PCR were able to amplify at least one of the O-antigen cluster genes (Table 4). Thus, it remains a possibility that a relatively small set of O-antigen gene sets is present among *A. baumannii* isolates. Previous characterization of the O-antigen diversity among isolates from the *A. baumannii*-*A. calcoaceticus* complex by use of monoclonal antibodies showed considerable variation in reactivity, indicating multiple distinct lipopolysaccharide modifications, even among closely related isolates (34).

Two-component regulatory systems. Bacterial two-component systems, consisting of a sensor histidine kinase and a response regulator, enable changes in gene expression in response to external stimuli (6, 16). Nineteen two-component systems were identified in *A. baumannii* AB0057 (see Table S5 in the supplemental material). Most of these are also present in the other clinical isolates. The downstream target genes for most of these remain unknown, but some are likely to play important roles in infection. The AdeRS pair regulates a multidrug efflux pump, contributing to resistance to aminoglycosides, tetracycline, erythromycin, chloramphenicol, trimethoprim, and fluoroquinolones (27, 28). AdeRS proteins are not present in AB900, SDF, or ADP1.

Two two-component systems that are likely to be involved in controlling resistance to heavy metals were found, including *cusSR* (30) (AB57_0660-1) and a less-well-characterized pair encoded by AB57_2550-1. The *cusSR* genes are absent from AB307-0294 and ACICU, along with the likely target genes involved in copper resistance. The *cusSR* genes are also missing from ADP1, while the likely target genes involved in copper resistance are present. In ATCC 17978, the regulatory and

TABLE 2—*Continued*

PCR result with primer[b]												
AB57_ 0106	AB57_ 0107	AB57_ 0108	AB57_ 0109	ABAYE 3806	ABAYE 3807	ABAYE 3808	ABAYE 3809	ABAYE 3810	ABAYE 3811	ABAYE 3812	ABAYE 3813	ABAYE 3814
–	–	–	–	–	–	–	–	–	–	–	–	–
+	+	+	+	–	–	–	–	–	–	–	–	–
+	+	+	+	–	–	–	–	–	–	–	–	–
+	+	+	+	–	–	–	–	–	–	–	–	–
+	+	+	+	–	–	–	–	–	–	–	–	–
+	+	+	+	–	–	–	–	–	–	–	–	–
+	+	+	+	–	–	–	–	–	–	–	–	–
+	+	+	+	–	–	–	–	–	–	–	–	–
–	+	–	–	+	+	+	+	+	+	+	+	+
+	+	+	+	–	–	–	–	–	–	–	–	–
–	–	–	–	+	–	+	–	–	–	–	–	–
–	–	–	–	–	–	–	–	–	–	–	–	+
–	+	–	–	+	+	+	+	+	+	+	+	+
–	–	–	–	–	–	–	–	–	–	–	–	–
–	–	–	–	–	–	–	–	–	–	–	–	–

likely target genes are present adjacent to one another, but the gene cluster is located in a nonsyntenic position relative to flanking genes in AB0057. The predicted CusS and CusR proteins have their best (non-*A. baumannii*) matches to proteins from several betaproteobacteria, suggesting that they are derived from a lateral transfer event into an *A. baumannii* ancestor following the split from *A. baylyi* ADP1.

At least one component of 11 of the 19 two-component systems that are present in the clinical isolates is absent from SDF, suggesting a reduced capacity to respond to environmental changes in this organism.

DISCUSSION

MDR in *A. baumannii* has been defined operationally as resistance to representatives of three or more of the following classes of antibiotics: quinolones (e.g., ciprofloxacin), extended-spectrum cephalosporins (e.g., ceftazidime and cefepime), β-lactam–β-lactamase inhibitor combinations (e.g., piperacillin-tazobactam), aminoglycosides (amikacin, gentamicin, and tobramycin), and carbapenems (e.g., imipenem and meropenem) (19). *A. baumannii* uses several strategies to evade antibiotics, including multiple detoxifying enzymes, efflux

TABLE 3. Distribution of O-antigen genes with second primer set

Isolate[a]	PCR/ESI-MS type[a]	PCR result with primer[b]											
		AB57_ 0094	AB57_ 0095	ABAYE 3806	ABAYE 3807	AB900_1	AB900_2	A1S_ 0053	A1S_ 0057	ACICU_ 00077	ACICU_ 00080	ABSDF 0078	ABSDF 0066
ATCC 17978		–	–	–	–	–	–	+	+	–	–	+	–
AB069	1	–	–	–	–	–	–	–	–	+	+	+	+
AB063	3	–	–	–	–	–	–	–	–	+	+	–	+
AB061	3	–	–	–	–	–	–	–	–	–	–	–	+
AB068	9	–	–	–	–	–	–	–	–	–	–	–	–
AB039	10	–	–	–	–	–	–	–	–	+	+	+	–
AB033	10	–	–	–	–	–	–	–	–	+	+	+	–
AB021	11	–	–	–	–	–	–	–	–	–	–	–	+
AB024	11	–	–	–	–	–	–	–	–	–	–	–	+
AB054	12	–	–	–	–	–	–	–	–	–	–	–	–
AB002	14	–	+	+	–	–	–	–	–	–	–	–	–
AB009	14	–	+	+	–	–	–	–	–	+	–	–	–
AB058	15	–	+	+	+	–	–	–	–	–	–	–	–
AB0057	15	+	+	–	–	–	–	–	–	–	–	–	–
AB070	16	–	–	+	–	+	–	+	–	–	–	–	–
AB900	19	–	–	–	–	+	+	–	–	–	–	–	–
AB051	24	+	+	–	–	+	–	–	–	–	–	+	–
AB041	24	–	-	–	–	+	–	–	–	–	–	+	–
AB074	39	–	+	+	–	+	–	–	–	–	–	–	–
AB307-0294	46	–	+	+	+	–	–	–	–	–	–	–	–
AB066	46	–	–	–	–	–	–	–	–	–	–	–	+
AB071	47	+	+	–	–	–	–	–	–	+	+	–	+
AB072	48	–	–	–	–	+	–	–	–	+	+	–	+

[a] Isolate and PCR/ESI-MS type information is from reference 19.
[b] Primer set prefixes indicate primers designed from O-antigen genes in the following isolates: AB57, AB0057; ABAYE, AYE; A1S, ATCC 17978; ABSDF, SDF; ACICU, ACICU; and AB900, AB900.

TABLE 4. O-antigen genes tested by PCR

ORF	Description
AB57_0094	VI polysaccharide biosynthesis protein VipA/TviB
AB57_0095	VI polysaccharide biosynthesis protein VipB/TviC
AB57_0096	Polysaccharide biosynthesis protein
AB57_0097	Conserved hypothetical protein
AB57_0099	Glycosyltransferase, group 1
AB57_0100	Hypothetical protein
AB57_0102	Putative glycosyltransferase family 1
AB57_0103	Glycosyltransferase, group 1
AB57_0104	UDP-glucose 4-epimerase
AB57_0105	Polyprenol phosphate:*N*-acetyl-hexosamine 1-phosphate transferase
AB57_0106	Acetyltransferase
AB57_0107	Nucleotide sugar epimerase/dehydratase
AB57_0108	UDP-glucose 4-epimerase
AB57_0109	Conserved hypothetical protein
ABAYE3806	Putative perosamine synthetase (WeeJ/Per)
ABAYE3807	Putative acetyltransferase (WeeI)
ABAYE3808	Putative UDP-galactose phosphate transferase (WeeH)
ABAYE3809	Putative glycosyltransferase family 1
ABAYE3810	Conserved hypothetical protein; putative polysaccharide polymerase
ABAYE3811	Putative polysaccharide polymerase
ABAYE3812	Putative glycosyltransferase family 1
ABAYE3813	Putative polysaccharide biosynthesis protein
ABAYE3814	Putative NAD-dependent epimerase/dehydratase (WbpP)
A1S_0053	MviM protein
A1S_0057	Capsular polysaccharide synthesis enzyme
ABSDF0066	Putative UDP-glucose/GDP-mannose dehydrogenase
ABSDF0078	Putative UDP-galactose phosphate transferase (WeeH)
ACICU_00077	CMP-*N*-acetylneuraminic acid synthetase
ACICU_00080	Sialic acid synthase

pumps, target site mutations, and gene regulatory changes. AB307-0294 is largely drug susceptible yet highly similar to the MDR strains AYE and AB0057. This prompted us to seek to explain the resistance phenotype on the basis of genetic differences between AB307-0294 and the MDR strains. Resistance to each tested antibiotic (Table 1) could be accounted for by the acquisition of a specific resistance determinant in AYE and AB0057. AB307-0294 has orthologs of the transporters and efflux pumps that are present in AYE and AB0057, but it appears that these alone are not sufficient to confer resistance to β-lactam and aminoglycoside antibiotics.

Among 74 isolates from WRAMC, resistance to the aminoglycosides amikacin and tobramycin was always associated with the presence of at least one aminoglycoside-modifying enzyme (AME) (19). In addition, a recent study of *A. baumannii* isolates in New York City showed that resistance to cefepime and tigecycline could be ascribed to increased expression of AdeABC in some isolates, while resistance to other cephalosporins and aminoglycosides was mediated by antimicrobial drug-inactivating enzymes and fluoroquinolone resistance was always associated with gyrase gene mutations (4). It is possible that upregulation of efflux pumps may be found to be sufficient to confer resistance to certain classes of antibiotics in other isolates. For example, one WRAMC isolate is ciprofloxacin resistant, despite carrying *gyrA* and *parC* alleles associated with drug susceptibility (54, 55), suggesting an alternative mechanism of resistance. Taken together, the extensive similarities between AB307-0294 and the MDR isolates imply that while drug efflux may be a contributor to clinically relevant antibiotic resistance, it is not the primary mechanism of MDR.

The RI is a dominant genomic feature in AYE and AB0057, exhibiting a large concentration of laterally transferred genes associated with antimicrobial resistance intermixed with a diverse set of transposon- and integron-related sequences that have presumably facilitated the transfer of this region of the genome into *A. baumannii.* The importance of the RI in contributing to the MDR phenotype is considerable in these isolates, with genes encoding resistance to cephalosporins, carbapenems, and aminoglycosides. In each of the MDR isolates, however, additional loci contribute to drug resistance. IS-flanked β-lactamase genes are found outside the RIs in AB0057 and ACICU, and cephalosporin resistance in AYE is likely due to an ISAba1 insertion adjacent to the $bla_{\mathrm{ADC\text{-}9}}$ gene. Furthermore, the RI found in AYE and AB0057, and to a lesser extent, ACICU, does not appear to be present in all MDR isolates based on PCR amplification of several genes located throughout the RI. Thus, it is likely that alternative genetic arrangements of resistance genes will be found as additional isolates are sequenced.

Quinolone resistance is primarily mediated by mutations in the housekeeping genes *gyrA* and *parC*, which are not RI associated. The *bla* genes (e.g., encoding TEM, OXA, VEB, and CTX-M) are frequently found in locations outside the RI, even in isolates that contain the RI. In ACICU, two copies of $bla_{\mathrm{OXA\text{-}58}}$ are present on a plasmid, and in AB0057, $bla_{\mathrm{OXA\text{-}23}}$ is located on the second island copy, ISAbaR4. In the MDR isolates analyzed to date, AMEs are associated with the RI. It remains to be determined whether AMEs are associated with RIs of novel structure in isolates that do not contain an RI analogous to those described in AYE, AB0057, and ACICU. In summary, evidence to support the notion that the RI is the sole, or even primary, genetic basis for clinically relevant MDR is still needed.

It is curious that the sequence of the >50-year-old isolate ATCC 17978 is not more divergent than those of other isolates, suggesting that although *A. baumannii* isolates differ by ~2% at the sequence level, there may be considerable stability in each clade. AYE and AB0057 were isolated more than a decade after AB307-0294 yet have diverged <0.1% at the nucleotide level compared with the older isolate. SDF also differs from the other *A. baumannii* isolates by ~2% at the DNA level, although it has also undergone a considerable reduction in gene number, presumably driven by the action of a large number of IS elements (51). It was argued that SDF was acquired by the louse directly from the bloodstream of an infected human in the course of a blood meal, since the louse gut is sterile (24). An alternative explanation is that SDF represents an *A. baumannii* lineage that is adapted for growth in the louse rather than in humans. Additional epidemiological surveys will be necessary to determine whether SDF-like *A. baumannii* isolates can be found in humans.

Antimicrobial resistance in *A. baumannii* arises by a combination of genetic changes and selective pressure. The following three classes of genetic alteration contribute to the acquisition

of a resistance phenotype: lateral gene transfer, gene amplification (by duplication and/or increased expression), and mutation of genes or their promoters (resulting in loss of function, enhancement of function, or gain of novel function). Each of these mechanisms is represented in *A. baumannii*. Further studies that address the balance among these strategies, the genetic and genomic architectures that support them, the role of mobile genetic elements, and the pace of genetic change will be facilitated by the sequences presented here and those of additional isolates that represent further examples of MDR and susceptible isolates of clinical significance.

ACKNOWLEDGMENTS

We gratefully acknowledge the financial support of a VA Merit Review grant from the Department of Veterans Affairs (R.A.B. and T.A.R.), NIH/NIAID grants AI072219 and AI063517 (R.A.B.), the STERIS Foundation (M.D.A.), and a U.S. Army Medical Research Acquisition Activity under contract W81XWH-05-1-0627 (T.A.R. and A.A.C.).

We thank the J. C. Venter Institute for making available the JCVI Annotation Service, which provided us with automatic annotation data and the manual annotation tool Manatee. We thank Nicholas Ornston for helpful discussions regarding the metabolic capacity of *Acinetobacter* species. We thank David Craft of WRAMC for providing *A. baumannii* isolates.

REFERENCES

1. **Abbott, A.** 2005. Medics braced for fresh superbug. Nature **436:**758.
2. **Ashburner, M., C. A. Ball, J. A. Blake, D. Botstein, H. Butler, J. M. Cherry, A. P. Davis, K. Dolinski, S. S. Dwight, J. T. Eppig, M. A. Harris, D. P. Hill, L. Issel-Tarver, A. Kasarskis, S. Lewis, J. C. Matese, J. E. Richardson, M. Ringwald, G. M. Rubin, and G. Sherlock.** 2000. Gene ontology: tool for the unification of biology. Nat. Genet. **25:**25–29.
3. **Barbe, V., D. Vallenet, N. Fonknechten, A. Kreimeyer, S. Oztas, L. Labarre, S. Cruveiller, C. Robert, S. Duprat, P. Wincker, L. N. Ornston, J. Weissenbach, P. Marliere, G. N. Cohen, and C. Medigue.** 2004. Unique features revealed by the genome sequence of *Acinetobacter* sp. ADP1, a versatile and naturally transformation competent bacterium. Nucleic Acids Res. **32:**5766–5779.
4. **Bratu, S., D. Landman, D. A. Martin, C. Georgescu, and J. Quale.** 2008. Correlation of antimicrobial resistance with beta-lactamases, the OmpA-like porin, and efflux pumps in clinical isolates of *Acinetobacter baumannii* endemic to New York City. Antimicrob. Agents Chemother. **52:**2999–3005.
5. **Brisse, S., D. Milatovic, A. C. Fluit, K. Kusters, A. Toelstra, J. Verhoef, and F. J. Schmitz.** 2000. Molecular surveillance of European quinolone-resistant clinical isolates of *Pseudomonas aeruginosa* and *Acinetobacter* spp. using automated ribotyping. J. Clin. Microbiol. **38:**3636–3645.
6. **Chang, C., and R. C. Stewart.** 1998. The two-component system. Regulation of diverse signaling pathways in prokaryotes and eukaryotes. Plant Physiol. **117:**723–731.
7. **Clinical and Laboratory Standards Institute.** 2005. Performance standards for antimicrobial disk susceptibility testing. M100–S15, 15th informational supplement. Clinical and Laboratory Standards Institute, Wayne, PA.
8. **Curtis, N. A., D. Orr, G. W. Ross, and M. G. Boulton.** 1979. Affinities of penicillins and cephalosporins for the penicillin-binding proteins of *Escherichia coli* K-12 and their antibacterial activity. Antimicrob. Agents Chemother. **16:**533–539.
9. **Damier-Piolle, L., S. Magnet, S. Bremont, T. Lambert, and P. Courvalin.** 2008. AdeIJK, a resistance-nodulation-cell division pump effluxing multiple antibiotics in *Acinetobacter baumannii*. Antimicrob. Agents Chemother. **52:** 557–562.
10. **Dijkshoorn, L., A. Nemec, and H. Seifert.** 2007. An increasing threat in hospitals: multidrug-resistant *Acinetobacter baumannii*. Nat. Rev. Microbiol. **5:**939–951.
11. **Dobrindt, U., B. Hochhut, U. Hentschel, and J. Hacker.** 2004. Genomic islands in pathogenic and environmental microorganisms. Nat. Rev. Microbiol. **2:**414–424.
12. **Ecker, J. A., C. Massire, T. A. Hall, R. Ranken, T. T. Pennella, C. Agasino Ivy, L. B. Blyn, S. A. Hofstadler, T. P. Endy, P. T. Scott, L. Lindler, T. Hamilton, C. Gaddy, K. Snow, M. Pe, J. Fishbain, D. Craft, G. Deye, S. Riddell, E. Milstrey, B. Petruccelli, S. Brisse, V. Harpin, A. Schink, D. J. Ecker, R. Sampath, and M. W. Eshoo.** 2006. Identification of *Acinetobacter* species and genotyping of *Acinetobacter baumannii* by multilocus PCR and mass spectrometry. J. Clin. Microbiol. **44:**2921–2932.
13. **Falagas, M. E., and P. I. Rafailidis.** 2007. Attributable mortality of *Acinetobacter baumannii*: no longer a controversial issue. Crit. Care **11:**134.
14. **Fournier, P. E., and H. Richet.** 2006. The epidemiology and control of *Acinetobacter baumannii* in health care facilities. Clin. Infect. Dis. **42:**692–699.
15. **Fournier, P. E., D. Vallenet, V. Barbe, S. Audic, H. Ogata, L. Poirel, H. Richet, C. Robert, S. Mangenot, C. Abergel, P. Nordmann, J. Weissenbach, D. Raoult, and J. M. Claverie.** 2006. Comparative genomics of multidrug resistance in *Acinetobacter baumannii*. PLoS Genet. **2:**e7.
16. **Galperin, M. Y.** 2005. A census of membrane-bound and intracellular signal transduction proteins in bacteria: bacterial IQ, extroverts and introverts. BMC Microbiol. **5:**35.
17. **Heritier, C., L. Poirel, and P. Nordmann.** 2006. Cephalosporinase over-expression resulting from insertion of ISAba1 in *Acinetobacter baumannii*. Clin. Microbiol. Infect. **12:**123–130.
18. **Hogg, J. S., F. Z. Hu, B. Janto, R. Boissy, J. Hayes, R. Keefe, J. C. Post, and G. D. Ehrlich.** 2007. Characterization and modeling of the *Haemophilus influenzae* core and supragenomes based on the complete genomic sequences of Rd and 12 clinical nontypeable strains. Genome Biol. **8:**R103.
19. **Hujer, K. M., A. M. Hujer, E. A. Hulten, S. Bajaksouzian, J. M. Adams, C. J. Donskey, D. J. Ecker, C. Massire, M. W. Eshoo, R. Sampath, J. M. Thomson, P. N. Rather, D. W. Craft, J. T. Fishbain, A. J. Ewell, M. R. Jacobs, D. L. Paterson, and R. A. Bonomo.** 2006. Analysis of antibiotic resistance genes in multidrug-resistant *Acinetobacter* sp. isolates from military and civilian patients treated at the Walter Reed Army Medical Center. Antimicrob. Agents Chemother. **50:**4114–4123.
20. **Iacono, M., L. Villa, D. Fortini, R. Bordoni, F. Imperi, R. J. Bonnal, T. Sicheritz-Ponten, G. De Bellis, P. Visca, A. Cassone, and A. Carattoli.** 2008. Whole-genome pyrosequencing of an epidemic multidrug-resistant *Acinetobacter baumannii* strain belonging to the European clone II group. Antimicrob. Agents Chemother. **52:**2616–2625.
21. **Jack, D. L., N. M. Yang, and M. H. Saier, Jr.** 2001. The drug/metabolite transporter superfamily. Eur. J. Biochem. **268:**3620–3639.
22. **Juhas, M., P. M. Power, R. M. Harding, D. J. Ferguson, I. D. Dimopoulou, A. R. Elamin, Z. Mohd-Zain, D. W. Hood, R. Adegbola, A. Erwin, A. Smith, R. S. Munson, A. Harrison, L. Mansfield, S. Bentley, and D. W. Crook.** 2007. Sequence and functional analyses of *Haemophilus* spp. genomic islands. Genome Biol. **8:**R237.
23. **Karlin, S.** 2001. Detecting anomalous gene clusters and pathogenicity islands in diverse bacterial genomes. Trends Microbiol. **9:**335–343.
24. **La Scola, B., and D. Raoult.** 2004. *Acinetobacter baumannii* in human body louse. Emerg. Infect. Dis. **10:**1671–1673.
25. **Lee, N. Y., H. C. Lee, N. Y. Ko, C. M. Chang, H. I. Shih, C. J. Wu, and W. C. Ko.** 2007. Clinical and economic impact of multidrug resistance in nosocomial *Acinetobacter baumannii* bacteremia. Infect. Control Hosp. Epidemiol. **28:**713–719.
26. **Lockhart, S. R., M. A. Abramson, S. E. Beekmann, G. Gallagher, S. Riedel, D. J. Diekema, J. P. Quinn, and G. V. Doern.** 2007. Antimicrobial resistance among gram-negative bacilli causing infections in intensive care unit patients in the United States between 1993 and 2004. J. Clin. Microbiol. **45:**3352–3359.
27. **Magnet, S., P. Courvalin, and T. Lambert.** 2001. Resistance-nodulation-cell division-type efflux pump involved in aminoglycoside resistance in *Acinetobacter baumannii* strain BM4454. Antimicrob. Agents Chemother. **45:**3375–3380.
28. **Marchand, I., L. Damier-Piolle, P. Courvalin, and T. Lambert.** 2004. Expression of the RND-type efflux pump AdeABC in *Acinetobacter baumannii* is regulated by the AdeRS two-component system. Antimicrob. Agents Chemother. **48:**3298–3304.
29. **Mathee, K., G. Narasimhan, C. Valdes, X. Qiu, J. M. Matewish, M. Koehrsen, A. Rokas, C. N. Yandava, R. Engels, E. Zeng, R. Olavarietta, M. Doud, R. S. Smith, P. Montgomery, J. R. White, P. A. Godfrey, C. Kodira, B. Birren, J. E. Galagan, and S. Lory.** 2008. Dynamics of *Pseudomonas aeruginosa* genome evolution. Proc. Natl. Acad. Sci. USA **105:**3100–3105.
30. **Munson, G. P., D. L. Lam, F. W. Outten, and T. V. O'Halloran.** 2000. Identification of a copper-responsive two-component system on the chromosome of *Escherichia coli* K-12. J. Bacteriol. **182:**5864–5871.
31. **Murat, D., P. Bance, I. Callebaut, and E. Dassa.** 2006. ATP hydrolysis is essential for the function of the Uup ATP-binding cassette ATPase in precise excision of transposons. J. Biol. Chem. **281:**6850–6859.
32. **Nemec, A., M. Maixnerova, T. J. van der Reijden, P. J. van den Broek, and L. Dijkshoorn.** 2007. Relationship between the AdeABC efflux system gene content, netilmicin susceptibility and multidrug resistance in a genotypically diverse collection of *Acinetobacter baumannii* strains. J. Antimicrob. Chemother. **60:**483–489.
33. **Niu, C., K. M. Clemmer, R. A. Bonomo, and P. N. Rather.** 2008. Isolation and characterization of an autoinducer synthase from *Acinetobacter baumannii*. J. Bacteriol. **190:**3386–3392.
34. **Pantophlet, R., J. A. Severin, A. Nemec, L. Brade, L. Dijkshoorn, and H. Brade.** 2002. Identification of *Acinetobacter* isolates from species belonging to the *Acinetobacter calcoaceticus-Acinetobacter baumannii* complex with monoclonal antibodies specific for O antigens of their lipopolysaccharides. Clin. Diagn. Lab. Immunol. **9:**60–65.
35. **Perez, F., A. M. Hujer, K. M. Hujer, B. K. Decker, P. N. Rather, and R. A.**

Bonomo. 2007. The global challenge of multidrug-resistant *Acinetobacter baumannii*. Antimicrob. Agents Chemother. **51:**3471–3484.
36. **Poirel, L., O. Menuteau, N. Agoli, C. Cattoen, and P. Nordmann.** 2003. Outbreak of extended-spectrum beta-lactamase VEB-1-producing isolates of *Acinetobacter baumannii* in a French hospital. J. Clin. Microbiol. **41:**3542–3547.
37. **Raymond, C. K., E. H. Sims, A. Kas, D. H. Spencer, T. V. Kutyavin, R. G. Ivey, Y. Zhou, R. Kaul, J. B. Clendenning, and M. V. Olson.** 2002. Genetic variation at the O-antigen biosynthetic locus in *Pseudomonas aeruginosa*. J. Bacteriol. **184:**3614–3622.
38. **Robenshtok, E., M. Paul, L. Leibovici, A. Fraser, S. Pitlik, I. Ostfeld, Z. Samra, S. Perez, B. Lev, and M. Weinberger.** 2006. The significance of *Acinetobacter baumannii* bacteraemia compared with *Klebsiella pneumoniae* bacteraemia: risk factors and outcomes. J. Hosp. Infect. **64:**282–287.
39. **Schmidt, H., and M. Hensel.** 2004. Pathogenicity islands in bacterial pathogenesis. Clin. Microbiol. Rev. **17:**14–56.
40. **Scott, P., G. Deye, A. Srinivasan, C. Murray, K. Moran, E. Hulten, J. Fishbain, D. Craft, S. Riddell, L. Lindler, J. Mancuso, E. Milstrey, C. T. Bautista, J. Patel, A. Ewell, T. Hamilton, C. Gaddy, M. Tenney, G. Christopher, K. Petersen, T. Endy, and B. Petruccelli.** 2007. An outbreak of multidrug-resistant *Acinetobacter baumannii-calcoaceticus* complex infection in the US military health care system associated with military operations in Iraq. Clin. Infect. Dis. **44:**1577–1584.
41. **Shen, K., J. Gladitz, P. Antalis, B. Dice, B. Janto, R. Keefe, J. Hayes, A. Ahmed, R. Dopico, N. Ehrlich, J. Jocz, L. Kropp, S. Yu, L. Nistico, D. P. Greenberg, K. Barbadora, R. A. Preston, J. C. Post, G. D. Ehrlich, and F. Z. Hu.** 2006. Characterization, distribution, and expression of novel genes among eight clinical isolates of *Streptococcus pneumoniae*. Infect. Immun. **74:**321–330.
42. **Shen, K., S. Sayeed, P. Antalis, J. Gladitz, A. Ahmed, B. Dice, B. Janto, R. Dopico, R. Keefe, J. Hayes, S. Johnson, S. Yu, N. Ehrlich, J. Jocz, L. Kropp, R. Wong, R. M. Wadowsky, M. Slifkin, R. A. Preston, G. Erdos, J. C. Post, G. D. Ehrlich, and F. Z. Hu.** 2006. Extensive genomic plasticity in *Pseudomonas aeruginosa* revealed by identification and distribution studies of novel genes among clinical isolates. Infect. Immun. **74:**5272–5283.
43. **Smith, M. G., T. A. Gianoulis, S. Pukatzki, J. J. Mekalanos, L. N. Ornston, M. Gerstein, and M. Snyder.** 2007. New insights into *Acinetobacter baumannii* pathogenesis revealed by high-density pyrosequencing and transposon mutagenesis. Genes Dev. **21:**601–614.
44. **Snel, B., P. Bork, and M. A. Huynen.** 1999. Genome phylogeny based on gene content. Nat. Genet. **21:**108–110.
45. **Stokes, H. W., and R. M. Hall.** 1989. A novel family of potentially mobile DNA elements encoding site-specific gene-integration functions: integrons. Mol. Microbiol. **3:**1669–1683.
46. **Su, X. Z., J. Chen, T. Mizushima, T. Kuroda, and T. Tsuchiya.** 2005. AbeM, an H^+-coupled *Acinetobacter baumannii* multidrug efflux pump belonging to the MATE family of transporters. Antimicrob. Agents Chemother. **49:**4362–4364.
47. **Sunenshine, R. H., M. O. Wright, L. L. Maragakis, A. D. Harris, X. Song, J. Hebden, S. E. Cosgrove, A. Anderson, J. Carnell, D. B. Jernigan, D. G. Kleinbaum, T. M. Perl, H. C. Standiford, and A. Srinivasan.** 2007. Multidrug-resistant *Acinetobacter* infection mortality rate and length of hospitalization. Emerg. Infect. Dis. **13:**97–103.
48. **Talbot, G. H., J. Bradley, J. E. Edwards, Jr., D. Gilbert, M. Scheld, and J. G. Bartlett.** 2006. Bad bugs need drugs: an update on the development pipeline from the Antimicrobial Availability Task Force of the Infectious Diseases Society of America. Clin. Infect. Dis. **42:**657–668.
49. **Tauch, A., S. Schneiker, W. Selbitschka, A. Puhler, L. S. van Overbeek, K. Smalla, C. M. Thomas, M. J. Bailey, L. J. Forney, A. Weightman, P. Ceglowski, T. Pembroke, E. Tietze, G. Schroder, E. Lanka, and J. D. van Elsas.** 2002. The complete nucleotide sequence and environmental distribution of the cryptic, conjugative, broad-host-range plasmid pIPO2 isolated from bacteria of the wheat rhizosphere. Microbiology **148:**1637–1653.
50. **Tomaras, A. P., C. W. Dorsey, R. E. Edelmann, and L. A. Actis.** 2003. Attachment to and biofilm formation on abiotic surfaces by *Acinetobacter baumannii*: involvement of a novel chaperone-usher pili assembly system. Microbiology **149:**3473–3484.
51. **Vallenet, D., P. Nordmann, V. Barbe, L. Poirel, S. Mangenot, E. Bataille, C. Dossat, S. Gas, A. Kreimeyer, P. Lenoble, S. Oztas, J. Poulain, B. Segurens, C. Robert, C. Abergel, J. M. Claverie, D. Raoult, C. Medigue, J. Weissenbach, and S. Cruveiller.** 2008. Comparative analysis of *Acinetobacters*: three genomes for three lifestyles. PLoS ONE **3:**e1805.
52. **van Dessel, H., L. Dijkshoorn, T. van der Reijden, N. Bakker, A. Paauw, P. van den Broek, J. Verhoef, and S. Brisse.** 2004. Identification of a new geographically widespread multiresistant *Acinetobacter baumannii* clone from European hospitals. Res. Microbiol. **155:**105–112.
53. **Vaneechoutte, M., D. M. Young, L. N. Ornston, T. De Baere, A. Nemec, T. Van Der Reijden, E. Carr, I. Tjernberg, and L. Dijkshoorn.** 2006. Naturally transformable *Acinetobacter* sp. strain ADP1 belongs to the newly described species *Acinetobacter baylyi*. Appl. Environ. Microbiol. **72:**932–936.
54. **Vila, J., J. Ruiz, P. Goni, and T. Jimenez de Anta.** 1997. Quinolone-resistance mutations in the topoisomerase IV parC gene of *Acinetobacter baumannii*. J. Antimicrob. Chemother. **39:**757–762.
55. **Vila, J., J. Ruiz, P. Goni, A. Marcos, and T. Jimenez de Anta.** 1995. Mutation in the *gyrA* gene of quinolone-resistant clinical isolates of *Acinetobacter baumannii*. Antimicrob. Agents Chemother. **39:**1201–1203.
56. **Villegas, M. V., and A. I. Hartstein.** 2003. *Acinetobacter* outbreaks, 1977–2000. Infect. Control Hosp. Epidemiol. **24:**284–295.
57. **Yancey, P. H.** 2005. Organic osmolytes as compatible, metabolic and counteracting cytoprotectants in high osmolarity and other stresses. J. Exp. Biol. **208:**2819–2830.
58. **Ye, J., L. Fang, H. Zheng, Y. Zhang, J. Chen, Z. Zhang, J. Wang, S. Li, R. Li, and L. Bolund.** 2006. WEGO: a web tool for plotting GO annotations. Nucleic Acids Res. **34:**W293–W297.

MAJOR ARTICLE

Penicillin-Binding Protein 7/8 Contributes to the Survival of *Acinetobacter baumannii* In Vitro and In Vivo

Thomas A. Russo,[1,2,3,4,5] Ulrike MacDonald,[2,4] Janet M. Beanan,[2,4] Ruth Olson,[2,4] Ian J. MacDonald,[3,4] Shauna L. Sauberan,[2,5] Nicole R. Luke,[2,3,5] L. Wayne Schultz,[3,6,7] and Timothy C. Umland[3,6,7]

[1]Veterans Administration Western New York Healthcare System and [2]The Witebsky Center for Microbial Pathogenesis, [3]Center of Excellence in Bioinformatics and Life Sciences, and Departments of [4]Medicine, [5]Microbiology, and [6]Structural Biology, State University of New York–Buffalo, and [7]Hauptman-Woodward Medical Research Institute, Buffalo, New York

Background. *Acinetobacter baumannii* is a bacterial pathogen of increasing medical importance. Little is known about genes important for its survival in vivo.

Methods and results. Screening of random transposon mutants of the model pathogen AB307–0294 identified the mutant AB307.27. AB307.27 contained its transposon insertion in *pbpG,* which encodes the putative low-molecular-mass penicillin-binding protein 7/8 (PBP-7/8). AB307.27 was significantly killed in ascites ($P < .001$), but its growth in Luria-Bertani broth was similar to that of its parent, AB307–0294 ($P = .13$). The survival of AB307.27 was significantly decreased in a rat soft-tissue infection model ($P < .001$) and a rat pneumonia model ($P = .002$), compared with AB307–0294. AB307.27 was significantly killed in 90% human serum in vitro, compared with AB307–0294 ($P < .001$). Electron microscopy demonstrated more coccobacillary forms of AB307.27, compared with AB307–0294, suggesting a possible modulation in the peptidoglycan, which may affect susceptibility to host defense factors.

Conclusions. These findings demonstrate that PBP-7/8 contributes to the pathogenesis of *A. baumannii*. PBP-7/8 either directly or indirectly contributes to the resistance of AB307–0294 to complement-mediated bactericidal activity. An understanding of how PBP-7/8 contributes to serum resistance will lend insight into the role of this low-molecular-mass PBP whose function is poorly understood.

Acinetobacter organisms are emerging pathogens of increasing medical importance [1]. Historically, *Acinetobacter* organisms have been considered primarily as health care–associated pathogens, accounting for 1%–3% of hospital-acquired infections and 2%–10% of infections in intensive care units [2–5]. Importantly, the incidence of *Acinetobacter* infection is increasing worldwide [3, 5, 6]. Favored sites of infection include the respiratory tract, particularly in ventilated patients (*Acinetobacter* infections accounted for 6.9% of hospital-acquired pneumonias in 2003, based on National Nosocomial Infections Surveillance system data), the urinary tract, intravascular access devices, surgical sites, and pressure or diabetic ulcers. Mortality rates associated with *Acinetobacter* infection range from 19% to 54% [6]. Interestingly, *Acinetobacter baumannii* has been described as an uncommon cause of severe community-acquired pneumonia, usually in persons with a comorbid condition (e.g., alcoholics), with the preponderance of cases reported from warm and humid geographic locales [7, 8]. Furthermore, the importance of *Acinetobacter* infections in war-related injuries is now established [9–12]. Finally, *Acinetobacter* organisms emerged as important pathogens in survivors of the Asian tsunami in 2004 [13].

An increasing incidence of infections due to strains with a high level of antibiotic resistance is making treatment challenging [14–16]. Particularly problematic are panresistant strains; rates of infection due to such strains

Received 25 April 2008; accepted 9 September 2008; electronically published 13 January 2009.

Potential conflicts of interest: none reported.

Financial support: US Department of Veterans Affairs (VA Merit Review to T.A.R.); US Army Medical Research Acquisition Activity (contract W81XWH-05–1-0627 to T.A.R.); University at Buffalo Interdisciplinary Research Development Fund (to T.A.R., L.W.S., and T.C.U.).

Reprints or correspondence: Dr. Thomas A. Russo, Dept. of Medicine, Div. of Infectious Diseases, 3435 Main St., Biomedical Research Bldg., Rm. 141, Buffalo, NY 14214 (trusso@acsu.buffalo.edu).

The Journal of Infectious Diseases 2009; 199:513–21

0022-1899/2009/19904-0007$15.00
DOI: 10.1086/596317

are greater outside of the United States. Safe, reliable therapeutic agents with predictable activity against *A. baumannii* are presently nonexistent [17, 18].

The need for an increased understanding of *Acinetobacter* infection pathogenesis, identification of virulence factors, and identification and testing of vaccine candidates and new antimicrobial targets is more pressing than ever [17, 18]. To identify genes important for growth and survival, we performed random mutagenesis on *A. baumannii* strain AB307–0294, which our research group has been studying as a model pathogen [19]. We hypothesized that screening this mutant pool for diminished or absent growth on plates made from human ascites would be an efficient means to identify such factors. As a result of this screen, the AB307–0294 mutant derivative AB307.27 was identified. AB307.27 contains its transposon insertion in *pbpG,* which encodes the putative low-molecular-mass penicillin-binding protein 7/8 (PBP-7/8) in *Acinetobacter* organisms. PBP-7/8 is a hydrolase/endopeptidase that hydrolyzes the D-ananyl-ε-meso-2,6-diaminopimelyl cross-bridge bond in high-molecular-mass sacculi [20]. However, there was no discernible change in phenotype in an *Escherichia coli* PBP-7 mutant, as assessed by growth in laboratory medium [21] and by fluorescence-activated cell sorting [22]. PBP-8 is a OmpT-mediated degradation product of PBP-7, and PBP-7 and PBP-8 have been shown in vitro to stabilize and enhance soluble lytic transglycosylase 70 [20, 23, 24]. PBP-7 is absent from gram-positive bacteria. The precise role of PBP-7/8 in gram-negative bacteria is unclear. It appears to be nonessential for normal cell elongation but has been implicated as an accessory enzyme that modulates cell morphology and in daughter cell separation [22, 25–27]. In this report, we describe a novel phenotype for PBP-7/8 in *A. baumannii*. This protein contributes to growth and survival of *A. baumannii* in human ascites in vitro and in vivo in rat soft-tissue infection and pneumonia models. These data lend new insight into the role of the low-molecular mass penicillin-binding proteins in clinically relevant environments.

MATERIALS AND METHODS

Bacterial strains and media. *A. baumannii* strain 307–0294 (blood isolate; sequence type 15 and clonal group 1 [28]) was isolated from a patient hospitalized at Erie County Medical Center (Buffalo, NY) in 1994. AB307–0294 was grown in Luria-Bertani medium, unless stated otherwise. The strain was maintained at −80°C in 50% Luria-Bertani broth and 50% glycerol. Ascites plates consisted of 80% human ascites (pH 7.3; ascites were not sterilized by filtration but were confirmed by culture as sterile) and 20% water. Two-hundred milliliters of water and 15 g of Bacto agar were autoclaved and cooled to 45°C, 800 mL of ascites and kanamycin (final concentration, 40 μg/mL) were added, and plates were poured. For quantitative growth curves, the following were used: 100% human ascites, Luria-Bertani medium, and 100% human urine pooled from 4 healthy donors and filter sterilized before use. Strains were grown overnight in Luria-Bertani medium and diluted in the medium in which the growth curve was being determined, with starting titers ranging from 1×10^4 to 1×10^5 cfu/mL in a final volume of 2 mL. Incubations were at 37°C in a shaking water bath (120 rpm/min). Aliquots were removed at 0, 3, 6, and 24 h, and 10-fold serial dilutions in 1 × PBS were performed to determine the bacterial concentration.

Transposon mutagenesis and screen for lack of growth on ascites plates. Electrocompetent cells were generated by growing AB307–0294 in Mueller-Hinton broth to an $Å_{600}$ of around 0.4. Fifteen milliliters of cells were washed once with 1 mL of ice-cold sterile mqH_2O, followed by 2 washes with 10% ice-cold, sterile glycerol. After the last wash, cells were resuspended in 75 μL and either used immediately or stored at −80°C before use. EZ-Tn5<kan-2>Tnp Transposome (60 ng in 3 μL [Epicentre Biotechnologies]) was electroporated into 75 μL of electrocompetent AB307–0294 (Bio-Rad Gene Pulser; 25 mF/2.5 kV/200 Ohm), using a 0.2-cm gap, in an ice-cold EP chamber (Bio-Rad Laboratories). Immediately after electroporation, cells were resuspended in SOC medium (Invitrogen) and grown at 37°C for 1 h. Aliquots were then plated on Mueller-Hinton plates supplemented with kanamycin (40 μg/mL), and isolated colonies were purified on the same medium. These AB307–0294 mutants (presumably AB307–0294::Tn5<kan-2>) were subsequently gridded onto ascites-kanamycin plates. AB307–0294 mutants that were confirmed to have minimal or no growth on the ascites-kanamycin plates were numbered consecutively and stored at −80°C.

DNA sequencing and analysis. The location of the transposon insertion in mutant derivatives of AB307–0294 was determined by chromosomal sequencing. Chromosomal DNA was prepared from the AB307–0294 mutants of interest by using a Qiagen Genomic-tip 100/G purification column (Qiagen). Cycle sequencing was performed off of the EZ-Tn5 <Kan-2> Transposon (Epicentre Biotechnologies), using the BigDye Terminator v3.1 cycle sequencing kit (Applied Biosystems) in accordance with the protocol for sequencing genomic DNA. The KAN-2 FP-1 forward primer included in the transposon kit was used. Cycle sequencing was performed on 10- or 20-μL reactions with the following PCR protocol: step 1, 96°C for 2 min; step 2, 96°C for 30 s, 50°C for 10 s, and 60°C for 4 min for 50 cycles; and step 3, 4°C, ramping 1°C/s. Cycle sequencing products were prepared for sequencing by use of the CleanSEQ (Agencourt) reaction cleanup reagent in accordance with the manufacturer's instructions. Sanger sequencing was performed with a 3130xl Genetic Analyzer DNA sequencer (Applied Biosystems). Sequence comparisons were performed via BLAST analysis of the nonredundant GenBank database.

Cloning of pbpG and construction of a complemented derivative of AB307.27 (PBP-7/8 negative). *pbpG* and 178 bases

upstream and 150 bases downstream were cloned via PCR-mediated amplification (forward primer: 5'-GCTGACGAGCTC-CAATGGAATGACAAAATTAGCAA-3'; reverse primer: 5'-CCT-AGTACCGGTCAATGGACCAAGTAAAAGATTCG-3'). Primers contained capped *Sac*I and *Age*I sites to facilitate ligation into the vector pNLAC1 (tetracycline and ampicillin resistant). The cloned *pbpG* was confirmed to be identical to that in strain AB307–0294 by bidirectional DNA sequencing. The pNLAC1::*pbpG* construct was electroporated into AB307.27, generating the complemented strain AB307.27/pNLAC1::*pbpG*. pNLAC1 without insert was electroporated into AB307–0294 and AB307.27, generating the control strains AB307/pNLAC1 and AB307.27/pNLAC1.

Structural analysis. A 3-dimensional homology model of PBP-7/8 (PBP-78A) was created using the automated first approach mode in SWISS-MODEL [29–31]. The sequence of AB307–0294 PBP-7/8 was entered in FASTA format and submitted to the SWISS-MODEL server (available at: http://swissmodel.expasy.org/workspace/index.php?func=modelling_simple1&userid=USERID&token=TOKEN). A BLAST value E-limit for choosing the best template was set to 0.00001. The model PBP-7/8 was returned in Protein Data Bank format. The PBP-7/8 model, the best template, and other templates with identity scores of >25% were superimposed using the secondary structure matching module in Coot [32]. A primary sequence alignment for all templates was performed with ClustalW2 (available at: http://www.ebi.ac.uk/Tools/clustalw2/index.html), using the default settings [33]. The superimposed structures were examined in 3 dimensions, using the graphical display in Coot [34]. The sequence alignment was adjusted by hand to correspond to the overlap of residues in 3-dimensional space.

Rat soft-tissue infection model. The rat pneumonia and soft-tissue infection model animal studies were reviewed and approved by the University at Buffalo and Veterans Administration Institutional Animal Care Committee. An established Long-Evans rat soft-tissue infection model was used as reported elsewhere [35].

Rat pneumonia model. An established Long-Evans rat model for studying pulmonary damage was used as reported elsewhere [36, 37].

Serum bactericidal assay. Complement-mediated bactericidal assays were performed as previously described [38].

Transmission electron microscopy (TEM). TEM was performed as described elsewhere [39].

Statistical analyses. Data are presented as mean values (±SEM). *P* values of .05/*n* (where *n* is the number of comparisons) are considered statistically significant, based on use of Bonferroni correction for multiple comparisons, and *P* values of >.05/*n* but <.05 are considered as representing a trend. To normalize in vitro and in vivo data, $\log_{10}$-transformed values were used. The area under each curve was calculated, and the areas were compared using 2-tailed unpaired *t* tests (Prism 4 for MacIntosh [GraphPad Software]).

RESULTS

Identification of AB307–0294 PBP-7/8. To identify factors in *Acinetobacter* organisms that are necessary for growth and survival in human infection, we used an experimental approach that was a modification of the method we previously used to identify virulence factors in extraintestinal pathogenic *E. coli* [40, 41]. First, random transposon mutagenesis was performed, and transposon mutants were selected on plates with nutrient-rich laboratory medium (i.e., Mueller-Hinton agar). Next, mutants were gridded onto ascites plates, which consisted of 80% human ascites (fluid that accumulates in the peritoneal cavity in pathologic states) and agar. Ascites plates are an ex vivo modified minimal medium and in essence are roughly reflective of inflammatory extracellular fluid, a common environment for extracellular bacterial pathogens such as *Acinetobacter* organisms. This screen resulted in the identification of AB307.27. Quantitative growth curves confirmed that AB307.27 was significantly killed in ascites ($P < .001$), but its growth in laboratory medium (i.e., Luria-Bertani broth) was similar to growth of its parent AB307–0294 ($P = .13$) (figure 1*A*). Chromosomal sequencing, priming off of the EZ-Tn5 <Kan-2> transposon, was performed on DNA purified from AB307.27. The transposon insertion within AB307.27 was in *pbpG* (between nucleotides 462 and 463), which encoded a putative D-alanyl-D-alanine endopeptidase or PBP-7/8. The complete sequence of AB307–0294 PBP-7/8 and its surrounding genes was determined (Genbank accession number EU676123). The open reading frame of *pbpG* contained 1023 nucleotides, which encoded a protein of 340 amino acids with a predicted molecular weight of 35,949 Da. Because the direction of transcription for a putative threonine synthase, encoded by the open reading frame 3' to *pbpG,* was in the opposite direction, the transposon insertion in *pbpG* should not have a polar effect. To confirm this, quantitative growth curves were performed in ascites with the constructs AB307–0294/pNLAC1 (a wild-type parent containing the cloning vector without an insert), AB307.27/pNLAC1 (a PBP-7/8 mutant derivative of AB307–0294 containing the cloning vector without an insert), and AB307.27/pNLAC1::*pbpG* (a PBP-7/8 mutant derivative containing cloned *pbpG*). Growth of the wild-type parent AB307–0294/pNLAC1 was similar to growth of the complemented mutant AB307.27/pNLAC1::*pbpG* ($P = .17$), confirming that inactivation of PBP-7/8 was responsible for decreased growth in ascites. As expected, the non-complemented strain AB307.27/pNLAC1 demonstrated a significant decrease in survival in ascites, compared with AB307–0294/pNLAC1 ($P < .001$) and AB307.27/pNLAC1::*pbpG* ($P < .001$) (figure 1*B*).

In silico analysis of AB307–0294 PBP-7/8. The SWISS-MODEL server created a model covering residues 92–332 of

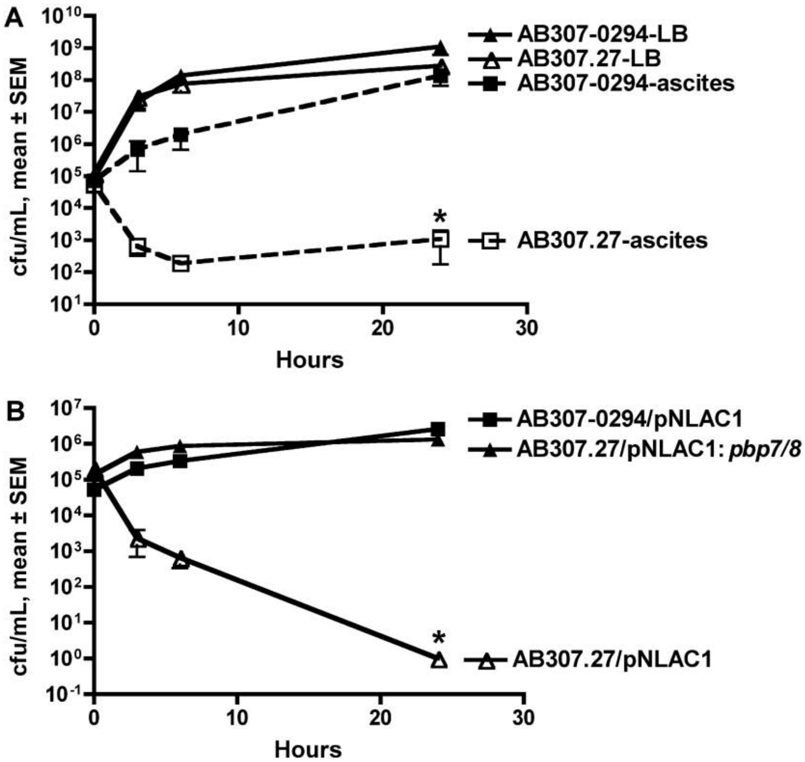

Figure 1. Growth/kill curve for *Acinetobacter baumannii* strains AB307–0294 (wild-type) and derivatives in Luria-Bertani medium and 100% human ascites. *A,* Growth of AB307–0294 and AB307.27 was assessed at 0, 3, 6, and 24 h in each medium. Growth of AB307–0294 ($n = 4$) and AB307.27 ($n = 4$) in Luria-Bertani medium was similar ($P = .13$, by a 2-tailed unpaired t test). In contrast, survival of AB307.27 ($n = 6$) was significantly decreased in ascites, compared with AB307–0294 ($n = 6$) ($^*P < .001$). *B,* Growth of AB307–0294/pNLAC1 (a wild-type parent containing a cloning vector without an insert), AB307.27/pNLAC1 (a penicillin-binding protein [PBP]–7/8 mutant derivative of AB307–0294 containing a cloning vector without an insert), and AB307.27/pNLAC1::*pbp7/8* (a PBP-7/8 mutant derivative containing cloned *pbp7/8*) was assessed at 0, 3, 6, and 24 h in ascites. Growth of AB307–0294/pNLAC1 ($n = 4$) and AB307.27/pNLAC1::*pbp7/8* ($n = 4$) was similar ($P = .17$). In contrast, survival of AB307.27/pNLAC1 ($n = 3$) was significantly decreased in ascites, compared with AB307–0294/pNLAC1 ($^*P < .001$) and AB307.27/pNLAC1::*pbp7/8* ($^*P < .001$).

PBP-7/8, resulting in a final E-score of 3.56e-16. PBP-5 from *E. coli* (Protein Data Bank code 1nj4) was chosen as the best template (27% identity to PBP-7/8) [42]. Other homologous proteins with crystal structures available and >25% identity with PBP-7/8 were PBP-4 from *Staphylococcus aureus* (Protein Data Bank code 1tvf) (Rajashankar et al., unpublished data), PBP-3 from *Streptococcus pneumoniae* (Protein Data Bank code 1xp4) [43], and DD-transpeptidase from *Streptomyces* strain K15 (Protein Data Bank code 1skf) [44]. Surprisingly, even with the low levels of sequence identity, the active site residue motifs SXXK, SXN, and KTG were completely conserved (figure 2). The superposition of all structures placed the active site residues within a root mean square deviation of 1.5 Å from their positions in each structure. Although the sequences surrounding the active site residues were varied, there was strict conservation of the secondary structural elements creating the active site scaffold (figure 2).

```
PBP78A    121---IASITKL MTAVVT ADA--- (34) ---RAEV LLFALMKS ENPAAA ALARTY --- (87 )---NINLSKTG YI--340
PBP5E      95---PASLTKM MTSYVI GQA--- (41) ---VSQL IRGINLQS GNDACV AMADFA --- (85 )---NVDGIKTG HT--427
PBP4SA     59---PASMTKL MTMYLT LEA--- (39) ---IADL LQITVSNS SNAAAL ILAKKV -- (102 )---GTDGLKTG SS--369
PBP3SP     39---IASITKL ITVYLV YEA--- (38) ---VEEL LEATLVSS ANSAAI ALAEKI -- (102 )---GFDGLKTG TT--379
DDPEPS     33---TGSTTKI MTAKVV LAQ--- (36) ---VRQL LYGLMLPS GCDAAY ALADKY --- (99 )---GAIGVKTG SG--262
SS                HHHHHHHHHHHHHHH               HHHHHHHHHTTTHHHHHHHHH                SSSSSSSSS
```

Figure 2. Structural alignment of the AB307–0294 penicillin-binding protein 7/8 (PBP-7/8) model (PBP78A) with homologous PBP crystal structures. The conserved active site residue motifs SXXK, SXN, and KTG are boxed. The secondary structural (SS) elements α-helix (H), β-strand (S), and turn (T) that arrange the active site residues are conserved in each structure. Although PBP78A has low identity with PBP5E (27%), the secondary structural elements serve to present the conserved active site residues in 3-dimensional space. Structures of other homologous proteins are PBP-5 from *Escherichia coli* (PBP5E; Protein Data Bank [PDB] code 1nj4), PBP-4 from *Staphylococcus aureus* (PBP4SA; PDB code 1tvf), PBP3 from *Streptococcus pneumoniae* (PBP3SP; PDB code 1xp4), and DD-transpeptidase from *Streptomyces* strain K15 (DDPEPS; PDB code 1skf). Structures were superimposed using the SSM superposition module of Coot [33].

Table 1. Homology of AB307–0294 PBP-7/8 with other homologues/orthologues.

This table is available in its entirety in the electronic edition of the *Journal of Infectious Diseases*.

Next, the DNA/predicted protein homology of AB307–0294 PBP-7/8 was compared with various homologues/orthologues (table 1, which appears only in the electronic edition of the *Journal*). Finally, a promoter prediction analysis was performed on the 5' DNA sequence to the predicted transcriptional start site of *pbpG* (BPROM [SoftBerry]; available at: http://www.softberry.com/berry.phtml?topic=bprom&group=programs&subgroup=gfindb). A putative promoter, whose transcription is predicted to be directed by the σ^{70} factor, was identified.

AB307.27 (PBP-7/8 negative) has an abnormal morphology. The cell morphology of AB307.27 (PBP-7/8) was assessed via TEM. When grown in logarithmic phase in Luria-Bertani medium, more coccobacillary forms of AB307.27 (PBP-7/8 negative) were observed, compared with its wild-type parent AB307-0294; however, both coccobacillary and bacillary forms were seen with each strain (figure 3). This finding suggests that AB307.27 may possess an abnormal peptidoglycan and suggests that, in *Acinetobacter* organisms, PBP-7/8 may play a more critical role in modulating cell morphology than has been described for other species [22].

AB307.27 (PBP-7/8 negative) is killed in the rat soft-tissue infection model. An in vivo validation of our in vitro findings was needed to confirm that PBP-7/8 was a factor that contributed to *Acinetobacter* infection. Initially, we compared the growth/survival of AB307–0294 (wild-type) and its isogenic derivative AB307.27 (PBP-7/8 negative) in a rat model of soft-tissue infection. A major advantage of this infection model is that multiple samples can be obtained over time from each animal, making it time- and cost-efficient for initial assessment of strains in vivo. Furthermore, it is clinically relevant given that *A. baumannii* has been increasingly recognized as a cause a variety of soft-tissue infections [10, 12]. Compared with AB307–0294, AB307.27 demonstrated a significant decrease in survival in this

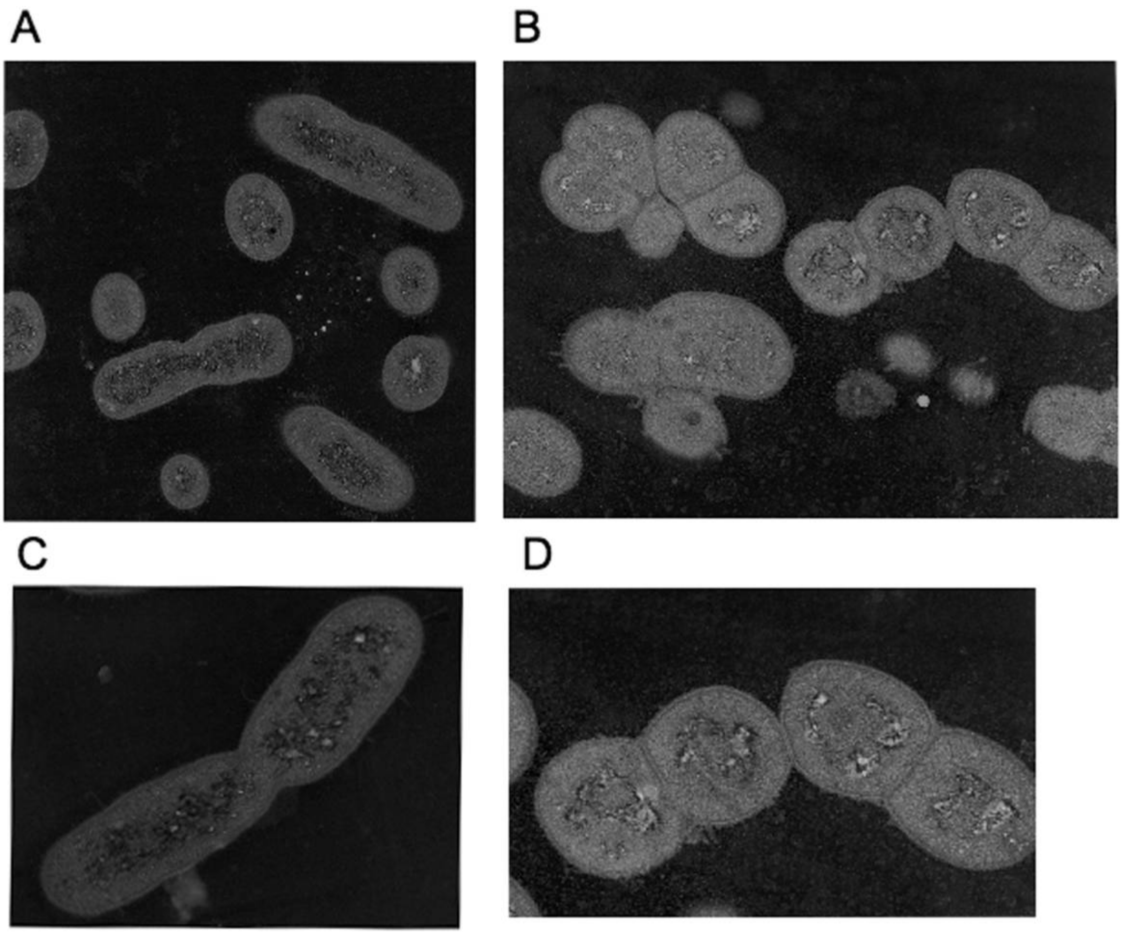

Figure 3. Transmission electron microscopy was performed on AB307–0294 (wild-type) and AB307.27 (penicillin-binding protein 7/8 negative) as described elsewhere [39]. Cells were grown in Luria-Bertani medium in logarithmic phase. *A* and *C,* AB307–0294 (10,000× and 20,000× original magnification, respectively); *B* and *D,* AB307.27 (10,000× and 20,000× original magnification, respectively).

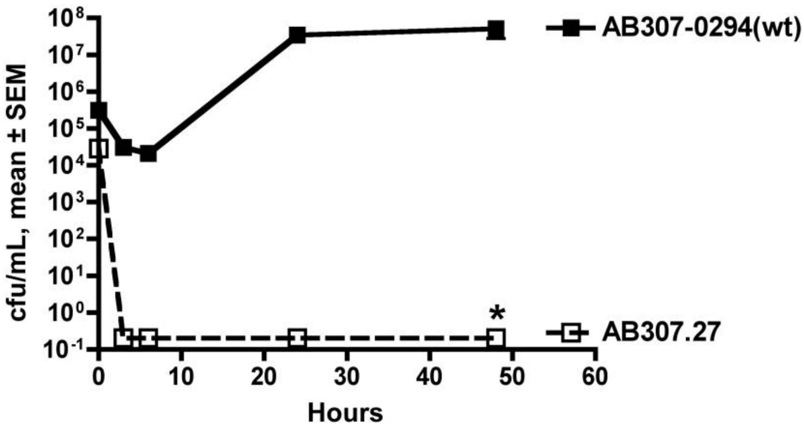

Figure 4. Survival of *Acinetobacter baumannii* strain 307–0294 (wild-type [wt]) and its isogenic derivative AB307.27 (penicillin-binding protein 7/8 negative) in the rat soft-tissue infection model. Rats were prepared and challenged with AB307–0294 and AB307.27 as described elsewhere [35]. Bacterial titers were determined at 0, 3, 6, 24, and 48 h. Survival of AB307.27 ($n = 4$–6 for each time point) was significantly decreased in this model, compared with AB307–0294 ($n = 5$ for each time point) (*$P < .001$, by a 2-tailed unpaired *t* test).

model ($P < .001$) (figure 4). These data demonstrate that PBP-7/8 is important for the survival of AB307–0294 in soft-tissue infection.

AB307.27 (PBP-7/8 negative) is killed in the rat pneumonia model. Next, we compared the growth and survival of AB307–0294 (wild-type) and its isogenic derivative AB307.27 (PBP-7/8 negative) in a rat pneumonia model, another common type of *Acinetobacter* infection. Compared with AB307–0294, AB307.27 demonstrated a significant decrease in survival in this model ($P = .002$) (figure 5). These data demonstrate that PBP-7/8 is important for the survival of AB307–0294 in pulmonary infection.

AB307.27 demonstrates an increase in susceptibility to complement-mediated bactericidal activity. The innate response is instrumental in determining whether extracellular bacterial pathogens such as *Acinetobacter* organisms are successfully cleared or establish an infection. The complement system is a critical component of the host's innate immune system. Therefore, we assessed whether AB307.27 had increased susceptibility to complement-mediated bactericidal activity, compared with its parent, AB307–0294. Compared with AB307–0294, AB307.27 demonstrated a significant decrease in survival in 90% human serum ($P < .001$) (figure 6). These data support the concept that complement-mediated bactericidal activity in vivo is at least one mechanism responsible for the clearance of AB307.27 in the rat soft-tissue infection and pneumonia models.

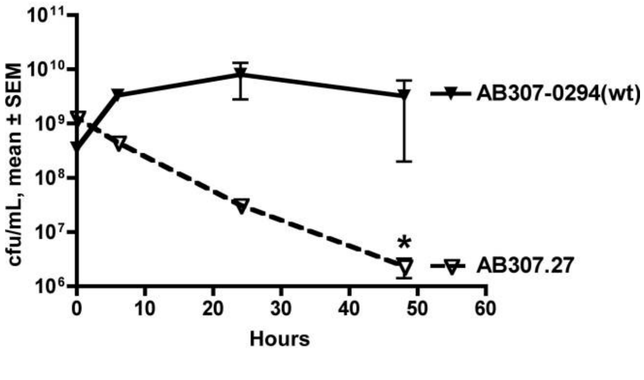

Figure 5. Survival of *Acinetobacter baumannii* strain 307–0294 (wild-type [wt]) and its isogenic derivative AB307.27 (penicillin-binding protein 7/8 negative) in the rat pneumonia model. Rats were challenged with 3.9×10^8 cfu of 307–0294 and 1.3×10^9 cfu of AB307.27 by intratracheal instillation, and total lung bacterial titers were determined at 0, 6, 24, and 48 h. Survival of AB307.27 ($n = 3$) was significantly decreased in this model, compared with AB307–0294 ($n = 3$) (*$P < .002$, by a 2-tailed unpaired *t* test).

Growth of AB307.27 (PBP-7/8 negative) in human urine is similar to that of AB307–0294 (wild-type). The growth of AB307–0294 and AB307.27 in human urine was assessed because the urinary tract is another site that *Acinetobacter* organisms commonly infect. However, in urine, complement levels are low and anticomplement activity may be present [45, 46]. The growth of AB307–0294 and AB307.27 was similar in human urine ($P = .07$) (figure 7). These data demonstrate that PBP-7/8 is not important for the growth/survival of AB307–0294 in human urine.

DISCUSSION

To our knowledge, this is the first report to describe a role for PBP-7/8 in the pathogenesis of infection. We demonstrated that the PBP-7/8–deficient mutant AB307.27, an isogenic derivative of the wild-type *A. baumannii* strain AB307–0294, was killed in human ascites (figure 1). Next, we demonstrated that AB307.27 was also killed in vivo in rat soft-tissue infection and pneumonia models (figures 4 and 5), both important types of *Acinetobacter* infection. We then demonstrated that AB307.27 was killed in 90% human serum in vitro (figure 6). TEM demonstrated more

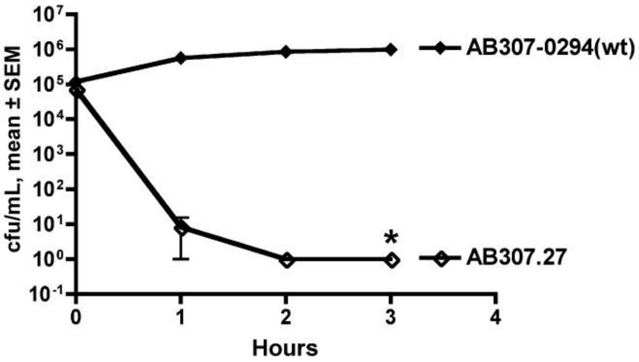

Figure 6. Effect of 90% normal human serum on the viability of the *Acinetobacter baumannii* strain AB307–0294 (wild-type [wt]) and its isogenic derivative AB307.27 (penicillin-binding protein 7/8 negative). Assays were performed as described elsewhere [38]. All strains were also assessed in the presence of 90% heat-inactivated (at 56°C for 30 min) normal human serum, and their growth was similar; therefore these data are not shown. Bacterial titers were determined at 0, 1, 2, and 3 h. Survival of AB307.27 ($n = 4$) was significantly decreased, compared with AB307–0294 ($n = 4$) (*$P < .001$, by a 2-tailed unpaired t test).

coccobacillary forms of AB307.27, compared with AB307–0294 (figure 3), suggesting a possible modulation in the peptidoglycan, which may affect susceptibility to host defense factors. Finally, the growth of AB307.27 was similar to AB307–0294 in human urine (figure 7), an environment in which complement levels are low and anticomplement activity may be present [45, 46]. Taken together, these results demonstrate that PBP-7/8 contributes to the pathogenesis of *A. baumannii* in the rat soft-tissue infection and pneumonia models. Furthermore, PBP-7/8 either directly or indirectly contributes to the resistance of AB307–0294 to complement-mediated bactericidal activity.

PBPs and their role in peptidoglycan synthesis have been extensively reviewed [27, 47, 48]. In brief, bacterial peptidoglycan consists of cross-linked N-acetylglucosamine and N–acetylmuramic acid glycan chains. It is a critical cell structure that provides the bacterium shape and is instrumental in resisting various physical forces [27, 47, 49]. PBPs have been classified as having a high or low molecular mass. High-molecular-mass PBPs enable peptidoglycan polymerization and insertion into the preexisiting cell wall [27, 47]. low-molecular-mass PBPs contribute to cell separation and peptidoglycan remodeling [22, 27, 49]. The low-molecular-mass PBPs have been less well studied than the high-molecular-mass class A and class B enzymes [47, 48]. However, in limited studies involving *E. coli,* low-molecular-mass PBPs, including PBP-7/8, have in general been shown not to be essential when grown in Luria-Bertani medium [21, 22, 25, 26]. PBP-7/8 has been postulated to play a role in cell wall remodeling [20, 50]. In contrast to AB307–0294, in *Salmonella* organisms the expression of PBP-7 is under the direction of the σ^s factor and is induced in carbon-starved medium (starvation-stress response), but a PBP-7–negative mutant was equally virulent as its wild-type parent after oral gavage in a BALB/c mouse sepsis model [50]. Therefore, the dramatic phenotype observed with AB307.27 both in human serum and ascites in vitro and in rat pneumonia and soft-tissue infection models was novel and surprising. We have established that at least 1 mechanism for this phenotype is an increase in susceptibility to complement-mediated bactericidal activity (figure 6). It remains possible that PBP-7/8 directly or indirectly contributes to the resistance of AB307–0294 to the bactericidal activity mediated by professional phagocytes or antimicrobial peptides, but these possibilities were not directly assessed in this report. The increase in coccobacillary forms of AB307.27, compared with AB307–0294, suggests that its peptidoglycan may be altered. However, further quantitative definition of the probable abnormalities in the peptidoglycan in AB307.27 via flow cytometry and/or biochemical methods are required to confirm that the peptidoglycan is truly abnormal in AB307.27 (PBP-7/8 negative)

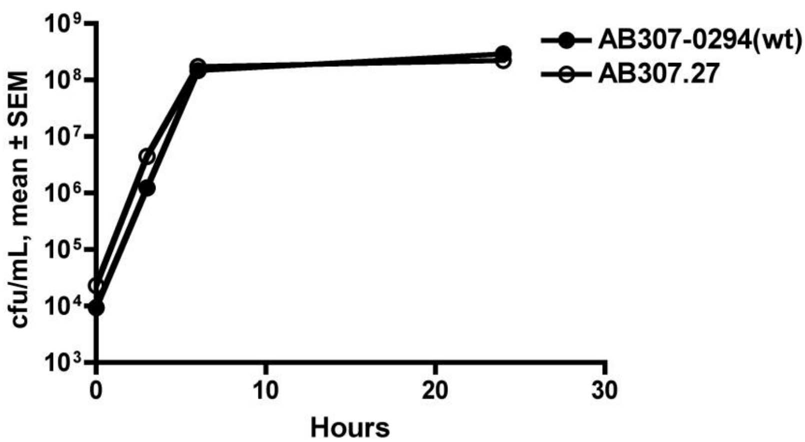

Figure 7. Growth/kill curve for *Acinetobacter baumannii* strain AB307–0294 (wild-type [wt]) and its isogenic derivative AB307.27 (penicillin-binding protein 7/8 negative) in 100% human urine. Growth of AB307–0294 and AB307.27 was assessed at 0, 3, 6, and 24 h in 100% human urine. Growth of AB307–0294 ($n = 4$) and AB307.27 ($n = 3$) in urine was similar ($P = .07$, by a 2-tailed unpaired t test).

and, if so, to define the nature of the change. Furthermore, whether this is a direct or an indirect result of the loss of PBP-7/8 is unresolved. A direct effect, resulting in an alteration in the structure of peptidoglycan due to the loss of PBP-7/8, would seem most likely. However, because PBP-7/8 is a hydrolase, one might predict that overexpression, not a lack of expression, would increase the susceptibility of the bacterium to complement-mediated bactericidal activity. An indirect effect on other PBP or glycolases (e.g., soluble lytic transglycosylase 70), which in turn affects the peptidoglycan structure, or an indirect effect independent of peptidoglycan remain possibilities. Future studies that assess binding of various proteins in the complement system will generate new insights on the mechanism by which PBP-7/8 contributes to complement resistance.

Selection for transposon mutant derivatives of AB307–0294 on laboratory medium and then screening for essentiality on ascites plates were critical for the efficiency of our approach. This simple innovation enabled us able to identify, in one step, genes that are both essential and expressed in vivo. The strength of this approach is that it is unbiased and highly efficient. We did not select the targets but allowed the genetic screen, designed to identify the phenotype of in vivo essentially, to dictate the choices. Furthermore, although we did not identify genes that are essential for growth in laboratory medium, we were able to identify those that are essential for growth/survival in ascites but not Mueller-Hinton medium, a more interesting mutant set. Subsequent identification of the gene into which the transposon inserted in mutants of interest by chromosomal sequencing and an in vivo assessment in the soft-tissue infection model resulted in a relatively efficient approach for identifying previously unrecognized and unknown virulence factors, as well as potential drug targets.

In summary, we have established that PBP-7/8 is critical for the survival of *A. baumannii* strain AB307–0294 in the rat soft-tissue infection and pneumonia models. Furthermore, PBP-7/8 either directly or indirectly contributes to the resistance of AB307–0294 to complement-mediated bactericidal activity. An understanding of how PBP-7/8 contributes to serum resistance will lend insight into the role of this low-molecular-mass PBP whose function is poorly understood.

Acknowledgments

We thank Steven R. Gill for assistance with the promoter prediction analysis and Thomas W. Loehfelm for helpful discussions regarding the construction of the cloning vector pNLAC1.

References

1. Munoz-Price LS, Weinstein RA. *Acinetobacter* infection. N Engl J Med **2008**; 358:1271–81.
2. Fournier PE, Richet H. The epidemiology and control of *Acinetobacter baumannii* in health care facilities. Clin Infect Dis **2006**; 42:692–9.
3. Richet H, Fournier PE. Nosocomial infections caused by *Acinetobacter baumannii*: a major threat worldwide. Infect Control Hosp Epidemiol **2006**; 27:645–6.
4. Joly-Guillou ML. Clinical impact and pathogenicity of *Acinetobacter*. Clin Microbiol Infect **2005**; 11:868–73.
5. Falagas ME, Karveli EA. The changing global epidemiology of *Acinetobacter baumannii* infections: a development with major public health implications. Clin Microbiol Infect **2007**; 13:117–9.
6. Gaynes R, Edwards JR. Overview of nosocomial infections caused by gram-negative bacilli. Clin Infect Dis **2005**; 41:848–54.
7. Anstey NM, Currie BJ, Hassell M, Palmer D, Dwyer B, Seifert H. Community-acquired bacteremic *Acinetobacter* pneumonia in tropical Australia is caused by diverse strains of *Acinetobacter baumannii,* with carriage in the throat in at-risk groups. J Clin Microbiol **2002**; 40:685–6.
8. Chen MZ, Hsueh PR, Lee LN, Yu CJ, Yang PC, Luh KT. Severe community-acquired pneumonia due to *Acinetobacter baumannii*. Chest **2001**; 120:1072–7.
9. Tong MJ. Septic complications of war wounds. JAMA **1972**; 219:1044–7.
10. Centers for Disease Control and Prevention. *Acinetobacter baumannii* infections among patients at military medical facilities treating injured US service members, 2002–2004. MMWR **2004**; 53:1063–6.
11. Scott P, Deye G, Srinivasan A, et al. An outbreak of multidrug-resistant *Acinetobacter baumannii-calcoaceticus* complex infection in the US military health care system associated with military operations in Iraq. Clin Infect Dis **2007**; 44:1577–84.
12. Davis KA, Moran KA, McAllister CK, Gray PJ. Multidrug-resistant *Acinetobacter* extremity infections in soldiers. Emerg Infect Dis **2005**; 11:1218–24.
13. Maegele M, Gregor S, Steinhausen E, et al. The long-distance tertiary air transfer and care of tsunami victims: injury pattern and microbiological and psychological aspects. Crit Care Med **2005**; 33:1136–40.
14. Rice LB. Challenges in identifying new antimicrobial agents effective for treating infections with *Acinetobacter baumannii* and *Pseudomonas aeruginosa*. Clin Infect Dis **2006**; 43(Suppl):S100–5.
15. Perez F, Hujer AM, Hujer KM, Decker BK, Rather PN, Bonomo RA. Global challenge of multidrug-resistant *Acinetobacter baumannii*. Antimicrob Agents Chemother **2007**; 51:3471–84.
16. Sunenshine RH, Wright MO, Maragakis LL, et al. Multidrug-resistant *Acinetobacter* infection mortality rate and length of hospitalization. Emerg Infect Dis **2007**; 13:97–103.
17. Paterson DL, Doi Y. A step closer to extreme drug resistance (XDR) in gram-negative bacilli. Clin Infect Dis **2007**; 45:1179–81.
18. Talbot GH, Bradley J, Edwards JE Jr, Gilbert D, Scheld M, Bartlett JG. Bad bugs need drugs: an update on the development pipeline from the Antimicrobial Availability Task Force of the Infectious Diseases Society of America. Clin Infect Dis **2006**; 42:657–68.
19. Loehfelm TW, Luke NR, Campagnari AA. Identification and characterization of an *Acinetobacter baumannii* biofilm-associated protein. J Bacteriol **2008**; 190:1036–44.
20. Romeis T, Holtje JV. Penicillin-binding protein 7/8 of *Escherichia coli* is a DD-endopeptidase. Eur J Biochem **1994**; 224:597–604.
21. Denome SA, Elf PK, Henderson TA, Nelson DE, Young KD. *Escherichia coli* mutants lacking all possible combinations of eight penicillin binding proteins: viability, characteristics, and implications for peptidoglycan synthesis. J Bacteriol **1999**; 181:3981–93.
22. Meberg BM, Paulson AL, Priyadarshini R, Young KD. Endopeptidase penicillin-binding proteins 4 and 7 play auxiliary roles in determining uniform morphology of *Escherichia coli*. J Bacteriol **2004**; 186:8326–36.
23. Henderson TA, Dombrosky PM, Young KD. Artifactual processing of penicillin-binding proteins 7 and 1b by the OmpT protease of *Escherichia coli*. J Bacteriol **1994**; 176:256–9.
24. Romeis T, Holtje JV. Specific interaction of penicillin-binding proteins 3 and 7/8 with soluble lytic transglycosylase in *Escherichia coli*. J Biol Chem **1994**; 269:21603–7.
25. Priyadarshini R, de Pedro MA, Young KD. Role of peptidoglycan amidases in the development and morphology of the division septum in *Escherichia coli*. J Bacteriol **2007**; 189:5334–47.

26. Priyadarshini R, Popham DL, Young KD. Daughter cell separation by penicillin-binding proteins and peptidoglycan amidases in *Escherichia coli*. J Bacteriol **2006**; 188:5345–55.
27. Sauvage E, Kerff F, Terrak M, Ayala JA, Charlier P. The penicillin-binding proteins: structure and role in peptidoglycan biosynthesis. FEMS Microbiol Rev **2008**; 32:234–58.
28. Ecker JA, Massire C, Hall TA, et al. Identification of *Acinetobacter* species and genotyping of *Acinetobacter baumannii* by multilocus PCR and mass spectrometry. J Clin Microbiol **2006**; 44:2921–32.
29. Arnold K, Bordoli L, Kopp J, Schwede T. The SWISS-MODEL workspace: a web-based environment for protein structure homology modelling. Bioinformatics **2006**; 22:195–201.
30. Guex N, Peitsch MC. SWISS-MODEL and the Swiss-PdbViewer: an environment for comparative protein modeling. Electrophoresis **1997**; 18: 2714–23.
31. Schwede T, Kopp J, Guex N, Peitsch MC. SWISS-MODEL: an automated protein homology-modeling server. Nucleic Acids Res **2003**; 31: 3381–5.
32. Emsley P, Cowtan K. Coot: model-building tools for molecular graphics. Acta Crystallogr D Biol Crystallogr **2004**; 60:2126–32.
33. Larkin MA, Blackshields G, Brown NP, et al. Clustal W and Clustal X version 2.0. Bioinformatics **2007**; 23:2947–8.
34. Krissinel E, Henrick K. Secondary-structure matching (SSM), a new tool for fast protein structure alignment in three dimensions. Acta Crystallogr D Biol Crystallogr **2004**; 60:2256–68.
35. Russo TA, Beanan JM, Olson R, et al. Rat pneumonia and soft-tissue infection models for the study of *Acinetobacter baumannii* biology. Infect Immun **2008**; 76:3577–86.
36. Russo TA, Bartholomew LA, Davidson BA, et al. Total extracellular surfactant is increased but abnormal in a rat model of gram-negative bacterial pneumonia. Am J Physiol Lung Cell Molec Physiol **2002**; 283: L655–63.
37. Russo TA, Davidson BA, Carlino-MacDonald UB, Helinski JD, Priore RL, Knight PR 3rd. The effects of *Escherichia coli* capsule, O-antigen, host neutrophils, and complement in a rat model of gram-negative pneumonia. FEMS Microbiol Lett **2003**; 226:355–61.
38. Russo T, Sharma G, Brown C, Campagnari A. The loss of the O4 antigen moiety from the lipopolysaccharide of an extraintestinal isolate of *Escherichia coli* has only minor effects on serum sensitivity and virulence in vivo. Infect Immun **1995**; 63:1263–9.
39. Nazareth H, Genagon SA, Russo TA. Extraintestinal pathogenic *Escherichia coli* survives within neutrophils. Infect Immun **2007**; 75:2776–85.
40. Russo TA, Jodush ST, Brown JJ, Johnson JR. Identification of two previously unrecognized genes *(guaA, argC)* important for uropathogenesis. Mol Microbiol **1996**; 22:217–29.
41. Russo T, Carlino U, Mong A, Jodush S. Identification of genes in an extraintestinal isolate of *Escherichia coli* with increased expression after exposure to human urine. Infect Immun **1999**; 67:5306–14.
42. Nicholas RA, Krings S, Tomberg J, Nicola G, Davies C. Crystal structure of wild-type penicillin-binding protein 5 from *Escherichia coli:* implications for deacylation of the acyl-enzyme complex. J Biol Chem **2003**;278: 52826–33.
43. Morlot C, Pernot L, Le Gouellec A, et al. Crystal structure of a peptidoglycan synthesis regulatory factor (PBP3) from *Streptococcus pneumoniae*. J Biol Chem **2005**; 280:15984–91.
44. Fonze E, Vermeire M, Nguyen-Disteche M, Brasseur R, Charlier P. The crystal structure of a penicilloyl-serine transferase of intermediate penicillin sensitivity: the DD-transpeptidase of streptomyces K15. J Biol Chem **1999**; 274:21853–60.
45. Acquatella H, Little PJ, de Wardener HE, Coleman JC. The effect of urine osmolality and pH on the bactericidal activity of plasma. Clin Sci **1967**; 33:471–80.
46. Beeson PB, Rowley D. The anticomplementary effect of kidney tissue; its association with ammonia production. J Exp Med **1959**; 110:685–97.
47. Macheboeuf P, Contreras-Martel C, Job V, Dideberg O, Dessen A. Penicillin binding proteins: key players in bacterial cell cycle and drug resistance processes. FEMS Microbiol Rev **2006**; 30:673–91.
48. Stewart GC. Taking shape: control of bacterial cell wall biosynthesis. Mol Microbiol **2005**; 57:1177–81.
49. Vollmer W, Joris B, Charlier P, Foster S. Bacterial peptidoglycan (murein) hydrolases. FEMS Microbiol Rev **2008**; 32:259–86.
50. Kenyon WJ, Nicholson KL, Rezuchova B, et al. σ^s-dependent carbon-starvation induction of *pbpG* (PBP 7) is required for the starvation-stress response in *Salmonella enterica* serovar Typhimurium. Microbiology **2007**; 153:2148–58.

INFECTION AND IMMUNITY, Aug. 2008, p. 3577–3586 Vol. 76, No. 8
0019-9567/08/$08.00+0 doi:10.1128/IAI.00269-08

Rat Pneumonia and Soft-Tissue Infection Models for the Study of *Acinetobacter baumannii* Biology$^{\nabla}$

Thomas A. Russo,[1,2,3,4,5]* Janet M. Beanan,[2,4] Ruth Olson,[2,4] Ulrike MacDonald,[2,4] Nicole R. Luke,[3,4,5] Steven R. Gill,[4,5,6] and Anthony A. Campagnari[3,4,5]

Veterans Administration Western New York Healthcare System,[1] Department of Medicine,[2] Department of Microbiology,[3] The Witebsky Center for Microbial Pathogenesis,[4] Center of Excellence in Bioinformatics and Life Sciences,[5] and Department of Oral Biology,[6] University at Buffalo-State University of New York, Buffalo, New York 14214

Received 26 February 2008/Accepted 28 May 2008

***Acinetobacter baumannii* is a bacterial pathogen of increasing medical importance. Little is known about its mechanisms of pathogenesis, and safe reliable agents with predictable activity against *A. baumannii* are presently nonexistent. The availability of relevant animal infection models will facilitate the study of *Acinetobacter* biology. In this report we tested the hypothesis that the rat pneumonia and soft-tissue infection models that our laboratory had previously used for studies of extraintestinal pathogenic *Escherichia coli* were clinically relevant for *A. baumannii*. Advantages of these models over previously described models were that the animals were not rendered neutropenic and they did not receive porcine mucin with bacterial challenge. Using the *A. baumannii* model pathogen 307-0294 as the challenge pathogen, the pneumonia model demonstrated all of the features of infection that are critical for a clinically relevant model: namely, bacterial growth/clearance, an ensuing host inflammatory response, acute lung injury, and, following progressive bacterial proliferation, death due to respiratory failure. We were also able to demonstrate growth of 307-0294 in the soft-tissue infection model. Next we tested the hypothesis that the soft-tissue infection model could be used to discriminate between the inherent differences in virulence of various *A. baumannii* clinical isolates. The ability of *A. baumannii* to grow and/or be cleared in this model was dependent on the challenge strain. We also hypothesized that complement is an important host factor in protecting against *A. baumannii* infection in vivo. In support of this hypothesis was the observation that the serum sensitivity of various *A. baumannii* clinical isolates in vitro roughly paralleled their growth/clearance in the soft-tissue infection model in vivo. Lastly we hypothesized that the soft-tissue infection model would serve as an efficient screening mechanism for identifying gene essentiality for drug discovery. Random mutants of 307-0294 were initially screened for lack of growth in human ascites in vitro. Selected mutants were subsequently used for challenge in the soft-tissue infection model to determine if the disrupted gene was essential for growth in vivo. Using this approach, we have been able to successfully identify a number of genes essential for the growth of 307-0294 in vivo. In summary, these models are clinically relevant and can be used to study the innate virulence of various *Acinetobacter* clinical isolates and to assess potential virulence factors, vaccine candidates, and drug targets in vivo and can be used for pharmacokinetic and chemotherapeutic investigations.**

Acinetobacter species are highly prevalent in the environment and have been cultured from moist skin in healthy humans, but increased colonization of skin and respiratory and gastrointestinal tracts occurs in individuals in long-term care and hospital facilities. The overwhelming majority of infections described until recently have been acquired mainly in hospitals, to a lesser degree in long-term care facilities, and only rarely from the community. *Acinetobacter baumannii* accounts for 1 to 3% of hospital-acquired infections and 2 to 10% of infections in intensive care units (14, 33, 49). Both sporadic and epidemic infections occur, usually after the first week of hospitalization (3, 13, 14, 19, 51). Importantly, the incidence of *Acinetobacter* infection is increasing worldwide (13, 16, 33). The respiratory tract, particularly in ventilated patients (6.9% of hospital-acquired pneumonias in 2003 based on National Nosocomial Infection Surveillance System data); the urinary tract; intravenous devices; surgical sites; and decubitus or diabetic ulcers are favored sites of infection. Mortality rates associated with *Acinetobacter* infection range from 19 to 54% (16). Interestingly, *A. baumannii* has been reported to uncommonly cause severe community-acquired pneumonia, usually in abnormal hosts (e.g., alcoholics), with the preponderance of cases reported from warm and humid geographic locales (1, 2, 6). Further, the importance of *Acinetobacter* infections in war-related injuries is now established. *A. baumannii* was the most common gram-negative bacillus recovered from traumatic injuries to the lower extremities during the Vietnam War (48). Most recently a new series of infections due to *A. baumannii* has been reported in U.S. service members injured in Iraq, Kuwait, and Afghanistan (5, 10, 11, 18, 44). The majority of patients sustained traumatic injuries, and infectious syndromes included soft-tissue infection, osteomyelitis, pneumonia, and bacteremia (30). Lastly, *Acinetobacter* emerged as an important pathogen in survivors of the Asian tsunami in 2004 (15, 24). In summary, the changing epidemiology and incidence of infections due to *Acinetobacter* establish it as a pathogen of increasing medical importance.

In many centers the incidence of infections due to highly

* Corresponding author. Mailing address: Department of Medicine, Division of Infectious Diseases, University at Buffalo, 3435 Main St., Biomedical Research Building (Room 141), Buffalo, NY 14214. Phone: (716) 829-2674. Fax: (716) 829-3889. E-mail: trusso@acsu.buffalo.edu.
$^{\nabla}$ Published ahead of print on 9 June 2008.

antibiotic-resistant strains is making treatment challenging (17, 29, 32, 45, 47, 50). Particularly problematic are panresistant strains. In a 1999 New York City outbreak, 12% of *A. baumannii* isolates were resistant to all standard antimicrobials (23). These rates are higher outside the United States. Safe reliable agents with predictable activity against *A. baumannii* are presently nonexistent.

The need for an increased understanding of *Acinetobacter* pathogenesis, identification of virulence factors, and the identification and testing of vaccine candidates and new antimicrobial targets is more pressing than ever (28, 46). In order to accomplish these goals it is critical to identify/develop relevant animal models of infection. To date, *Acinetobacter* has been used in a variety of animal models, including murine (21, 22, 25, 26, 31, 36) and guinea pig (4) pneumonia models, a rat thigh infection model (27), and a rabbit endocarditis model (35). However, the clinical relevance and suitability of these models vary depending on the hypothesis being tested. In this report we tested the hypothesis that the rat pneumonia and soft-tissue infection models that our laboratory had previously used for studies of extraintestinal pathogenic *Escherichia coli* were clinically relevant for studying *A. baumannii* infection. Next we tested the hypothesis that the soft-tissue infection model could be used to discriminate between the inherent differences in virulence of various *A. baumannii* clinical isolates. We also hypothesized that complement is an important host factor in protecting against *A. baumannii* infection in vivo. Lastly we hypothesized that the soft-tissue infection model would serve as an efficient screening mechanism for establishing gene essentiality for drug discovery. The results suggest that these models are well suited and clinically relevant for testing and answering a variety of questions related to infections due to *A. baumannii*.

MATERIALS AND METHODS

Bacterial strains and media. *A. baumannii* strain 307-0294 (blood isolate, sequence type 15 [ST15], clonal group 1 based on the work of Ecker et al. [12]) was isolated from a patient hospitalized at Erie County Medical Center, Buffalo, NY. *A. baumannii* strains 853 (OIFC031) (blood isolate, ST11, clonal group II), 855 (OIFC075) (axillary isolate, ST14, clonal group III), 900 (OIFC111) (perineal isolate, ST19, clonal group undetermined), and 979 (OIFC327) (environmental isolate, ST24, clonal group undetermined) were isolated from infected military personnel serving in Iraq and Afghanistan (kindly provided by David Craft and Paul Scott of the Walter Reed Army Medical Center). All strains were grown in Luria-Bertani (LB) medium unless stated otherwise and were maintained at −80°C in 50% LB broth and 50% glycerol. Ascites plates consisted of 80% human ascites and 20% water. Two hundred milliliters of water and 15 g of Bacto agar were autoclaved and cooled to 45°C, 800 ml of ascites and kanamycin (40-μg/ml final concentration) was added, and plates were poured. For quantitative growth curves in ascites, 100% human ascites was utilized.

Rat pneumonia model. The rat pneumonia and soft-tissue infection model animal studies were reviewed and approved by the University at Buffalo and Veterans Administration Institutional Animal Care Committee. An established rat (Long-Evans) model for studying pulmonary damage was used as reported previously (39, 41). In brief, Long-Evans rats (250 to 300 g) were anesthetized with 3.5% halothane in 100% oxygen until unconscious and then maintained at 3.5% halothane. The trachea was exposed surgically, and a 4-in. piece of 1-0 silk was slipped under the trachea to facilitate instillation of the inoculum. The animals were suspended in a supine position on a 60°-incline board. Pulmonary instillation of bacteria prepared in 1× phosphate-buffered saline (PBS) (pH 7.4) was introduced intratracheally (1.2 ml/kg of body weight) via a 1-ml syringe and 26-gauge needle, and the incision was closed with surgical staples. Animals were sacrificed at 3, 6, 24, 48, 72, and 168 h postinoculation for assessments of bacterial growth/clearance, the pulmonary inflammatory response, and lung injury. At harvest, halothane anesthesia was performed, a fraction of inspired oxygen (FiO_2) of 98% was administered, and a midline incision was made through the peritoneum and thoracic cavity. An arterial blood gas sample was obtained from the descending aorta in a 1-ml heparinized syringe. The pulmonary vasculature was flushed of residual blood by injecting the right ventricle with 20 ml of 1× Hanks' balanced salt solution plus 7.5% $NaHCO_3$ (pH 7.2) using a 22-gauge needle. Next, bronchoalveolar lavage (BAL) was performed with 15 ml of normal saline (37°C) that was administered into the lungs by gravity via a tracheal cannula. The recovered BAL fluid (BALF) was kept on ice. A 500-μl aliquot of recovered BALF was removed for subsequent measurement of bacterial CFU. The remaining BALF was centrifuged at 1,500 × *g* to pellet the cellular fraction. The supernatant was removed and frozen at −80°C for cytokine/chemokine assessments (see subsequent section on pulmonary inflammatory response). The cellular fraction was resuspended in 3 ml of ice-cold 1× PBS, carefully layered over 2 ml of cold-filtered 2% bovine serum albumin in 1× PBS, centrifuged at 150 × *g*, and resuspended in 4 ml of ice-cold 1× PBS. Lastly, the lungs were removed and kept at 4°C.

(i) Assessment of bacterial growth/clearance. Intact, excised post-BAL lungs were weighed and suspended in normal saline to a total weight of 10 g (assumed to equate to 10 ml). The addition of saline served as a vehicle for homogenization and to generate a constant volume for each so that titers could be easily calculated. Lungs were then homogenized on ice (three bursts of 3-s duration each) using a Polytron PT-2000 homogenizer (Brinkman Instruments, Westbury, NY). Total *Acinetobacter* titers were determined by enumerating combined bacteria in BALF plus post-BAL lung tissue as described previously (41).

(ii) Assessment of the pulmonary host response. ***(a)*** **Measurement of rat TNF-α, IL-1β, and CINC-1 levels in BALF.** Sandwich enzyme-linked immunosorbent assays utilizing commercial antibodies and standards (R&D Systems Inc., Minneapolis, MN) were employed in measuring levels of rat tumor necrosis factor alpha (TNF-α), interleukin-1β (IL-1β), and cytokine-induced neutrophil chemoattractant 1 (CINC-1) as described previously (40).

(b) **Measurement of BALF cell counts.** A 50-μl aliquot was diluted 1:200 in Isoton II solution (Beckman Coulter), and the leukocyte concentration was determined using a Multisizer 3 Coulter Counter (Beckman Coulter). A cytoslide was prepared by diluting cells to a final concentration of 5×10^4 leukocytes, using a Cytospin 3 cytocentrifuge (Shandon, Pittsburgh, PA), staining with Diff-Quik reagents (Baxter, Miami, FL), and examination by light microscopy (Nikon Microscope ECLIPSE 80i; Nikon Instruments Inc., Melville, NY).

(iii) Assessment of lung injury. Arterial blood oxygenation was measured (ABL5; Radiometer America, Westlake, OH) and reported as the arterial partial pressure of oxygen divided by the fraction of inspired oxygen (PaO_2/FiO_2 ratio). Albumin concentrations in cell-free BAL were measured by enzyme-linked immunosorbent assay using a polyclonal rabbit anti-mouse albumin antibody (a gift from Daniel Remick, University of Michigan, Ann Arbor, MI) and horseradish peroxidase-labeled goat anti-rabbit immunoglobulin (Pharmingen, San Diego, CA) (9). Rat albumin (Sigma, St. Louis, MO) was used as a standard.

Rat soft-tissue infection model. Long-Evans rats (200 to 250 g) were anesthetized as described for the pneumonia model. A subcutaneous space was created on the back of each rat by injecting 50 ml of air subcutaneously and then injecting a mixture of sterile vegetable oil (975 μl) and croton oil (25 μl) in the space created. After 7 days this resulted in an encapsulated "pouch" that was filled with an exudative fluid (pouch fluid), mimicking a subcutaneous abscess. This model has been well characterized (7, 8). It is a dynamic model, as evidenced by the fact that neutrophils will migrate into the pouch in response to appropriate stimuli. Bacteria can be introduced into the pouch, and pouch fluid can be easily removed over time, enabling the study of both microbial and host responses. On day 8, approximately 5×10^6 CFU of the *A. baumannii* strain being assessed was injected into the pouches of anesthetized animals, resulting in estimated starting pouch concentrations of 1×10^5 to 2×10^5 CFU/ml. Within 1 minute after the bacteria were injected into the pouch, 0.5 ml of pouch fluid was removed to measure the actual starting bacterial titer. Fluid aliquots (0.5 ml) were subsequently obtained from anesthetized animals 3, 6, 24, and 48 h after the initial bacterial challenge, and bacterial titers were determined by enumerating bacterial CFU in pouch fluid by serial 10-fold dilutions in 1× PBS.

Serum bactericidal assay. Complement-mediated bactericidal assays were performed by measuring the change in bacterial titer over time in the presence of 90% active or inactive (heated at 56°C for 30 min) human serum. An input bacterial titer of approximately 1×10^5 CFU was utilized, and titers were measured at 0, 1, 2, and 3 h as described previously (38, 43).

Transposon mutagenesis and screen for lack of growth on ascites plates. Electrocompetent cells were generated by growing AB307-0294 in Mueller-Hinton (MH) broth to an A_{600} of around 0.4. Fifteen milliliters of cells was washed once with 1 ml of ice-cold sterile milli-Q-filtered H_2O (Millipore, Billerica, MA), followed by two washes with 10% ice-cold, sterile glycerol. After the last wash, the cells were

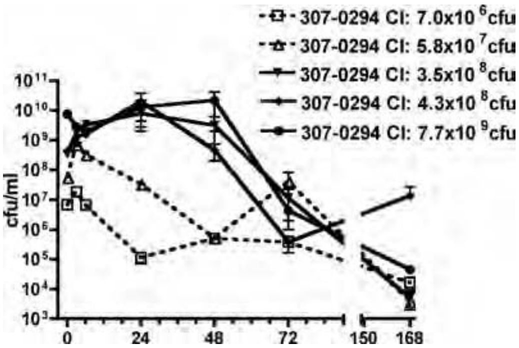

FIG. 1. Growth/clearance of different titers of *A. baumannii* strain 307-0294 in the rat pneumonia model. Rats were challenged with 7.0 × 10^6, 5.8 × 10^7, 3.5 × 10^8, 4.3 × 10^8, and 7.7 × 10^9 CFU of 307-0294 (blood isolate, ST15, clonal group 1) by intratracheal instillation, and total lung bacterial titers were determined at 0, 3, 6, 24, 48, 72, and 168 h. Data are means ± standard errors of the means for n = 3 for each challenge titer and time point.

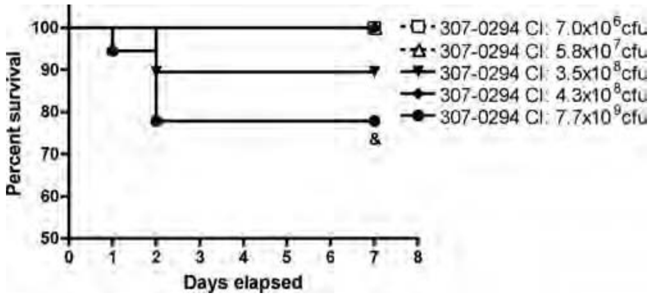

FIG. 2. Survival of rats in the pneumonia model post-challenge with different titers of *A. baumannii* strain 307-0294. Rats were challenged with 7.0 × 10^6 (n = 18), 5.8 × 10^7 (n = 19), 3.5 × 10^8 (n = 19), 4.3 × 10^8 (n = 18), and 7.7 × 10^9 (n = 18) CFU of 307-0294 by intratracheal instillation, and survival was recorded. There was a trend for increased survival in rats challenged with 7.0 × 10^6 and 5.8 × 10^7 CFU compared to rats challenged with 7.7 × 10^9 CFU (&, P = 0.03).

resuspended in 75 μl and either used immediately or stored at −80°C prior to use. EZ-Tn5<kan-2>Tnp Transposome (60 ng in 3 μl) (Epicentre Biotechnologies; catalog no. TSM99K2; Madison, WI) was electroporated into 75 μl electrocompetent AB307 (Bio-Rad Gene Pulser; 25 mF/2.5 kV/200 Ω) using an 0.2-cm-gap, ice-cold EPchamber (Bio-Rad Laboratories, Hercules, CA). Immediately after electroporation cells were resuspended in S.O.C. medium (Invitrogen, Carlsbad, CA) and grown at 37°C for 1 h. Aliquots were then plated on MH plates supplemented with kanamycin (40 μg/ml), and isolated colonies were purified on the same medium. These 307 mutants (presumably 307-0294::Tn5<kan-2>) were subsequently gridded onto ascites-kanamycin plates. 307-0294 mutants that were confirmed to have minimal or no growth on the ascites-kanamycin plates were numbered consecutively and stored at −80°C.

DNA sequencing and analysis. The location of the transposon insertion in mutant derivatives of 307-0294 was determined by chromosomal sequencing. Chromosomal DNA was prepared from the 307 mutants of interest by using a Qiagen DNeasy tissue kit (Qiagen, Valencia, CA) following the protocol for gram-negative bacteria. UV spectroscopy was used to determine concentrations. DNA was used immediately or frozen at −20°C. Cycle sequencing was performed off the EZ-Tn5<kan-2> Transposon (Epicentre Biotechnologies) using the BigDye Terminator v3.1 Cycle Sequencing Kit (Applied Biosystems), following the protocol for sequencing genomic DNA. The KAN-2 FP-1 forward primer included in the transposon kit was used. Cycle sequencing was performed on 20-μl reaction mixtures with the following protocol: 96°C for 5 min, 96°C for 30 s, 50°C for 10 s, 60°C for 4 min (40 cycles)/4°C, and ramping at 1°C/s. Next DNA was precipitated by adding 30 ml of 80% isopropanol to each reaction mixture. Reaction mixtures were allowed to stand in the dark for 15 min and then centrifuged for 15 min at 2,097 × g at 4°C in a 5415 R refrigerated centrifuge (Eppendorf). Supernatant was removed, and 70% ethanol was added to each reaction mixture. Reaction mixtures were again centrifuged for 15 min at 2,097 × g and 4°C. Supernatants were removed, and reaction mixtures were air dried for 10 min in the dark. Afterwards 20 ml HiDi formamide (Applied Biosystems) was added to each reaction mixture. Each was vortexed for 15 s. Sanger sequencing was performed on a 3130xl Genetic Analyzer DNA sequencer (Applied Biosystems) according to the manufacturer's protocol. Sequence comparisons were performed via BLAST analysis of the nonredundant GenBank sequences.

Statistical analyses. Data are presented as means ± standard errors of the means. P values of 0.05/n (n = number of comparisons) are considered statistically significant based on the Bonferroni correction for multiple comparisons, and P values of >0.05/n but <0.05 are considered as representing a trend. In vivo and in vitro data were shown to be normally distributed by the Kolmogorov-Smirnov normality test (P > 0.10, alpha = 0.05) (Prism 4 for MacIntosh; GraphPad Software Inc.) and were analyzed using two-tailed unpaired t or log rank tests.

RESULTS

The rat pneumonia model is clinically relevant for assessing *Acinetobacter* infection. *Acinetobacter* is capable of causing both community-acquired and nosocomial pneumonia. Therefore, we tested the hypothesis that the immunocompetent rat pneumonia model that our laboratory had previously used for studies of extraintestinal pathogenic *E. coli* was clinically relevant for *A. baumannii* (39–42). The pertinent features of gram-negative bacterial pneumonia were evaluated: namely, bacterial growth (or clearance), the ensuing host inflammatory response, acute lung injury, and death due to respiratory failure following progressive bacterial proliferation.

Bacterial growth/clearance. Rats underwent intratracheal challenge with various titers (7.0 × 10^6 to 7.7 × 10^9 CFU) of *A. baumannii* strain 307-0294 (blood isolate, ST15, clonal group 1) to determine whether growth or clearance occurred in this in vivo pneumonia model over 7 days (Fig. 1). Overall, growth/clearance roughly correlated with the magnitude of the challenge inoculum. For the highest challenge titer (7.7 × 10^9 CFU) net growth occurred over the first 48 h, and for the next two highest challenge titers (3.5 × 10^8 and 4.3 × 10^8 CFU) net growth occurred over the first 24 h. However, by 72 h net clearance occurred for all challenge titers. By day 7, although clearance occurred for all challenge titers, it was not complete. Taken together, these data support the contention that *A. baumannii* is able to survive and grow in the rat pneumonia model and that this is dependent on the challenge inoculum.

Survival. Rats underwent intratracheal challenge with various titers (7.0 × 10^6 to 7.7 × 10^9 CFU) of 307-0294 to determine if mortality occurred in this in vivo pneumonia model over 7 days (Fig. 2). No deaths occurred after challenge with 7.0 × 10^6 (n = 18), 5.8 × 10^7 (n = 19), and 4.3 × 10^8 (n = 18) CFU. Two and four deaths occurred 24 to 48 h after challenge with 3.5 × 10^8 (n = 19) and 7.7 × 10^9 (n = 18) CFU, respectively. There was a trend for increased survival in rats challenged with 7.0 × 10^6 and 5.8 × 10^7 CFU compared to rats challenged with 7.7 × 10^9 CFU (P = 0.03). These data support the contention that *A. baumannii* is able to cause lethal pulmonary infection in the rat pneumonia model and that this is dependent on the challenge inoculum. Further, growth/clearance (see "Bacterial growth/clearance" above), oxygenation, and BALF albumin data (see "Acute lung injury" below) suggest that death, at least in part, is due to progressive bacterial proliferation and associated respiratory failure.

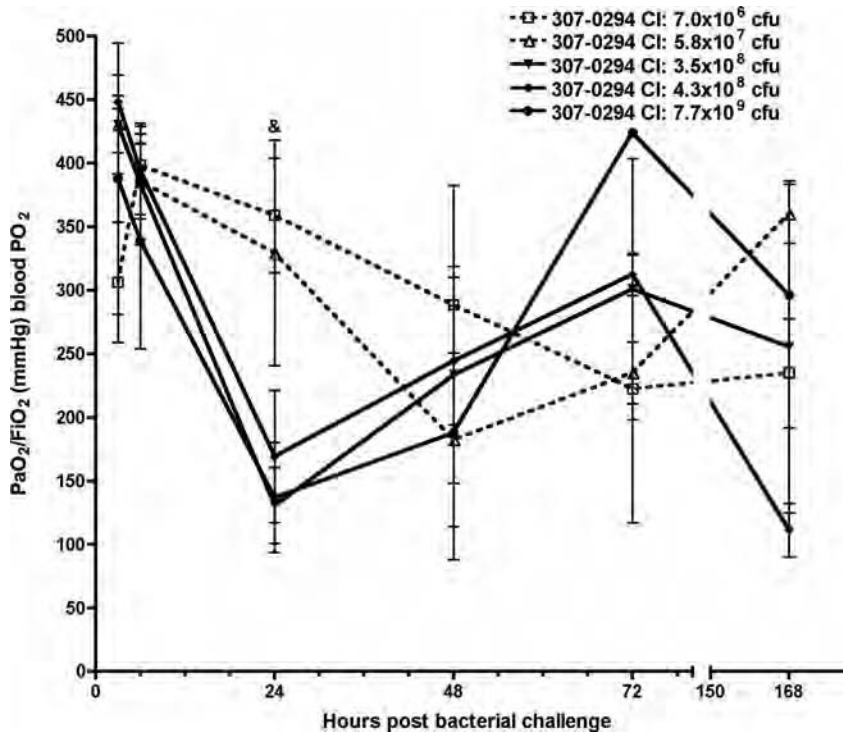

FIG. 3. Oxygenation concentration from rats at 3, 6, 24, 48, 72, and 168 h post-challenge with different titers of *A. baumannii* strain 307-0294. Rats were given 7.0×10^6, 5.8×10^7, 3.5×10^8, 4.3×10^8, and 7.7×10^9 CFU of 307-0294 by intratracheal instillation, and aortic blood was obtained at 3, 6, 24, 48, 72, and 168 h for determination of PaO_2/FiO_2 (mm Hg). There was a trend for increased oxygenation at 24 h in rats challenged with 7.0×10^6 CFU compared to rats challenged with 3.5×10^8 and 7.7×10^9 CFU (&, $P = 0.02$ and 0.04, respectively). Data are means ± standard errors of the means for $n = 3$ for each challenge titer and time point.

Acute lung injury. To determine the effect of *A. baumannii* on acute lung injury, arterial oxygenation (PaO_2/FiO_2 ratio) and BALF albumin were measured at 3, 6, 24, 48, 72, and 168 h following challenge of rats with various titers of 307-0294. After challenge with 307-0294, the decreases in oxygenation levels, which reflect acute lung injury, were similar and most pronounced with the three highest challenge inocula (3.5×10^8 to 7.7×10^9 CFU). A lesser effect on oxygenation was observed with the two lowest challenge inocula (7.0×10^6 and 5.8×10^7 CFU) (Fig. 3). The greatest decrease in oxygenation occurred at 24 h for the three highest 307-0294 challenge inocula (3.5×10^8 to 7.7×10^9 CFU), at 48 h for the next highest challenge inoculum (5.8×10^7 CFU), and at 72 h for the lowest challenge inoculum (7.0×10^6 CFU). Levels recovered thereafter but not back to baseline. There was a trend for increased oxygenation at 24 h in rats challenged with 7.0×10^6 CFU compared to rats challenged with 3.5×10^8 and 7.7×10^9 CFU ($P = 0.02$ and 0.04, respectively). These data demonstrated that when *A. baumannii* was able to grow (e.g., 307-0294 challenge inocula of 3.5×10^8 to 7.7×10^9 CFU), the decrease in oxygenation was greatest and occurred more quickly than when *A. baumannii* was cleared (e.g., 307-0294 challenge inocula of 7.0×10^6 and 5.8×10^7 CFU).

Leakage of albumin from the vasculature into the alveolar spaces is another measure of acute lung injury. After challenge with 307-0294, the increases in BALF albumin levels were similar and most pronounced with the three highest challenge inocula (3.5×10^8 to 7.7×10^9 CFU) and a lesser effect on BALF albumin was observed with the two lowest challenge inocula (7.0×10^6 and 5.8×10^7 CFU) (Fig. 4). The greatest increase in BALF albumin occurred at 24 h for the three highest 307-0294 challenge inocula (3.5×10^8 to 7.7×10^9 CFU) and at 6 h for the two lowest challenge inocula (5.8×10^7 and 7.0×10^6 CFU); levels decreased thereafter. There was a significant decrease or trend toward a significant decrease in the concentration of BALF albumin at various times in rats challenged with 7.0×10^6 and 5.8×10^7 CFU compared to rats challenged with 3.5×10^8, 4.3×10^8, and 7.7×10^9 CFU (Fig. 4). These data demonstrated that the increase in BALF albumin was greatest when *A. baumannii* was able to grow (e.g., 307-0294 challenge inocula of 3.5×10^8 to 7.7×10^9 CFU) compared to when *A. baumannii* was cleared (e.g., 307-0294 challenge inocula of 7.0×10^6 and 5.8×10^7 CFU).

Host inflammatory response. To determine the effect of *A. baumannii* on pulmonary levels of TNF-α, IL-1β, and CINC-1 in vivo, these mediators were assessed in cell-free BALF supernatants at 3, 6, 24, 48, 72, and 168 h following challenge of rats with various titers of 307-0294. After challenge with 307-0294, levels of TNF-α, IL-1β, and CINC-1 were barely measurable after a challenge inoculum of 7.0×10^6 CFU, increased after a challenge inoculum of 5.7×10^7 CFU, and were of similar orders of magnitude after challenge inocula of 3.5×10^8, 4.3×10^8, and 7.7×10^9 CFU (Fig. 5A to C). After challenge with 307-0294, TNF-α and CINC-1 levels peaked at 6 h and essentially were at the limit of detection by 72 h (Fig. 5A and C), whereas IL-1β levels peaked at 24 h and were at the

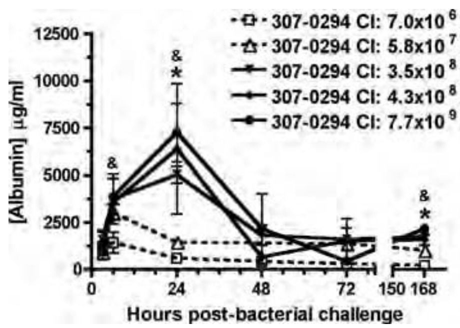

FIG. 4. BALF albumin concentration from rats at 3, 6, 24, 48, 72, and 168 h post-challenge with different titers of *A. baumannii* strain 307-0294. Rats were given 7.0×10^6, 5.8×10^7, 3.5×10^8, 4.3×10^8, and 7.7×10^9 CFU of 307-0294 by intratracheal instillation, and cell-free BALF was obtained at 3, 6, 24, 48, 72, and 168 h for determination of albumin. There was a significant decrease in the concentration of BALF albumin at 24 h in rats challenged with 7.0×10^6 and 5.8×10^7 CFU compared to rats challenged with 3.5×10^8 CFU (*, $P = 0.0008$ and 0.002, respectively) and at 168 h in rats challenged with 7.0×10^6 and 5.8×10^7 CFU compared to rats challenged with 3.5×10^8 CFU (*, $P = 0.006$ and 0.008, respectively). There was a trend for a decrease in the concentration of BALF albumin at 6 h in rats challenged with 7.0×10^6 CFU compared to rats challenged with 4.3×10^8 CFU (&, $P = 0.03$), at 24 h in rats challenged with 7.0×10^6 and 5.8×10^7 CFU compared to rats challenged with 7.7×10^9 CFU (&, $P = 0.01$ and 0.02, respectively), and at 168 h in rats challenged with 7.0×10^6 CFU compared to rats challenged with 4.3×10^8 CFU (&, $P = 0.01$). Data are means $\pm$ standard errors of the means for $n = 3$ for each challenge titer and time point.

limit of detection by 72 h (Fig. 5B). There was a significant decrease or trend toward a significant decrease in TNF-α, IL-1-β, and CINC-1 levels at various times in rats challenged with 7.0×10^6 and 5.8×10^7 CFU compared to rats challenged with 3.5×10^8, 4.3×10^8, and 7.7×10^9 CFU (Fig. 5). These data demonstrated that after challenge with 307-0294 levels of TNF-α, IL-1β, and CINC-1 increased with increasing challenge inocula from 7.0×10^6 to 3.5×10^8 CFU and reached plateau levels thereafter. Further, levels of these early proinflammatory cytokines decreased after 6 h for TNF-α and CINC-1 and after 24 h for IL-1β. These data support the contention that the magnitude of the challenge inoculum is the dominant factor affecting levels of TNF-α, IL-1β, and CINC-1.

Pulmonary neutrophils present in BALF were also assessed after challenge with various titers of 307-0294 (except for the 7.7×10^9 CFU challenge inoculum). Neutrophil counts peaked at 6 h and decreased thereafter (Fig. 6). The total numbers of neutrophils were similar after challenge with all titers of 307-0294, except after challenge with the lowest titer (7.0×10^6 CFU) at 24, 48, 72, and 168 h, where there was a significant decrease or a trend toward a significant decrease in the number of neutrophils compared to that for rats challenged with 5.7×10^7, 3.5×10^8, and 4.3×10^8 CFU (Fig. 6). The timing of maximal neutrophil counts corresponded to the timing of maximal TNF-α and CINC-1 levels, but unlike cytokines, neutrophil counts decreased more slowly and persisted for 168 h. Further, the maximal neutrophil response was seen even with the lowest 307-0294 challenge titers.

Taken together, these data demonstrate that bacterial growth, acute lung injury, and an appropriate host inflammatory response occur in the rat pneumonia model after challenge with *Acinetobacter*. This supports our hypothesis that the immunocompetent rat pneumonia model is clinically relevant for assessing *A. baumannii* infection.

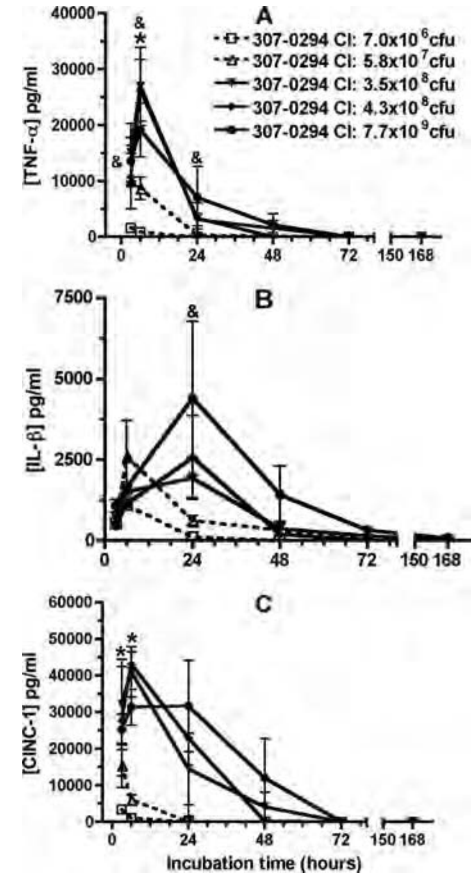

FIG. 5. TNF-α, IL-1β, and CINC-1 cell-free BALF concentrations from rats at 3, 6, 24, 48, 72, and 168 h post-challenge with different titers of *A. baumannii* strain 307-0294. (A) TNF-α. (B) IL-1β. (C) CINC-1. Rats were given 7.0×10^6, 5.8×10^7, 3.5×10^8, 4.3×10^8, and 7.7×10^9 CFU of 307-0294 (blood isolate, ST15, clonal group 1) by intratracheal instillation, and BALF was obtained for determination of cytokine/chemokine levels at 3, 6, 24, 48, 72, and 168 h. (A) There was a significant decrease in TNF-α levels at 6 h in rats challenged with 7.0×10^6 CFU compared to rats challenged with 4.3×10^8 CFU (*, $P = 0.01$) and a trend for decreased TNF-α levels at 3 h in rats challenged with 7.0×10^6 CFU compared to rats challenged with 7.7×10^9 CFU (&, $P = 0.049$), at 6 h in rats challenged with 7.0×10^6 CFU compared to rats challenged with 3.5×10^8 and 7.7×10^9 CFU (&, $P = 0.02$), at 6 h in rats challenged with 5.8×10^7 CFU compared to rats challenged with 4.3×10^8 CFU (&, $P = 0.04$), and at 24 h in rats challenged with 7.0×10^6 CFU compared to rats challenged with 3.5×10^8 CFU (&, $P = 0.04$). (B) There was a trend for decreased IL-1β levels at 24 h in rats challenged with 7.0×10^6 CFU compared to rats challenged with 3.5×10^8 CFU (&, $P = 0.04$). (C) There was a significant decrease in CINC-1 levels at 3 h in rats challenged with 7.0×10^6 CFU compared to rats challenged with 7.7×10^9 CFU (*, $P = 0.007$) and at 6 h in rats challenged with 7.0×10^6 compared to rats challenged with 3.5×10^8, 4.3×10^8, and 7.7×10^9 CFU (*, $P = 0.004$, 0.0003, and 0.004, respectively) and in rats challenged with 5.8×10^7 CFU compared to rats challenged with 3.5×10^8, 4.3×10^8, and 7.7×10^9 CFU (*, $P = 0.007$, 0.0006, and 0.008, respectively). Data are means $\pm$ standard errors of the means for $n = 3$ for each challenge titer and time point.

The rat soft-tissue infection model is clinically relevant for assessing *Acinetobacter* infection. Surgical sites, ulcers, and patients who have sustained traumatic (e.g., battlefield) in-

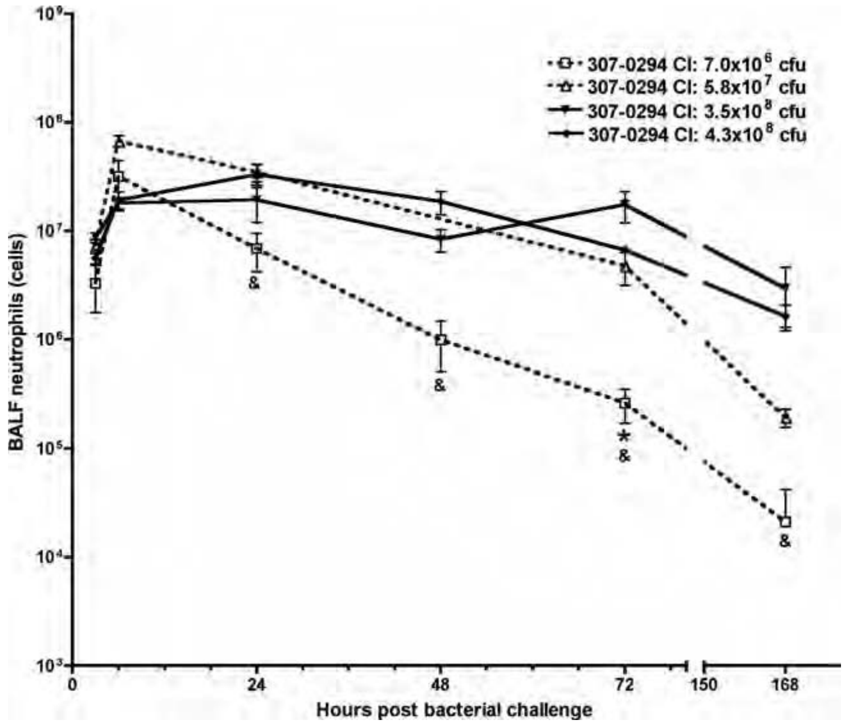

FIG. 6. Neutrophil numbers in BALF from rats at 3, 6, 24, 48, 72, and 168 h post-challenge with different titers of *A. baumannii* strain 307-0294. Rats were given 7.0×10^6, 5.8×10^7, 3.5×10^8, 4.3×10^8, and 7.7×10^9 CFU of 307-0294 by intratracheal instillation; BALF was collected at 3, 6, 24, 48, 72, and 168 h; and cells were harvested from BALF and then enumerated by Coulter counting. Neutrophil numbers are based on leukocyte differentials obtained from stained cytoslides (Materials and Methods). Cell counts were not done from animals challenged with 7.7×10^9 CFU. There was a significant decrease in the number of neutrophils at 72 h in rats challenged with 7.0×10^6 CFU compared to rats challenged with 4.3×10^8 CFU (*, $P = 0.0003$) and a trend for a decrease in the number of neutrophils at 24 h in rats challenged with 7.0×10^6 CFU compared to rats challenged with 5.7×10^7 and 4.3×10^8 CFU (&, $P = 0.019$ and 0.041, respectively), at 48 h in rats challenged with 7.0×10^6 CFU compared to rats challenged with 3.5×10^8 and 4.3×10^8 CFU (&, $P = 0.025$ and 0.019, respectively), at 72 h in rats challenged with 7.0×10^6 CFU compared to rats challenged with 3.5×10^8 CFU (&, $P = 0.037$), and at 168 h in rats challenged with 7.0×10^6 CFU compared to rats challenged with 5.7×10^7 and 4.3×10^8 CFU (&, $P = 0.022$ and 0.022, respectively). Data are means ± standard errors of the means for $n = 3$ for each challenge titer and time point.

juries have been at risk for soft-tissue infection due to *Acinetobacter* (30, 48). Therefore, we tested our hypothesis that the immunocompetent rat soft-tissue infection model is clinically relevant for assessing *A. baumannii* infection. In brief, a subcutaneous fluid-filled space is created that can be inoculated with the bacterial strain being assessed, samples can be withdrawn, and bacterial titers can be measured over time (for at least 7 days). The growth of 307-0294 was assessed over 48 h (Fig. 7). Clearance was observed over the first 6 h, followed by growth and achievement of plateau density by 24 h. The ability of 307-0294 to survive the host's defenses and proliferate within this soft-tissue environment is consistent with its ability to cause soft-tissue infection in humans. These data support our hypothesis that this model is clinically relevant and can be used to study *Acinetobacter* in this setting.

The rat soft-tissue infection model can be used to assess the relative virulence of various *A. baumannii* clinical isolates. Next we tested the hypothesis that the soft-tissue infection model could be used to discriminate between the inherent differences in virulence of various *A. baumannii* clinical isolates. The growth of 853 (OIFC031) (blood isolate, ST11, clonal group II), 855 (axillary isolate, ST14, clonal group III), 900 (perineal isolate, ST19, clonal group undetermined), and 979 (OIFC327) (environmental isolate, ST24, clonal group undetermined) was compared to that of 307-0294 in this model. Three patterns were observed: growth (979), clearance (853), or a variable degree of clearance over 3 to 6 h followed by different rates of growth (855 > 307-0294 > 900) (Fig. 7). There was a significant decrease or trend toward a significant decrease in survival of 853 and 900 at various times compared to 307-0294, 855, and 979. This model was quite sensitive in differentiating the abilities of different *A. baumannii* strains to survive in vivo. Interestingly, although the number of strains assessed was small, one might predict that survival of the blood isolates 307-0294 and 853 would be the greatest, but this was not the case. These data support our hypothesis that this model can be used to discriminate between the inherent differences in virulence of various *A. baumannii* clinical isolates.

Serum sensitivity of *Acinetobacter* isolates in vitro correlates with their growth in the soft-tissue infection model. Complement and neutrophils are innate host defense factors known to be active in the soft-tissue infection model (7, 8). Since various strains of *Acinetobacter* were variably cleared in this model, we hypothesized that complement is an important host factor in protecting against *A. baumannii* infection in vivo. Therefore, the serum sensitivity of *A. baumannii*

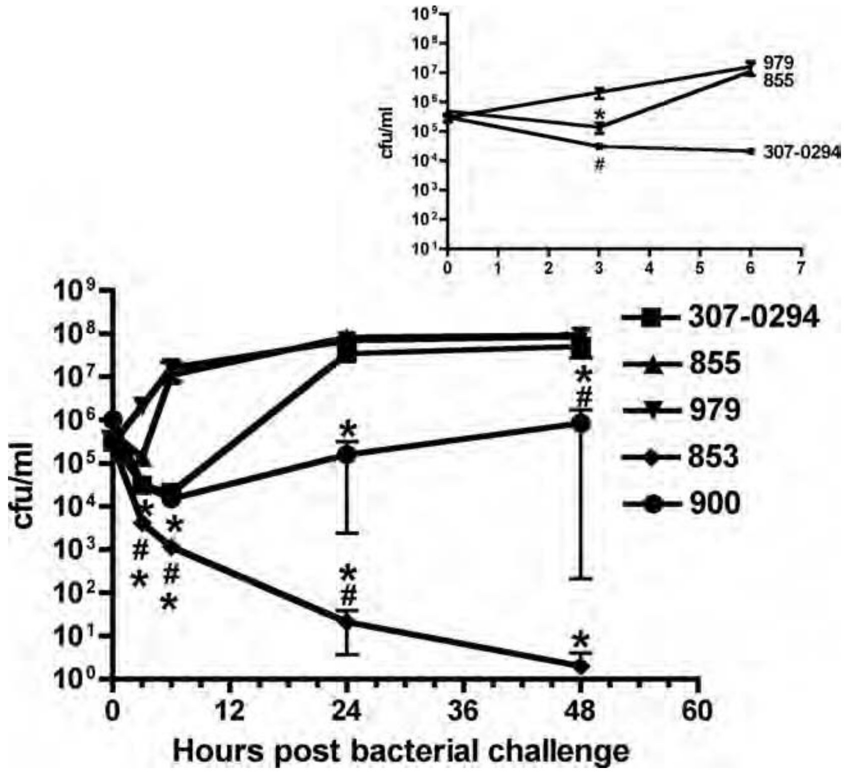

FIG. 7. Growth/clearance of *A. baumannii* strains 307-0294, 853, 855, 900, and 979 in the rat soft-tissue infection model. Rats were prepared and challenged with the bacterial strains being assessed as described in Materials and Methods. Bacterial titers were determined at 0, 3, 6, 24, and 48 h. There was a significant decrease or trend toward a significant decrease in survival of 853 and 900 at various times compared to 307-0294, 855, and 979. Data are means ± standard errors of the means for $n = 4$ to 9. *, 853 compared to 307-0294, $P < 0.001$ and 0.0005 at 3 and 6 h, respectively; *, 853 compared to 855, $P = 0.0004$ at 48 h; *, 853 compared to 979, $P = 0.0005$ and 0.003 at 24 and 48 h, respectively. #, 853 compared to 307-0294, $P = 0.045$ at 24 h; #, 853 compared to 855, $P = 0.03$ at 24 h; #, 853 compared to 979, $P = 0.02$ and 0.03 at 3 and 6 h, respectively; *, 900 compared to 307-0294, $P = 0.007$ at 24 h; *, 900 compared to 855, $P = 0.004$ and <0.0001 at 24 and 48 h, respectively; *, 900 compared to 979, $P = 0.002$, 0.005, <0.0001, and <0.0001 at 3, 6, 24, and 48 h, respectively; #, 900 compared to 307-0294, $P = 0.019$ at 48 h. (Inset) Enlargement of data from 307-0294, 855, and 979 from 0 to 6 h. There was both a trend and a significant difference in growth of 307-0294 and 855 compared to 979. *, 855 compared to 979, $P = 0.005$; #, 307-0294 compared to 979, $P = 0.02$.

strains 307-0294, 853, 855, 900, and 979 was assessed over 3 h in vitro (Fig. 8). All strains grew similarly in 90% serum that was heated at 56°C for 30 min to inactivate complement-mediated killing and LB medium (data not shown). When these strains were exposed to 90% active serum, the growth of 307-0294, 855, and 900 was similar. In contrast, 853 underwent an approximate 2-log killing and 900 underwent an approximate 0.5-log killing followed by recovery to the starting titer at 3 h; these differences were significant compared to 307-0294, 855, and 979. These data roughly correlate with growth/clearance in the soft-tissue infection model (Fig. 7). However, the soft-tissue infection model was more discriminatory, with 307-0294, 855, and 979 demonstrating differing growth/clearance capabilities, whereas in the serum sensitivity assay, the survival capabilities of 307-0294, 855, and 979 were similar. This is not surprising since multiple host defense factors (e.g., professional phagocytes and antimicrobial peptides) in addition to complement are present in the soft-tissue infection model. Nonetheless, these data support our hypothesis that complement is one host defense factor that contributes to the clearance of *A. baumannii* in vivo.

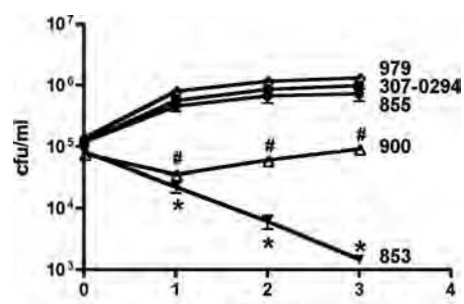

FIG. 8. Effect of 90% normal human serum on the viability of the *A. baumannii* strains 307-0294, 853, 855, 900, and 979 in vitro. Assays were performed as described in Materials and Methods. All strains were also assessed in the presence of 90% heat-inactivated (56°C for 30 min) normal human serum, and their growth rates were similar; therefore, these data are not shown. The survival of 853 and 900 was significantly decreased compared to that of 307-0294, 855, and 979. Data are means ± standard errors of the means for $n = 4$ to 6. *, 853 compared to 307-0294, 855, and 979. P is <0.0001 for all comparisons between 853 and 307-0294 and 979. P is <0.0001, 0.0006, and 0.002 for 853 compared to 855 for 1, 2, and 3 h, respectively. #, 900 compared to 307-0294, 855, and 979. P is < 0.0001, 0.0006, and <0.0001 for 900 compared to 307-0294; $P = 0.002$, 0.008, and 0.009 for 900 compared to 855; $P = 0.0004$, <0.0001, and < 0.0001 for 900 compared to 979 for 1, 2, and 3 h, respectively.

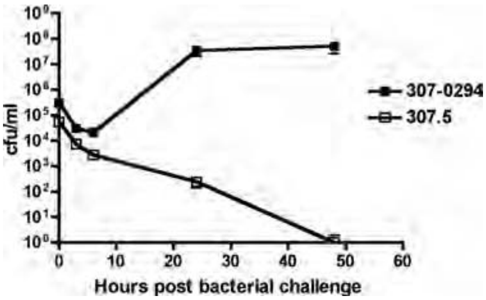

FIG. 9. Growth/clearance of *A. baumannii* strain 307-0294 and its mutant derivative 307.5 in the rat soft-tissue infection model. Rats were prepared and challenged with the bacterial strains being assessed as described in Materials and Methods. Bacterial titers were determined at 0, 3, 6, 24, and 48 h.

The rat soft-tissue infection model can be used to efficiently assess gene essentiality in vivo. Because safe reliable agents with predictable activity against *A. baumannii* are presently nonexistent, there is a need to identify new antimicrobial targets in *Acinetobacter*. Although multiple approaches to accomplish this goal exist, a starting point for one strategy is to identify *Acinetobacter* genes essential for growth. The rat soft-tissue infection model is an efficient model for assessing in vivo growth/survival because multiple samples can be obtained from a single animal over time. Therefore, we hypothesized that the soft-tissue infection model would serve as an effective screening tool for establishing gene essentiality for drug discovery. We randomly mutagenized 307-0294 using the transposon EZ-Tn5<kan-2>. Mutants isolated on MH plates containing kanamycin were subsequently gridded onto ascites plates supplemented with kanamycin. Chromosomal sequencing (using primers from the ends of EZ-Tn5<kan-2>) was performed on mutants that displayed no or minimal growth on ascites plates, enabling the localization of the transposon insertion. One of these mutants (307.5) contains a transposon insertion in the gene that codes for phosphoribosylaminoimidazole-succinocarboxamide synthase. Quantitative growth curves performed in LB medium demonstrated that there was no difference in growth between 307-0294 and 307.5 (data not shown). To test our hypothesis that the soft-tissue infection model could be used to establish gene essentiality in vivo, we assessed the growth of AB307.5 in this model (Fig. 9). 307.5, a mutant derivative of 307-0294, was cleared, thereby supporting our hypothesis.

DISCUSSION

Acinetobacter is a pathogen of increasing medical importance (13, 14, 19, 33). Little is known about its mechanisms of pathogenesis, vaccine candidates have not been identified, and an increasing proportion of strains are highly resistant to antimicrobials (29, 32). The availability of clinically relevant animal infection models will facilitate studies on the innate virulence of various *Acinetobacter* clinical isolates, potential virulence factors, vaccine candidates, and drug targets in vivo and can be used for pharmacokinetic and chemotherapeutic investigations. In this report we tested the hypotheses that the rat pneumonia and soft-tissue infection models that our laboratory had previously used for studies of extraintestinal pathogenic *E. coli* were clinically relevant for assessing *A. baumannii* (37, 41, 42). The lung is an important site of *Acinetobacter* infection in humans, and after challenge with *A. baumannii*, the pneumonia model demonstrated all of the features of infection that are critical for a clinically relevant model: namely, bacterial growth/clearance, an ensuing host inflammatory response, acute lung injury, and death due to respiratory failure following progressive bacterial proliferation (Fig. 1 to 6). Soft tissue has been increasingly recognized as an important site of *Acinetobacter* infection in battlefield injuries, surgical sites, and ulcers (5, 11, 18). We were also able to demonstrate growth of 307-0294 in the soft-tissue infection model, as occurs in soft-tissue infection, thereby supporting our hypothesis. We also hypothesized that the soft-tissue infection model could be used to discriminate between the inherent levels of virulence possessed by various *Acinetobacter* strains. In support of this, various patterns of growth were observed for the *Acinetobacter* strains tested (Fig. 7). Although it is beyond the scope of this report, these biologic data could be used in conjunction with molecular epidemiologic data as a means of predicting the virulence of *Acinetobacter* isolates. Given the variable growth of *Acinetobacter* strains in the soft-tissue infection model and the fact that complement is an active host defense factor in this site, we hypothesized that complement is an important host factor in protecting against *A. baumannii* infection in vivo. Growth/clearance of the *A. baumannii* strains in the soft-tissue infection model roughly correlated with growth/clearance in in vitro serum sensitivity studies (Fig. 8), thereby supporting this hypothesis. Lastly, we supported our hypothesis that the soft-tissue infection model could be used to establish the essentiality of *Acinetobacter* genes in vivo, an important characteristic for potential drug targets (Fig. 9). Although we did not utilize these models to assess vaccine candidates or virulence factors, it is self-evident that they can be used for this purpose as well.

The models described in this report have certain advantages over the previously described *Acinetobacter* animal infection models (4, 21, 22, 25–27, 31, 36). First, it is critical to be able to have bacterial growth over a significant period of time in a pneumonia model. In our rat model, with the highest challenge inocula we were able to demonstrate growth for 24 to 48 h post-bacterial challenge (Fig. 1). Further, at the highest challenge inocula some rats succumbed to infection (Fig. 2). Given that at these challenge inocula significant acute lung injury also occurred (Fig. 3 to 4), it is reasonable to infer that these animals died from respiratory insufficiency (as opposed to "cytokine storm"). Since we did not perform blood cultures in these animals, we cannot exclude the possibility of concomitant bacteremia, which could also contribute to mortality in this setting. However, even if bacteremia did occur in these animals, bacteremia also occurs in severe pneumonia in humans and as a result does not make this model less relevant. Taken together, these data support this model as being particularly relevant for studying all aspects of *Acinetobacter* pneumonia: namely, bacterial growth/clearance, acute lung injury, and the host response. In contrast, bacteria are often cleared in murine pneumonia models. Therefore, in the majority of *Acinetobacter* murine pneumonia models reported on to date, the animals received porcine mucin with the bacterial challenge (4, 25, 26, 34, 36) or were rendered neutropenic (20, 21), permutations

that are not present in most patients who develop *Acinetobacter* pneumonia. In one report that used a murine model, *Acinetobacter* grew over the first 4 h but underwent significant clearance by 24 h (22). A major advantage of the soft-tissue infection model is that multiple sampling can be performed over time in each animal, making it time and cost efficient for initial assessment of strains in vivo. In contrast, in the pneumonia models and thigh infection model (27) animals need to be euthanized for measurement of bacterial growth/clearance, injury, and the host response. Further, in the thigh infection model animals were rendered neutropenic (27). Although the lungs and soft tissue are clearly different host environments that contain different growth and host defense factors, clinical isolates and mutant derivatives of 307-0294 that were cleared in the soft-tissue infection model were also cleared when assessed in the pneumonia model (data not shown). Although we did not measure the host response in our *A. baumannii* studies, this can be done in the soft-tissue infection model as previously reported (7, 8). Therefore, the soft-tissue infection model is more cost-effective and high throughput for answering certain biologic questions. It would appear that this model could be used for an initial, efficient means to assess the growth/clearance of *Acinetobacter* in vivo.

Although it was not the main goal of this report, interesting aspects of *A. baumannii* biology were illuminated during this study. The soft-tissue infection model was more discriminating for growth differences between strains than for in vitro serum sensitivity testing (Fig. 7 and 8). This is not surprising since in the soft-tissue infection model host factors critical in protecting against extracellular bacterial pathogens like *Acinetobacter* are present including complement, antimicrobial peptides, and professional phagocytes. Second, *A. baumannii* strains 307-0294 and 853 were both blood isolates but displayed diametrically opposed growth/clearance patterns in vivo. These data highlight the fact that the innate virulence of clinical isolates may not necessarily be predicted by site of isolation.

In summary, we have supported our hypotheses on the utility of rat pneumonia and soft-tissue infection models for studying *Acinetobacter* biology. Both of the models described in this report are clinically relevant and possess certain advantages over previously described models. These models can be used to study the innate virulence of various *Acinetobacter* clinical isolates and to assess potential virulence factors, vaccine candidates, and drug targets in vivo and can be used for pharmacokinetic and chemotherapeutic investigations.

ACKNOWLEDGMENTS

We gratefully acknowledge the financial support of a VA Merit Review from the Department of Veterans Affairs (T.A.R.) and a US Army Medical Research Acquisition Activity under contract W81XWH-05-1-0627 (T.A.R. and A.C.).

REFERENCES

1. **Anstey, N. M., B. J. Currie, M. Hassell, D. Palmer, B. Dwyer, and H. Seifert.** 2002. Community-acquired bacteremic *Acinetobacter* pneumonia in tropical Australia is caused by diverse strains of *Acinetobacter baumannii*, with carriage in the throat in at-risk groups. J. Clin. Microbiol. **40:**685–686.
2. **Anstey, N. M., B. J. Currie, and K. M. Withnall.** 1992. Community-acquired Acinetobacter pneumonia in the Northern Territory of Australia. Clin. Infect. Dis. **14:**83–91.
3. **Bergogne-Berezin, E., and K. J. Towner.** 1996. *Acinetobacter* spp. as nosocomial pathogens: microbiological, clinical, and epidemiological features. Clin. Microbiol. Rev. **9:**148–165.
4. **Bernabeu-Wittel, M., C. Pichardo, A. Garcia-Curiel, M. E. Pachon-Ibanez, J. Ibanez-Martinez, M. E. Jimenez-Mejias, and J. Pachon.** 2005. Pharmacokinetic/pharmacodynamic assessment of the in-vivo efficacy of imipenem alone or in combination with amikacin for the treatment of experimental multiresistant *Acinetobacter baumannii* pneumonia. Clin. Microbiol. Infect. **11:**319–325.
5. **Centers for Disease Control and Prevention.** 2004. *Acinetobacter baumannii* infections among patients at military medical facilities treating injured U.S. service members, 2002–2004. MMWR Morb. Mortal. Wkly. Rep. **53:**1063–1066.
6. **Chen, M. Z., P. R. Hsueh, L. N. Lee, C. J. Yu, P. C. Yang, and K. T. Luh.** 2001. Severe community-acquired pneumonia due to *Acinetobacter baumannii*. Chest **120:**1072–1077.
7. **Dalhoff, A., G. Frank, and G. Luckhaus.** 1982. The granuloma pouch: an in vivo model for pharmacokinetic and chemotherapeutic investigations. I. Biochemical and histological characterization. Infection **10:**354–360.
8. **Dalhoff, A., G. Frank, and G. Luckhaus.** 1983. The granuloma pouch: an in vivo model for pharmacokinetic and chemotherapeutic investigations. II. Microbiological characterization. Infection **11:**41–46.
9. **Davidson, B., P. Knight, J. Helinski, N. Nader, T. Shanley, and K. Johnson.** 1999. The role of tumor necrosis factor-alpha in the pathogenesis of aspiration pneumonitis in rats. Anesthesiology **91:**486–499.
10. **Davis, K. A., K. A. Moran, C. K. McAllister, and P. J. Gray.** 2005. Multidrug-resistant Acinetobacter extremity infections in soldiers. Emerg. Infect. Dis. **11:**1218–1224.
11. **Department of Veterans Affairs.** 2004. Update of the Colleagues' Letter sent April 23, 2004 concerning *Acinetobacter baumannii.* Department of Veterans Affairs, Veterans Health Administration, Washington, DC.
12. **Ecker, J. A., C. Massire, T. A. Hall, R. Ranken, T. T. Pennella, C. A. Ivy, L. B. Blyn, S. A. Hofstadler, T. P. Endy, P. T. Scott, L. Lindler, T. Hamilton, C. Gaddy, K. Snow, M. Pe, J. Fishbain, D. Craft, G. Deye, S. Riddell, E. Milstrey, B. Petruccelli, S. Brisse, V. Harpin, A. Schink, D. J. Ecker, R. Sampath, and M. W. Eshoo.** 2006. Identification of *Acinetobacter* species and genotyping of *Acinetobacter baumannii* by multilocus PCR and mass spectrometry. J. Clin. Microbiol. **44:**2921–2932.
13. **Falagas, M. E., and E. A. Karveli.** 2007. The changing global epidemiology of *Acinetobacter baumannii* infections: a development with major public health implications. Clin. Microbiol. Infect. **13:**117–119.
14. **Fournier, P. E., and H. Richet.** 2006. The epidemiology and control of *Acinetobacter baumannii* in health care facilities. Clin. Infect. Dis. **42:**692–699.
15. **Garzoni, C., S. Emonet, L. Legout, R. Benedict, P. Hoffmeyer, L. Bernard, and J. Garbino.** 2005. Atypical infections in tsunami survivors. Emerg. Infect. Dis. **11:**1591–1593.
16. **Gaynes, R., and J. R. Edwards.** 2005. Overview of nosocomial infections caused by gram-negative bacilli. Clin. Infect. Dis. **41:**848–854.
17. **Jain, R., and L. H. Danziger.** 2004. Multidrug-resistant Acinetobacter infections: an emerging challenge to clinicians. Ann. Pharmacother **38:**1449–1459.
18. **Johnson, E. N., T. C. Burns, R. A. Hayda, D. R. Hospenthal, and C. K. Murray.** 2007. Infectious complications of open type III tibial fractures among combat casualties. Clin. Infect. Dis. **45:**409–415.
19. **Joly-Guillou, M. L.** 2005. Clinical impact and pathogenicity of Acinetobacter. Clin. Microbiol. Infect. **11:**868–873.
20. **Joly-Guillou, M. L., M. Wolff, R. Farinotti, A. Bryskier, and C. Carbon.** 2000. In vivo activity of levofloxacin alone or in combination with imipenem or amikacin in a mouse model of *Acinetobacter baumannii* pneumonia. J. Antimicrob. Chemother. **46:**827–830.
21. **Joly-Guillou, M. L., M. Wolff, J. J. Pocidalo, F. Walker, and C. Carbon.** 1997. Use of a new mouse model of *Acinetobacter baumannii* pneumonia to evaluate the postantibiotic effect of imipenem. Antimicrob. Agents Chemother. **41:**345–351.
22. **Knapp, S., C. W. Wieland, S. Florquin, R. Pantophlet, L. Dijkshoorn, N. Tshimbalanga, S. Akira, and T. van der Poll.** 2006. Differential roles of CD14 and toll-like receptors 4 and 2 in murine Acinetobacter pneumonia. Am. J. Respir. Crit. Care Med. **173:**122–129.
23. **Landman, D., J. M. Quale, D. Mayorga, A. Adedeji, K. Vangala, J. Ravishankar, C. Flores, and S. Brooks.** 2002. Citywide clonal outbreak of multiresistant *Acinetobacter baumannii* and *Pseudomonas aeruginosa* in Brooklyn, N.Y.: the preantibiotic era has returned. Arch. Intern. Med. **162:**1515–1520.
24. **Maegele, M., S. Gregor, E. Steinhausen, B. Bouillon, M. M. Heiss, W. Perbix, F. Wappler, D. Rixen, J. Geisen, B. Berger-Schreck, and R. Schwarz.** 2005. The long-distance tertiary air transfer and care of tsunami victims: injury pattern and microbiological and psychological aspects. Crit. Care Med. **33:**1136–1140.
25. **Montero, A., J. Ariza, X. Corbella, A. Domenech, C. Cabellos, J. Ayats, F. Tubau, C. Borraz, and F. Gudiol.** 2004. Antibiotic combinations for serious infections caused by carbapenem-resistant *Acinetobacter baumannii* in a mouse pneumonia model. J. Antimicrob. Chemother. **54:**1085–1091.
26. **Pachon-Ibanez, M. E., F. Fernandez-Cuenca, F. Docobo-Perez, J. Pachon, and A. Pascual.** 2006. Prevention of rifampicin resistance in *Acinetobacter baumannii* in an experimental pneumonia murine model, using rifampicin

associated with imipenem or sulbactam. J. Antimicrob. Chemother. **58:**689–692.
27. **Pantopoulou, A., E. J. Giamarellos-Bourboulis, M. Raftogannis, T. Tsaganos, I. Dontas, P. Koutoukas, F. Baziaka, H. Giamarellou, and D. Perrea.** 2007. Colistin offers prolonged survival in experimental infection by multidrug-resistant *Acinetobacter baumannii*: the significance of co-administration of rifampicin. Int. J. Antimicrob. Agents **29:**51–55.
28. **Paterson, D. L., and Y. Doi.** 2007. A step closer to extreme drug resistance (XDR) in gram-negative bacilli. Clin. Infect. Dis. **45:**1179–1181.
29. **Perez, F., A. M. Hujer, K. M. Hujer, B. K. Decker, P. N. Rather, and R. A. Bonomo.** 2007. Global challenge of multidrug-resistant *Acinetobacter baumannii*. Antimicrob. Agents Chemother. **51:**3471–3484.
30. **Petersen, K., M. S. Riddle, J. R. Danko, D. L. Blazes, R. Hayden, S. A. Tasker, and J. R. Dunne.** 2007. Trauma-related infections in battlefield casualties from Iraq. Ann. Surg. **245:**803–811.
31. **Renckens, R., J. J. Roelofs, S. Knapp, A. F. de Vos, S. Florquin, and T. van der Poll.** 2006. The acute-phase response and serum amyloid A inhibit the inflammatory response to *Acinetobacter baumannii* pneumonia. J. Infect. Dis. **193:**187–195.
32. **Rice, L. B.** 2006. Challenges in identifying new antimicrobial agents effective for treating infections with *Acinetobacter baumannii* and *Pseudomonas aeruginosa*. Clin. Infect. Dis. **43:**S100–S105.
33. **Richet, H., and P. E. Fournier.** 2006. Nosocomial infections caused by *Acinetobacter baumannii*: a major threat worldwide. Infect. Control Hosp. Epidemiol. **27:**645–646.
34. **Rodriguez-Hernandez, M. J., L. Cuberos, C. Pichardo, F. J. Caballero, I. Moreno, M. E. Jimenez-Mejias, A. Garcia-Curiel, and J. Pachon.** 2001. Sulbactam efficacy in experimental models caused by susceptible and intermediate *Acinetobacter baumannii* strains. J. Antimicrob. Chemother. **47:**479–482.
35. **Rodriguez-Hernandez, M. J., M. E. Jimenez-Mejias, C. Pichardo, L. Cuberos, A. Garcia-Curiel, and J. Pachon.** 2004. Colistin efficacy in an experimental model of *Acinetobacter baumannii* endocarditis. Clin. Microbiol. Infect. **10:**581–584.
36. **Rodriguez-Hernandez, M. J., J. Pachon, C. Pichardo, L. Cuberos, J. Ibanez-Martinez, A. Garcia-Curiel, F. J. Caballero, I. Moreno, and M. E. Jimenez-Mejias.** 2000. Imipenem, doxycycline and amikacin in monotherapy and in combination in *Acinetobacter baumannii* experimental pneumonia. J. Antimicrob. Chemother. **45:**493–501.
37. **Russo, T., Y. Liang, and A. Cross.** 1994. The presence of K54 capsular polysaccharide increases the pathogenicity of *Escherichia coli in vivo*. J. Infect. Dis. **169:**112–118.
38. **Russo, T., G. Sharma, C. Brown, and A. Campagnari.** 1995. The loss of the O4 antigen moiety from the lipopolysaccharide of an extraintestinal isolate of *Escherichia coli* has only minor effects on serum sensitivity and virulence in vivo. Infect. Immun. **63:**1263–1269.
39. **Russo, T. A., L. A. Bartholomew, B. A. Davidson, J. D. Helinski, U. B. Carlino, P. R. Knight III, M. F. Beers, E. N. Atochina, R. H. Notter, and B. A. Holm.** 2002. Total extracellular surfactant is increased but abnormal in a rat model of gram-negative bacterial pneumonia. Am. J. Physiol. Lung Cell. Mol. Physiol. **283:**L655–L663.
40. **Russo, T. A., B. A. Davidson, J. M. Beanan, R. Olson, B. A. Holm, R. H. Notter, and P. R. Knight III.** 2007. Capsule and O-antigen from an extraintestinal isolate of *Escherichia coli* modulate cytokine levels in rat macrophages in vitro and in a rat model of pneumonia. Exp. Lung Res. **33:**337–356.
41. **Russo, T. A., B. A. Davidson, U. B. Carlino-MacDonald, J. D. Helinski, R. L. Priore, and P. R. Knight III.** 2003. The effects of *Escherichia coli* capsule, O-antigen, host neutrophils, and complement in a rat model of Gram-negative pneumonia. FEMS Microbiol. Lett. **226:**355–361.
42. **Russo, T. A., B. A. Davidson, S. A. Genagon, N. M. Warholic, U. Macdonald, P. D. Pawlicki, J. M. Beanan, R. Olson, B. A. Holm, and P. R. Knight III.** 2005. *E. coli* virulence factor hemolysin induces neutrophil apoptosis and necrosis/lysis in vitro and necrosis/lysis and lung injury in a rat pneumonia model. Am. J. Physiol. Lung Cell. Mol. Physiol. **289:**L207–L216.
43. **Russo, T. A., M. C. Moffitt, C. H. Hammer, and M. M. Frank.** 1993. Tn*phoA*-mediated disruption of K54 capsular polysaccharide genes in *Escherichia coli* confers serum sensitivity. Infect. Immun. **61:**3578–3582.
44. **Scott, P., G. Deye, A. Srinivasan, C. Murray, K. Moran, E. Hulten, J. Fishbain, D. Craft, S. Riddell, L. Lindler, J. Mancuso, E. Milstrey, C. T. Bautista, J. Patel, A. Ewell, T. Hamilton, C. Gaddy, M. Tenney, G. Christopher, K. Petersen, T. Endy, and B. Petruccelli.** 2007. An outbreak of multidrug-resistant *Acinetobacter baumannii-calcoaceticus* complex infection in the US military health care system associated with military operations in Iraq. Clin. Infect. Dis. **44:**1577–1584.
45. **Sunenshine, R. H., M. O. Wright, L. L. Maragakis, A. D. Harris, X. Song, J. Hebden, S. E. Cosgrove, A. Anderson, J. Carnell, D. B. Jernigan, D. G. Kleinbaum, T. M. Perl, H. C. Standiford, and A. Srinivasan.** 2007. Multidrug-resistant Acinetobacter infection mortality rate and length of hospitalization. Emerg. Infect. Dis. **13:**97–103.
46. **Talbot, G. H., J. Bradley, J. E. Edwards, Jr., D. Gilbert, M. Scheld, and J. G. Bartlett.** 2006. Bad bugs need drugs: an update on the development pipeline from the Antimicrobial Availability Task Force of the Infectious Diseases Society of America. Clin. Infect. Dis. **42:**657–668.
47. **Tognim, M. C., S. S. Andrade, S. Silbert, A. C. Gales, R. N. Jones, and H. S. Sader.** 2004. Resistance trends of Acinetobacter spp. in Latin America and characterization of international dissemination of multi-drug resistant strains: five-year report of the SENTRY Antimicrobial Surveillance Program. Int. J. Infect. Dis. **8:**284–291.
48. **Tong, M. J.** 1972. Septic complications of war wounds. JAMA **219:**1044–1047.
49. **van Dessel, H., T. E. Kamp-Hopmans, A. C. Fluit, S. Brisse, A. M. de Smet, L. Dijkshoorn, A. Troelstra, J. Verhoef, and E. M. Mascini.** 2002. Outbreak of a susceptible strain of Acinetobacter species 13 (sensu Tjernberg and Ursing) in an adult neurosurgical intensive care unit. J. Hosp. Infect. **51:**89–95.
50. **Van Looveren, M., and H. Goossens.** 2004. Antimicrobial resistance of Acinetobacter spp. in Europe. Clin. Microbiol. Infect. **10:**684–704.
51. **Villegas, M. V., and A. I. Hartstein.** 2003. Acinetobacter outbreaks, 1977–2000. Infect. Control Hosp. Epidemiol. **24:**284–295.

Editor: V. J. DiRita